FOR OFFICIAL USE ONLY

JPRS L/8461

16 May 1979

[redacted]

USSR

[redacted]

[redacted]

TRANSLATIONS ON USSR SCIENCE AND TECHNOLOGY

PHYSICAL SCIENCES AND TECHNOLOGY

(FOUO 28/79)

SELECTIONS FROM THE JOURNAL 'QUANTUM ELECTRONICS'

U. S. JOINT PUBLICATIONS RESEARCH SERVICE

[redacted]

FOR OFFICIAL USE ONLY

APPROVED FOR RELEASE: 2007/02/09: CIA-RDP82-00850R000100050032-0

NOTE

JPRS publications contain information primarily from foreign newspapers, periodicals and books, but also from news agency transmissions and broadcasts. Materials from foreign-language sources are translated; those from English-language sources are transcribed or reprinted, with the original phrasing and other characteristics retained.

Headlines, editorial reports, and material enclosed in brackets [] are supplied by JPRS. Processing indicators such as [Text] or [Excerpt] in the first line of each item, or following the last line of a brief, indicate how the original information was processed. Where no processing indicator is given, the information was summarized or extracted.

Unfamiliar names rendered phonetically or transliterated are enclosed in parentheses. Words or names preceded by a question mark and enclosed in parentheses were not clear in the original but have been supplied as appropriate in context. Other unattributed parenthetical notes within the body of an item originate with the source. Times within items are as given by source.

The contents of this publication in no way represent the policies, views or attitudes of the U.S. Government.

APPROVED FOR RELEASE: 2007/02/09: CIA-RDP82-00850R000100050032-0

JPRS L/8461

16 May 1979

TRANSLATIONS ON USSR SCIENCE AND TECHNOLOGY

PHYSICAL SCIENCES AND TECHNOLOGY

(FOUO 28/79)

SELECTIONS FROM THE JOURNAL 'QUANTUM ELECTRONICS'

Moscow KVANTOVAYA ELEKTRONIKA in Russian Vol 6 No 2, Feb 79
pp 267-273, 281-303, 317-348, 351-354, 357-363, 370-377,
394-397, 400-402, 408-411, 417-421

CONTENTS PAGE

PHYSICS

CONTENTS (Continued)

PHYSICS

UDC 621.375.826

HIGH-PRESSURE WIRE-TRIGGERED PULSED CO_2 LASER

Moscow KVANTOVAYA ELEKTRONIKA in Russian Vol 6, No 2, Feb79 pp 267-273

[Article by B. F. Gordiyets, B. Kosma, A. G. Sviridov and N. N. Sobolev, Physics Institute, imeni P. N. Lebedev AN USSR (Moscow), submitted 24 Jan 78]

[Text] A design is described of a wire-triggered CO_2 laser operating in a wide range of pressures (up to 3 atm). Discharge and laser radiation characteristics have been investigated experimentally. On the basis of the theoretical model of kinetic processes, the laser action characteristics are predicted over a wide range of discharge parameters. The theoretical results obtained are in good agreement with the experiments.

1. Introduction

In recent years, a great number of papers (see, for example, [1]) were dedicated to the development and investigation of various designs of pulsed CO_2 lasers with transverse discharge. This is due to the fact that this makes it possible to obtain large unit powers of laser infrared radiation, high power and efficiency at high pressures of active medium by comparatively simple means.

At present, there are high-pressure pulsed CO_2 lasers in which discharges are used with needle-shaped electrodes [2], double transverse discharges and discharges with preionization by ultraviolet radiation [4].

Interesting and comparatively simple is the design of a laser with preionization by means of additional wire electrodes [5]. Preliminary investigations [6] indicated a promising outlook for using this type of discharge at pressures higher than an atmosphere. Until now, however, a detailed analysis of the operation of this type of laser has not been made.

The goal of this paper is to make an installation with a stable pulsed glow discharge triggered by wire electrodes at pressures higher than an atmosphere,

as well as to obtain and investigate in detail the optimal modes of laser generation at a wavelength of 10.6 microns in a mixture of $CO_2 + N_2 + He$. Experimental data were compared to theoretical results.

2. Description of the Installation

Fig. 1 shows an arrangement of a discharge chamber. Aluminum electrodes 1 are placed in tube 2 made of vinyl plastic. The internal diameter of the tube is 8 cm and it is 60 cm long. Electrodes of the Rogovskiy shape, 43.5 cm long, are placed symmetrically with respect to the tube axis 1.4 cm from each other. Two tungsten wires 11, 0.2 mm in diameter, were stretched parallel to the electrodes equal distances from the axis (about 2 cm) for doing the preionozation. NaCl plates 3, 0.8 cm thick, are installed at Brewster's angle at the ends of the chamber. When investigating the discharge, the chamber was placed in an optical resonator 120 cm long, formed by a mirror with a gold coating on a quartz substrate with a 170 cm radius of curvature and a flat mirror made of germanium on which a dielectric was sprayed so that its coefficient of reflection was about 80 percent.

Voltage was applied to the chamber electrodes by a Marx generator consisting of five sections, each containing a capacity C =0.022 microfarads. The charging voltage of the capacitors of each section varied from 7 to 15 kv which made it possible to discharge from 2.7 to 12.3 joules, i.e., 0.067 to 0.29 joules/cm^3. The use of a Marx generator provided a five-fold multiplication of the charge voltage, increasing thereby the front steepness of the puncture. The ends of the wires providing preionization were connected to the cathode through two capacitors of 470 picofarads each.

To determine the power introduced into the discharge, discharge current pulses and electrode voltages were recorded in each experiment. This was done by means of an OK-17 two-beam oscillograph, which was shielded by a Faraday type metal cage. The current pulse was taken off a noninductive resistance shunt, while the voltage pulse was taken off a voltage divider containing a high ohm resistance and a matched RD-75 cable.

The shape of the pulse generation was recorded by a PEPI-1 modified pyroelectric receiver and an OK-17M oscillograph, which were also located in the Faraday box. A pulse was sent from the current measuring shunt to the second channel of the oscillograph so that it could measure the delay in the starting of the pulse generation with respect to the start of the current pulse, and determine simultaneously the time characteristics of generation and current pulses.

3. Results of Discharge Investigation

Durations of current and voltages pulses of the discharge did not exceed about 0.3 microseconds. The maximum electrode voltage (about 20 kv) coincided approximately in time with the current maximum (about 0.75 ka). An analysis

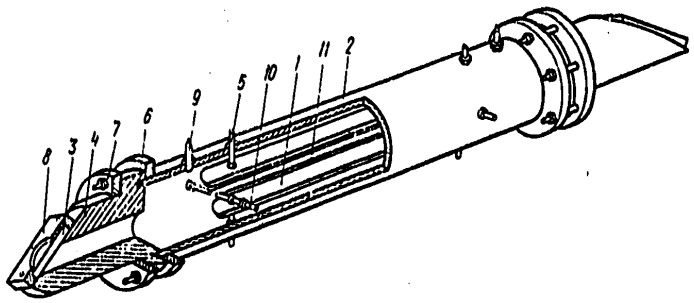

Fig. 1. Design of the laser chamber

1. Electrodes
2. Vinyl plastic tube
3. NaCl plate installed at Brewster's angle
4. Plexiglass coupling
5. Pins for supporting electrodes
6. Rubber lining
7. Flanges
8. Detent for the NaCl plate
9. Hole for admitting gas
10. Holder for preionozing wires
11. Tungsten wires for preionizing gas

of current and voltage indicated that the time relationship between field intensity E and current density j under our experimental conditions may be approximated by empirical formulas

$$E = E_0(1-e^{-mt})e^{-nt};\ j = j_0(1-e^{-m't})e^{-n't}, \qquad (1)$$

where the exponent of the indicators depend strongly on the distance between the electrodes and weakly on the compositions of the mixture, while j_o and E_o are unambiguously related to experimental peak values of current and voltage j_n and E_n .

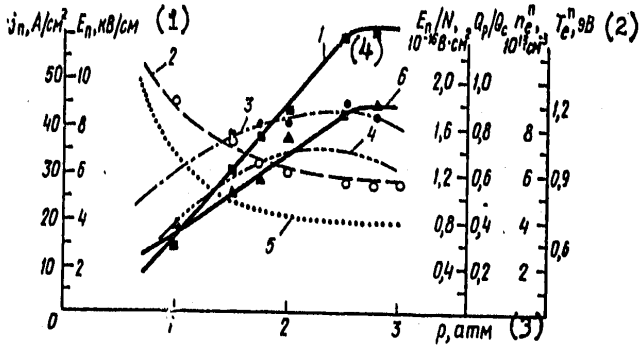

Fig. 2. Relationships between peak values of the electric field E_n (1), current density j_n (2), reduced intensity E_n/N (3), effective temperature T_e^n (4) and concentration n_e^n (5) of the discharge electrons, as well as the relationship between Q_p/Q_c (6) and total gas pressure p.

1. kv/cm
2. electron volt
3. atmosphere
4. v. cm^2

In all the experiments, the value of the cross section of the discharge, used in calculating the current density, was determined by the boundaries of the discharge trace, remaining on the electrodes after prolonged operation of the laser, and was about 30 cm^2 (length of discharge 43 cm and width 0.7 cm). The results of processing the oscillograms made it possible to obtain data on the values of E_n and j_n, as well as to calculate the relationship between the total energy put into discharge

$$Q_p = \int_0^\infty IU dt,$$

and energy Q_C, stored in the capacitor of the Marx generator. This data is shown in Fig. 2 for mixture CO_2: N_2: He=1:0.5:6.75 and Q_C=0.13 joules/cm^2.

This figure shows the relationship between the reduced field intensity E_n/N(N is the total number of gas particles per unit volume) As may be seen

from Fig. 2, raising the pressure from 1 to 2.6 atmospheres leads to a linear increase in $E_п$, while $j_п$ decreases with pressure. In region $p < 2.6$ atmospheres, the value of Q_p/Q_C is proportional to pressure and at p=3 atmospheres reaches about 89 percent. As the voltage on the capacitors increases, pressure p_o, at which parameters $E_п$, $j_п$ and Q_p/Q_C are saturated, increases. This makes it possible by increasing capacitor voltage, to obtain a uniform discharge at all higher pressures.

The value of E/N determines the effective temperature T_e of the discharge electrons and their drift velocity v. It follows from numerical calcualtions [7] that T_e (E/N) may be approximated to good accuracy by the formula

$$T_e = AE/N + B, \qquad (2)$$

where A is a constant depending on the composition of the mixture (for mixture $CO_2 + N_2$: He=2:9, A=0.52x10^{16} electron volt/voltxcm^2; B is the gas temperature, electron volt. It follows also from [7] that for a broad class of mixtures $CO_2 + N_2 + Ee$ the drift velocity is

$$v = (12{,}5 \cdot 10^{16}\ E/N + 27{,}5)\ \text{км/с}. \qquad (3)$$

Knowing the drift velocity of electrons and the current density, it is possible to find electron concentration n_e which, together with T_e, determines the energy imparted to the N_2 and CO_2 molecules:

$$n_e = 6{,}25 \cdot 10^{12}/(1{,}25 \cdot 10^{16}\ E/N + 2{,}75). \qquad (4)$$

Fig. 2 shows the relationships between the peak values of $T_e^п$ and $n_e^п$ in the pulse and the gas pressure found from (2) and (4). As seen from the figure, the values of $T_e^п$ and $n_e^п$ in the investigated pressure areas are found in the area of 0.9 electron volts and 4x10^{13}cm^{-3} respectively. We will note that $E_п$, $T_e^п$ and $n_e^п$ correspond to the moment of time when the current reaches maximum (peak) value. The relationship obtained of $E_п/N$ and the total gas pressure p is different from the one cited for pressures 0.1 to 1.0 atmospheres in [8]. A reduction in the value of $E_п/N$ with a reduction in pressure within the limits of 1.75 to 1.0 atmospheres is due to the strong ionization of the gas under these conditions, attested to by the high value of $n_e^п$. In

this case, strongly luminescent plasma jets are formed on the cathode surface, the lengths of which increase in the direction of the anode with pressure reduction in the discharge chamber; at pressures less than 0.75 atmospheres, the discharge changes to an arc discharge. Due to strong gas ionization, the peak value of electric field $E_п$ decreases faster with a reduction in gas pressure than in the usual case, when the volume between basic electrodes is filled with uniform diffusion glowing discharge. This leads not to an increase, but to a decrease of $E_п/N$ with the reduction in pressure.

4. Relationship Between the Energy of the Laser Pulse and Pressure and Accumulated Energy

We investigated the relationship between the energy of the laser pulse and the pressure at various values of accumulated energy. Experiments were conducted with a mixture CO_2:N_2:He=1:0.5:6.75 in a pressure range of 1 to 3 atmospheres and unit energies Q_C=0.067 to 0.29 joules/cm^3 when changing the charge voltage of one section V from 7 to 15 kv/section. The results are shown in Fig. 3 in the form of curves. It may be seen that the relationship between the radiation pulse energy and the pressure has a maximum, the position of which shifts to the side of greater pressures when the energy on the accumulating capacitors increases. Starting with $Q_C \gtrsim 0.13$ joules/cm^3, we did not reach the maximum of E_{izl} with respect to the pressure because the strength of the discharge chamber did not permit the creation of a pressure higher than 3 atmospheres.

It is well known that organic admixtures that have small ionization potentials may change the discharge characteristics [9]. To clarify the effect of such an admixture on the energy of laser radiation, we took an n-xylylol, which has an ionization potential of 8.44 electron volts and a transparency opening of 10 to 11 microns [10]. It was added to a working mixture of CO_2+ N_2+ He gases by passing this mixture or one of its components through a cuvette filled with saturated vapors of n-xylylol at room temperature.

In the presence of n-xylylol the discharge becomes visually more uniform and the radiation energy at $Q_C \gtrsim 0.13$ joules/cm^3 increase 1.5 to 2 times. At large additions of n-xylylol (when the mixture was passed through a cuvette with its vapors) laser generation did not originate.

5. Investigation of Discharge Characteristics and Laser Radiation. Comparison of an Experiment with Calculation

We will consider a theoretical model of a pulsed CO_2 laser we used for the physical interpretation of the experimental data.

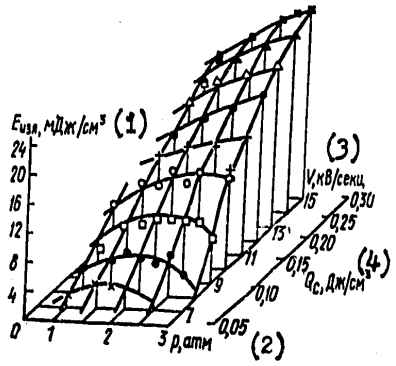

Fig. 3. Experimental relationship between unit output radiation energy E_{ize} and the total pressure p and unit accumulated energy Q_C.

1. E_{izl}, mjoules/cm^3
2. atmospheres
3. V, kv/section
4. Q_C, joules/cm^3

The basic physical concepts of the mechanixm that provides for the inverse population in CO_2 lasers were formulated in [11]. A system of kinetic equations based on the introduction of partial oscillating temperatures [13] was formulated in general form in [12] for relaxation processes of oscillating energy in multiatom molecules within the framework of a harmonic oscillator model. Our calculations were based on [12].

In view of the rapid energy exchange between symmetrical and unsymmetrical modes of CO_2, it was considered that the energies of these modes are in quasi-equilibrium with respect to each other. In kinetic equations for oscillating mode energies, besides members that characterize the collision processes of heavy particles, members were also introduced that describe the excitation and deactivation of oscillations by electrons, while for asymmetric and symmetric CO_2 modes -- members that describe relaxation in the field of laser radiation. For constant speeds of excitation of CO_2 and N_2 oscillations by electrons, analytical approximations of quantitative data [7] were selected.

Effective temperature T_e and concentration n_e of electrons, necessary for calculating velocities of excitation, were determined from formulas (2) and (4).

Equations of oscillating relaxations for CO_2 and N_2 written in this manner were solved on a computer jointly with equations for gas temperature and density of laser radiation flow within the resonator. In this case, new refined data for constant collision relaxation [14], probabilities for spontaneous radiational transition 001-100 to CO_2 and the widths of the lines for a shock mechanism of widening [15] were used.

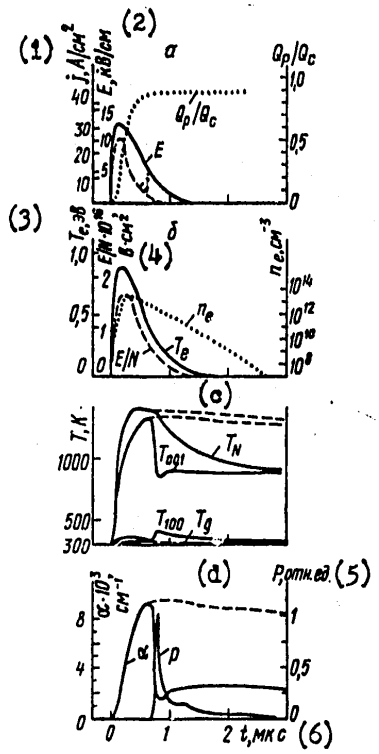

Fig. 4. Typical time characteristics of discharge (a), active medium (b) and laser radiation for mixture CO_2:N_2:He=1:2:13; pressure p=3 atmospheres at Q_c= 0.13 joules /cm^3. c -- gas temperature T and oscillating temperatures T_g, T_{001}, T_{100} of nitrogen molecules, asymmetric and deformation modes of CO_2 molecules in generation mode (solid lines) and amplification mode (broken line); d -- generation power P and amplification coefficient in generation mode (solid line) and amplification mode (broken line).

Fig. 4 (continued)

1. J, amp/cm^2
2. E, kv/cm
3. T_e, electron volts
4. T_e, electron volts
5. P, relative units
6. t, microseconds

Fig. 4 shows the approximate time relationships E, J, Q_p/Q_0 and E/N obtained on the basis of current and voltage oscillograms and formulas (1). This figure also shows time relationships n_e and T_e obtained on the basis of experimental data and formulas (2) and (4). Using paper [7] and the values of n_e and T_e shown in Fig. 4b, we found the gas and oscillation temperatures, indicators of oscillation and the power of generation. The results of each experiment were processed in this manner.

However, the basic attention in this paper was devoted to studying the effect of the discharge parameters on the energy of the radiation pulse. The greatest radiation energy is obtained at equal partial pressures of N_2 and CO_2. An increase of E_{izl} with pressure is due to two factors: an increase in the energy of Q_p, put into the discharge, and an increase of energies of Q_{N_2} and Q_{001}, put into N_2 oscillations and the asymmetric mode of CO_2. The relationships between pressure and ratios Q_{001}/Q_p, Q_{N_2}/Q_p $(Q_{100}+Q_{010})/Q_p$ $(Q_{100}+Q_{010}$ is the energy used for exciting the symmetrical and the deformation modes of CO_2), as well as the efficiency of laser generation are shown in Fig. 5. The increase of energy, put into oscillations, with pressure is due, in its turn, to an increase in the field intensity N_{max}/N in the area of 1 to 2.75 atmospheres (see Fig. 3), leading to an increase in the velocity of oscillation excitation.

Fig. 6 shows the relationships between the unit energy of laser excitation in the pulse and the unit accumulated energy for mixture CO_2:N_2:He=1:05:6.75 at a total pressure of 3 atmospheres. Here also the theory agrees well with the experiment. It was impossible to reach energy inputs greater than about 0.3 joules/cm^2 because for $Q_0 \approx 0.3$ joules/cm^3 the voltage applied to the capacitors reached values close to the allowed maximum.

A calculation of laser parameters of up to Q_0=4 joules/cm^3 was made to clarify the possibilities of raising E_{izl}. It may be seen from Fig. 6 that maximum energy in the Pulse E_{izl}=0.045 joules/cm^3 is reached at Q_0=1.1 joules/cm^3. A reduction of E_{izl} for a further increase in Q_0 is due to an increase in the population of the lower laser level due to an increase in gas temperature Tg. This leads to an increase in the residual energy of oscillations N_2 and

an asymmetrical mode of CO_2, i.e., to an oscillation energy which cannot be transformed into radiation. Fig. 6 also shows the calculated values of the efficiency and gas temperature 5 microseconds after the start of the pulse current. The reduction in efficiency with a reduction in Q_0 in the area of small Q_0 is due to the approach to the threshold of generation.

Besides energy, investigations were also made of the time characteristics of pulse generation: delay time with respect to the start of the current pulse and the total time τ_r *. Delay time $\Delta\tau$ is equal to the time after which the amplification coefficient becomes equal to losses, because the generation process can start only when they are equal. The relationship between $\Delta\tau$ and energy in storing capacitors is shown in Fig. 6. The reduction of $\Delta\tau$ with an increase in Q_0 in region $Q \lesssim 2$ joules/cm^3 is due to an increase in the amplification coefficient. However, at a further increase in Q_0, due to an increase in the gas temperature, α begins to decrease, which leads to an increase in $\Delta\tau$.

$\Delta\tau$ increases with an increase of N_2 content. This is due to the fact that with an increase in the N_2 content, the total energy that passes from the discharge into the oscillating mode of N_2 molecules increases and, at the same time, the velocity of its passage into the asymmetrical oscillating mode of CO_2 decreases. Because of this, an increase of the unsaturated amplification coefficient occurs more slowly, which leads to a corresponding increase in $\Delta\tau$. Measured and calculated versions of $\Delta\tau$ (p) were found to be small which is due to a reduction in the unsaturated amplification coefficient when the pressure increases.

6. Conclusion

The developed installation described in this paper and the cited theoretical and experimental investigations of laser radiation characteristics confirm, in our opinion, the promise of using a high pressure pulsed laser with $CO_2 + N_2 + He$ mixture triggered by additional wire electrodes.

The feed system used (Marx oscillator) and the installation itself are very simple and permit the obtaining of a stable discharge and laser generation for various compositions of the working mixture within wide intervals of gas pressures (higher than an atmosphere) and energies in the storage capacitors (Q_0=0.067 to 0.29 joules/cm^3).

Laser radiation in the pulse (about 27 mjoules/cm^3) obtained experimentally at p=3 atmospheres and Q_0=0.29 joules/cm^3 is not the maximum possible. The

*Calculated value $\Delta\tau$ depends weakly on the initial effective power W of spontaneous radiation on the laser transition. In our calculations, we used $W \sim 10^{-12}$ W/cm^2.

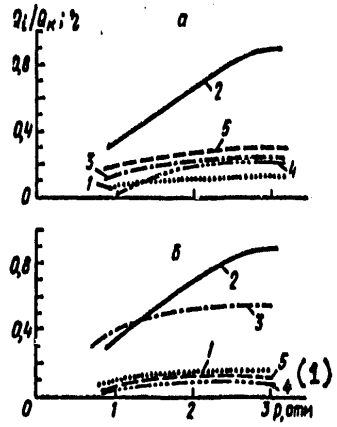

Fig. 5. Calculated relationships between the efficiency of laser generation $\eta = E_{izl}/Q_p$ (1) and ratios Q_p/Q_0 (2), Q_{N_2}/Q_p (3), Q_{001}/Q_p (4) and Q_{010} $Q_{100})$ $/Q_p$ (5) and total gas pressure p(Q_0 =0.13 joules/cm^3) for mixtures CO_2:N_2: He=1:0.25:5.62 (a) and 1:2:13.5 (b).

1. atmospheres

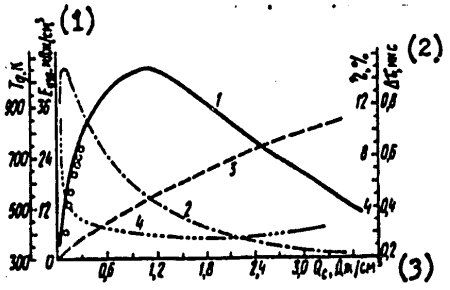

Fig. 6. Relationships between unit output energy of laser radiation E_{izl} (1) efficiency of laser generation $\eta = E_{izl}/Q_p$ (2), gas temperature T_g (3) and delay time $\Delta\tau$ of the generation pulse with respect to the start of the current start (4) and unit stored energy Q_0.

experiment shows the possibility of obtaining a stable discharge at higher p and Q_0, while the calculation shows that it is possible, in this case, to reach a radiation energy in the pulse $\gtrsim$ 50 mjoules/cm^3. A comparison of the theory and the experiment shows also that the theoretical model of kinetic processes in the laser pulse in mixture CO_2+N_2+He we used describes correctly and to a satisfactory accuracy these processes in a wide range of discharge parameter values.

BIBLIOGRAPHY

1. Kosma, B.; Sviridov, A. G. Preprint FIAN, Moscow, 1975, No 160.

2. Hidson, D. J.; Makios, V.; Morrison, R. W. Phys. Letts. 40A, 413 (1972).

3. Blanchard, M.; Gilbert, J.; Rheault, F.; Lachambre, J. L.; Fortin, R; Tremblay, R. J. J. Appl. Phys. 45, 1311 (1974).

4. Alcock, A. J.; Leopole, K.; Richardson, M. S. Appl. Phys. Letts, 23, 562 (1973).

5. Lamberton, H. M.; Pearson, P. R. Elecr. Letts, 141 (1971).

6. Kosma, B.; Sviridov, A. G.; Sobolev, N. N.; Shumskaya, L. I. "Brief Reports on Physics," FIAN, No 11 (1975).

7. Judd, O. P. J. Appl. Phys., 45, 4572 (1974).

8. Gordiyets,B. F.; Kosma, B.; Sviridov, A. G.; Sobolev, N. N. Preprint FIAN, Moscow, 1977 No 205.

9. Schriever, R. L. Appl. Phys. Letts, 20, 354 (1972).

10. Nakanisi, K. "Infrared Spectra and Structure of Organic Compounds." Moscow, MIR, 1965.

11. Sobolev, N. N.; Sokovikov, V. V. "Letters in ZhETF," 4, 363 (1966); 5, 122 (1967).

12. Biryukov, A. S.; Gordiyets,V. F.; ZHURNAL PRIKLADNOY MEKH'ANIKI I TEKHNICHESKOY FIZIKI, No 6, 29 (1972).

13. Gordiyets, B. F.; Sobolev, N. N.' Sokovikov, V. V.; Shelepin, L. A. Phys Letts, A25, 173 (1967).

14. Volkov, A. Yu.; Denin, A. I.; Logunov, A. N.; Kudryavtsev, Ye. M.; Sobolev, N. N. Preprint FIAN, Moscow, 1977, No 4.

15. Biryukov, A. S.; Volkov, A. Yu.; Kudryavtsev, Ye. M.; Serikov, R. I. KVANTOVAYA ELEKTRONIKA 3, 1748 (1976)

2291
CSO: 8144/1033

PHYSICS

UDC 621.378.33

ANALYSIS OF A CALCULATION MODEL OF THE PULSED CHEMICAL DF-CO_2 LASER

Moscow KVANTOVAYA ELEKTRONIKA in Russian Vol 6, No 2, Feb 79 pp 281-287

[Article by V. Ya. Agroskin, B. G. Bravy, G. K. Vasiliyev, V. I. Kiryanov, Institute of Chemical Physics AN USSR (Moscow), submitted 10 Feb 78]

[Text] Computer calculation has been performed of the characteristics of the pulsed chemical DF-CO_2 laser and the results have been compared with experimental data. Separate descriptions of the kinetics of the chemical reaction and laser action have been incorporated into the model. A correlation has been performed with the results of calculations obtained by other authors. The analysis demonstrates that existing models do not achieve satisfactory agreement with the experiment. The probable causes of the discrepancy are considered.

1. Introduction

Until now, a number of papers [1-4] have been written dedicated to the calculations of the pulse characteristics of a chemical DF-CO_2 laser with transfer of oscillation-excited energy in a chemical reaction from molecule DF to molecule CO_2, in which laser action occurs in band $00^01\text{-}10^00$ (λ=10.6 microns). In all papers, the analysis was made for mixture D_2-F_2-CO_2-O_2-(He), initiated by a pulsed gas-discharge tube (only in [2] was the initiation assumed to be instantaneous). In spite of the agreement noted between calculated and experimental values in them, it is impossible not to pay attention to certain special features of these calculations. Thus, in [3], the constant of the transmission velocity of oscillating energy from the DF molecule to the CO_2 molecule was assumed to be 3×10^{-13} cm^3/sec, which is considerably lower than the value determined later.

To obtain an agreement with the experiment, the author of [3] assumed the constant of velocity attenuation of DF by DF to be lower than the value known at present [8]. In paper [4], the numerical agreement with the experiment was obtained by increasing the experimentally obtained energy removal by 2.5 times, which the authors related to the single-mode operation of the laser.

We will note that in all the calculations made, a faster exchange was assumed between the laser level and the deformation mode ($k \sim 10^{-11}$ cm^3/sec [9]). However, there is a number of papers [10-17, 51] in which the velocity constant of this process is at least an order of magnitude lower (the spread can be even about two orders of magnitude). We will note that the precise value of this constant is unknown at present [50]. Nevertheless, for mixtures strongly (greater than 20 times) diluted by an inert gas, at low full pressure ($\lesssim$0.3 atmospheres) the indeterminacy of the value of this constant, apparently, is not essential, which is attested to by good (with the exception of the near-threshold area) qualitative and quantitative agreement between the calculation and the experiment in [1]. However, such mixtures, from the standpoint of efficient transformation of the chemical reaction energy to generation, do not have great interest.

It was considered necessary to make a calculation taking into account the latest data on relaxation and kinetic processes and compare it to the results of the latest experimental work. At the basis of the model considered in this paper, unlike the one proposed earlier, lies a parametric calculation of the chemical reaction kinetics [18] with a subsequent calculation of the characteristics of generation and oscillation relaxation on a computer. Thereby, as in experiment [19], we fixed the mode of the chemical reaction progress. In this way we also achieved considerable simplification of the computer program. Moreover, we varied the value of the constant of the lower laser level with a deformation mode. The aim was to achieve an understanding of the rules for the saturation of energy removal obtained in the experiment depending upon the initiation in some compositions, the lack of saturation in others and an S-type relationship for still others [19], as well as the relationship between energy removal and the CO_2 concentration [19]. We also considered it necessary to compare our calculation with that in [4].

Description of the Model

According to available experimental data [20-26] a photo-initiated chemical reaction in Mixture D_2-F_2-CO_2-O_2-He proceeds according to arrangement:

$$0.\ F_2 \xrightarrow{h\nu} 2F,$$

$$1.\ F + D_2 \rightarrow DF + D,$$
$$2.\ D + F_2 \rightarrow DF + F,$$
$$3.\ D + O_2 + M \rightarrow DO_2 + M,$$
$$4.\ D + DO_2 \rightarrow \begin{cases} D_2 + O_2 \\ 2OD \\ D_2O + O \end{cases}$$
$$5.\ F + O_2 + M \rightarrow FO_2 + M,$$
$$6.\ F + FO_2 + M \rightarrow F_2O_2 + M,$$
$$7.\ F + FO_2 \rightarrow F_2 + O_2,$$

where M is any molecule. The table shows the respective velocity constants. The efficiencies of molecules He, D_2, F_2, O_2, CO_2 and DF in trimolecular processes of breaks 3, 5, 6 are assumed equal respectively to 1; 2; 1; 1 [24, 22,26]; 4.5 [22] and 7 [27]. Velocity constants of processes 3-7 are assumed to be independent of the temperature [22-25].

The calculation utilized the initial condition at which, from our point of view, the most important experimental characteristics of the chemical reaction and generation [19] were obtained. The composition of the mixture was 5% D_2+5, 30% F_2+2, 80% CO_2+0.5; 1.6% O_2+He; the initial temperature $T \approx 300K$ and pressure p_0=1 atmosphere; the degree of dissociation of molecules F_2 during the entire initiation pulse α = 0 to 5%.

(1)

Процесс	T, K	k	(2) Размерность (4)	(3) Литература
1	300—2000	$1.5 \cdot 10^{-10} \exp(-1600/RT)$	см³/с	[20]
2	300—560	$1.5 \cdot 10^{-10} \exp(-2400/RT)$	см³/с	[21,22]
3	300	$2 \cdot 10^{-32}$, M=He	см⁶/с	[22—24]
4	300	$\sim 1 \cdot 10^{-10}$	см³/с	[22]
5	300	$0{,}8 \cdot 10^{-32}$, M=He	см⁶/с	[25,26]
6	300	$0{,}9 \cdot 10^{-31}$, M=Ar	см⁶/с	[25]
7	300	$< 2 \cdot 10^{-13}$	см³/с	[25]

1. Process
2. Dimension
3. Literature
4. cm^3/sec.

We will consider the role of the secondary processes of breaks in the chain of the generation stage when the basic share of energy radiation is removed, i.e., when the mixture temperature is still not too high (< 800K). It can easily be shown that process 7 can be neglected, since for $p \sim 1$ atmosphere its velocity is smaller by an order of magnitude than the velocity of process 6, Under the conditions of the experiment, contributions of primary process of breaks 3 and 5 are commensurate. In this case, as shown by evaluations, the role of the break process of chain 4, secondary with respect to process 3, although it must be considered, is nevertheless comparatively small. In such a case, the role of process 6 compared to 5 is still more insignificant, inasmuch as when it is reduced to a bimolecular constant its velocities at $p \approx 1$ atmosphere are only 2×10^{-12} cm^3/sec, which is about two orders of magnitude smaller than the corresponding value for process 4. For this reason, the contribution of process 6 can also be neglected. Naturally, for T > 800K, to describe the kinetics of the chemical reaction, it is necessary to take into account the processes of thermal dissociation of molecules F_2, as well asprocesses with the participation of OD and D_2O, whose role has still not

been studied enough as yet. However, for the purposes of this investigation this is not necessary and in the calculation we will only take into account processes 0-5*.

As shown by analysis, the kinetics of the photo-initiated reaction in a DF-CO_2 laser may be determined, as in an NF laser [18], by nondimensional parameters Δ, δ and up to a temperature of $T-T_0 \sim 800K$, taking into account the burning out of the mixture, by equations:

$$\frac{d\theta}{d\tau} = \frac{\Delta\delta\xi\eta}{1+\mu}\left(1-\frac{\gamma\theta}{\eta}\right)\exp\left[\theta/\left(1+\frac{RT_0}{E_2}\theta\right)\right],$$
$$\frac{d\xi}{d\tau} = \left(1-\frac{\gamma\theta}{\eta}\right)I(\tau) - \frac{\delta\xi}{1+\mu}\left(1+\mu\frac{k_3}{k_2}+\frac{k_4}{k_2^0}\Delta\gamma\zeta\right), \qquad (1)$$
$$\frac{d\zeta}{d\tau} = \frac{\delta\xi}{1+\mu}\left(1-\frac{k_4}{k_2^0}\Delta\gamma\zeta\right),$$

where

$$\Delta = \frac{4k_2^0(F_2^0)^2 q\alpha E_2}{c_v MRT_0^2 O_2^0 \sum_i k_{2i}M_i}; \qquad \delta = \omega^{-1}O_2^0\sum_i k_{2i}M_i;$$

$\theta=(T-T_0)E_2/RT_0^2$) -- relative heating of the mixture; $\xi=(D+F)/2\alpha F_2^0$, $\zeta=(DO_2)/2\alpha F_2^0$ -- nondimensional concentrations of atoms DF and radicals DO_2 respectively; $\tau=\omega t$ -- nondimensional time; ω^{-1} -- characteristic time of the initiating pulse; $\mu=F/D=K_2F_2/(k_1D_2)$ -- ratio of concentrations of of atoms F and D, $\gamma^{-1}=2_q E_2 F_2^0/(C_v MRT_0^2)$ -- nondimensional adiabatic temperature of the mixture; k_i^0, k_i -- velocity of constants of the i-th process at temperatures To and T respectively; D_2, F_2, M_i -- current concentrations of molecules; $M=\sum_i M_i$ -- total concentration of mixture; q -- thermal effect

*It should be noted that for a more than two-fold excess above the break threshold [49] it is possible to limit oneself only with 0-3,5 and even 0-3 (see, for example, [18].

of reaction; η -- share of reaction energy transformed into heat; R -- gas constant; E_i -- activation energy of the i-th process; c_v -- average specific heat of the mixture; $I(\tau)$ -- normalized form of the initiating pulse.

It is possible to obtain relationship $\beta(\tau)$ from (1) and the law for accumulating DF molecules with time. As shown by calculation this law approximates with good precision the relation $DF \sim \exp \Omega t$ practically to full burning out. The relationship obtained between Ω and initial values of Δ, δ has the same form as in [18]. We will note that if Δ and δ are considered constant in the course of the reaction, the value of Ω will differ by not more than 3%.

The calculation was made for the form of the initiating pulse nearest to the experimental [19]:

$$I(\tau) = \begin{cases} \beta_1 \tau^2, & 0 < \tau \leqslant \tau_m \\ \beta_2 \exp(-\tau), & \tau_m \leqslant \tau < \infty, \end{cases}$$

where β_1, β_2 -- constants; τ_m -- time for reaching the maximum pulse intensity.

We will now consider the models for the generation and relaxation processes (Fig. 1), considering that the reaction is developing according to the exponential law. The migration of energy from the oscillation-excited DF molecules in the course of the reaction occurs in accordance with arrangement:

8. $DF(v) + M \rightarrow DF(v-1) + M$,
9. $DF(1) + CO_2(00^00) \rightleftarrows DF(0) + CO_2(00^01)$,
10. $CO_2(00^01) + M \rightarrow CO_2(nm^l0) + M$,
11. $CO_2(00^01) + h\nu \rightarrow CO_2(10^00) + 2h\nu$,
12. $CO_2(10^00) + CO_2(00^00) \rightleftarrows CO_2(00^00) + CO_2(02^00)$,
13. $CO_2(02^00) + M \rightleftarrows CO_2(0m^l0) + M$,
14. $CO_2(01^10) + M \rightarrow CO_2(00^00) + M$.

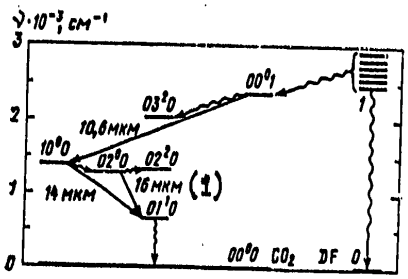

Fig. 1. Energy arrangement of levels and transitions between them for DF and CO_2 molecules ($03^{1}0$ should be read instead of $03^{2}0$).

1. microns

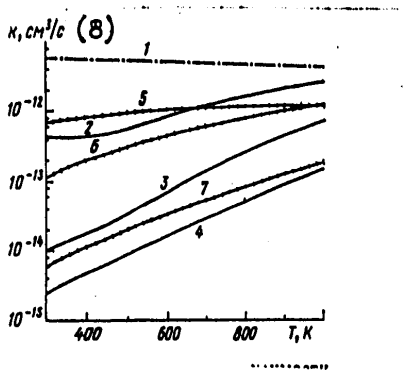

Fig. 2. Temperature dependence of the velocity constant. k_g(1) [5-7]; k_{10} for DF (2) [7,8]; CO_2 (3) [37-39] and He (4) [40,41]; k_{14} for D_2 (5) [42]; He (6) and CO_2 (7) [42,44].

8. cm^3/sec.

Here, 8 -- process of deactivation of the oscillation-excited DF molecule; 9 -- process of energy exchange between DF and CO_2 molecules; 10 -- deactivation of the upper laser level; 11 -- process of generation; 12 -- VV-exchange between Fermi resonance levels $10^0 0$-$02^0 0$; 13 -- exchange between Fermi-levels and the deformation mode; 14 -- process of VT-relaxation of the deformation mode. Inasmuch as in the entire interval of temperatures for all compositions of the mixture used [19] the process velocity 8 is smaller by an order of magnitude than the velocity of process 9, we will neglect it. Einstein's coefficient and shock half-widths for process 11 are taken from [28-30]. Process 12 is assumed to be rapid ($k_{12} \sim 11^{-11}$ cm^3/sec [31, 52]). The velocity constant of process 13 was varied within 10^{-13} to 11^{-11} in accordance with data [10-17, 51]. Temperature dependences of velocity constants of processes 9, 10, 14 are shown in Fig. 2. Temperature dependence of k_{10} for D_2 [32-35] at $T \gtrsim 300K$ is taken similar to CO_2. The value of k_{10} for F_2 is assumed constant and equal to 6×10^{-14} cm^3/sec. The process of the VT-relaxation of the deformation mode on molecules F_2 and DF was not taken into account (data for it is lacking). Also neglected were all relaxation processes with the participation of atoms.

In the calculated model, there were considered levels $00^0 0$, $00^0 1$, $10^0 0$, $02^0 0$ and all levels of the deformation mode for which Boltzman's distribution with temperature, different from the temperature of the medium and determined by the totality of all relaxation processes, was assumed. VV-exchange between DF and CO_2 molecules was considered in the approximation of a harmonic oscillator. The distribution of CO_2 molecules along the rotation levels was considered in equilibrium with temperature, equal to the temperature of the medium. Only the oscillation-rotation transition P_{20} of the $00^0 1$-$10^0 0$ band was considered in generation, inasmuch as, according to experimental data [19], practically all generation energy (70 to 80%) is liberated in it. It was assumed that the working modes of the resonator fill the volume of the active medium entirely because the experimentally measured divergence of the laser was about 15'. The length of the active zone was taken as 0.9 meters, of the resonator -- 2 meters and the reflecting surfaces of the meters -- 0.85 and 0.3 [19]. Volume losses in the active medium with a constant absorption coefficient 7×10^{-4} cm^{-1} [45] were taken into account. Diffraction losses were neglected. The power of laser radiation was calculated according to velocity equations.

Comparison of Calculated and Experimental Data

Fig. 3 shows the calculation results of the energy output of a laser depending upon the initial CO_2 concentration in the mixture with the variation of the velocity constant of the process 13. In the calculation, as in experiment [19], the mode of the reaction process was recorded (Ω=const). The calculation, as may be seen from the figure, shows that the best qualitative

agreement with the experiment is observed only at very high values of k_{13} ($\sim 10^{-11}$ cm^3/sec); the energy output increases monotonically with the increase in CO_2 concentration to about 20-30% and then practically does not change up to the full replacement of CO_2 by helium. A better quantitative agreement is obtained at low values of k_{13} ($\sim 10^{-13}$ cm^3/sec).

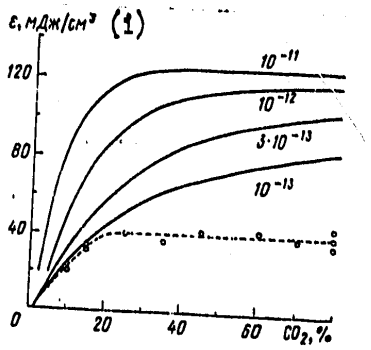

Fig. 3. Calculated relationships between unit energy output of the laser and the CO_2 concentration in the mixture for $\Omega = 1.4 \times 10^6$ sec^{-1} for indicated values of k_{13} and experimental data [19]

1. mjoules/cm^3

The relationship between energy output and the degree of dissociation of F_2 molecules in various composition mixtures is shown in Fig. 4. It may be seen that all relationships have thresholds and saturation (or trend to saturation) at $\alpha \sim 1\%$, which agrees qualitatively with the experiment. Mixture $10\%D_2 + 30\%F_2 + 59\%CO_2 + 1\%O_2$ is an exception for which there is not even qualitative agreement. A reduction in k_{13} to 3×10^{-13} cm^3/sec for a standard composition mixture ($5\%D_2 + 15\%F_2 + 25\%CO_2 + 1\%O_2 + 54\%$ He) leads to a better quantitative agreement, nevertheless, calculated values of energy output in this case are 1.5 to 2 times higher than the experimental. For a mixture $5\%D_2 + 15\%F_2 + 79.4\%CO_2 + 0.6\%O_2$, this excess is 2 to 3 times. A noticeable discrepancy between calculated and experimental data prompted us to compare the results of the quantitative analysis with published data for equal initial conditions. A calculation was made for this purpose of the relationship obtained in [4] between energy output from the F_2 content in the mixture

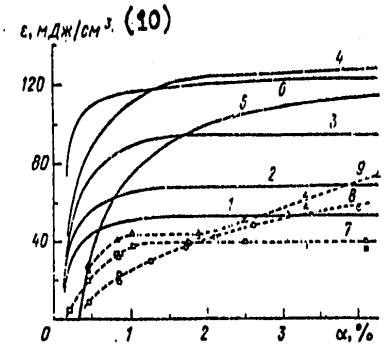

Fig. 4. Calculated values of unit energy output of laser and the degree of dissociation of F_2 molecules in a mixture of standard composition for $k_{13}=10^{-13}$(1); 3×10^{-13} (2); 10^{-12} (3) and $10^{-11}cm^3/sec$ (4) and in mixtures $5\%D_2+15\%F_2+59.4\%CO_2+0.6\%O_2$ (5), $10\%D_2+30\%F_2+59\%CO_2+1\%O_2$ (6); for $k_{13}=3\times10^{-13}cm^3/sec$, as well as experimental relationships for standard composition mixture (7) and mixtures 5 (8) and 6 (9) [19].

10. mjoules/cm^3

and full pressure. The value of K_{13} was assumed to be high ($\sim 10^{-11}cm^3/sec$) as if [4]. The comparison of results (Fig. 5) shows an entirely satisfactory agreement between our calculation and calculation [4], which shows the adequacy of both calculation models.

Discussion of Results

Based on the cited model, we will consider certain characteristic features of the calculated relationships obtained. Thus, the effect of $\varepsilon(\alpha)$ saturation may be explained by the fact that the moment of break in generation is due basically to the competition between the velocity of the chemical pumping up of the upper laser level, proportional [DF], and the velocity of its relaxation, proportional to exp [DF]. This competition depends only on the temperature of the mixture which, at the moment of the break of generation according to calculations, is about 900K and does not depend on α. This and all previous models do not explain the lack of saturation (S-shaped relationship in Fig. 4). Moreover, it also does not explain the relatively low temperatures of the experiment at $\alpha \lesssim 1\%$ [19]. Therefore, probably, the absolute values of calculated energy outputs are so high.

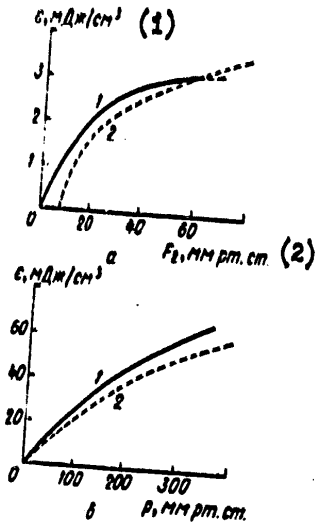

Fig. 5. Calculated relationships between unit energy outputs of a laser for α =0.15% and O_2/F_2=0.05 and the F_2 content in a mixture of composition of 10 mm of the mercury column of $D_2 + F_2$ + 60 mm of mercury column of CO_2 (a) and full pressure of a mixture of composition 10%D_2 + 30%F_2 + 60%CO_2 (b), (1[4], 2 -- this paper).

1. mjoules/cm^2

2. mm of mercury column

Calculations showed that absolute values of energy outputs depend strongly on values of k_{13}, with a better approximation to experimental values of energy outputs obtained at $k_{13} \sim 10^{-12}$-10^{-13} cm^3/sec and not 10^{-11}/cm^{3}sec as assumed in [1-4]. In favor of smaller values of this constant besides data [10-14, 16, 17], is also the fact of obtaining generation at transitions 10^01 - 01^10 (λ =14 microns) and 02^0 - 01^10 ($\lambda \approx$16 microns) [46, 47].

The general conclusion, to which an analysis of the obtained calculated values leads, may be formulated as follows. All models existing at present, including ours, although they are able to explain certain qualitative rules

for the behavior of a DF-CO_2 laser characteristic do not, as a whole, agree quantitatively with the experiment and do not explain certain qualitative patterns, for example the S-shaped relationship of ε (α) [19]. This may be due to the inaccuracy of several relaxation constants, in particular, k_{13}, k_{14} and partly k_{10} (for example relaxation $CO_2(00^01)$ on oscillation-excited DF^* molecules). Thus, if it is assumed that for DF^* $k_{10} \sim 10^{-11}$ cm^3/sec, then calculated relationship $\varepsilon(\alpha)$ for a standard mixture also coincides with the experimental quantitatively.

It is not ruled out that higher volumetric losses occur in a laser, depending on temperature in a complex manner. The divergence may also be due to the imperfection of the kinetic model. For example, the model does not take into account the chemical reaction between F_2 and CO_2 mentioned in [19] and whose role is still not clear enough. It is not ruled out that molecule COF_2 is formed in the course of this reaction as an intermediate product, which has a large absorption coefficient in the region of 10.6 microns ($\sim$0.01 cm^{-1} mm of the mercury column^{-1} [53]). Evaluations show that 1 to 2 mm of mercury column COF_2 can reduce the energy output of the laser by 2 to 3 times. To produce this amount of COF_2, for example, it is necessary to have, in the reaction of the fluorine with oscillation-excited CO_2 molecules, a value of effective velocity constant $\sim 10^{-14}$ cm^3/sec, which does not appear possible. The S-shaped nature of the relationship between the energy output of the laser and the initiation, which occurs for several mixtures, may be due to kinetic special features of accumulation and consumption of COF_2 in the course of the reaction, or the clearing of COF_2 at the laser transition for a sufficiently high density of generation power. It is possible that this reaction also makes a contribution to the generation energy.

Generally speaking, the high unit energy outputs ($\sim$0.1 joules/cm^3), obtained in the calculations, appear to be attainable, but at higher initiations or greater content of F_2 and CO_2 in the mixture, indicated by experimental results [19, 48].

BIBLIOGRAPHY

1. Pochler, T. O.; Pirkle, J. C.; Walker, R. E. IEEE J. QE-9, 83 (1973).

2. Kerber, R. L.; Cohen, N. IEEE J. QE-9, 94 (1973).

3. Igoshin, V. I. Trudy FIAN, 76, 117 (1974).

4. Kulakov, L. V.; Nikitin, A. I., Orayevskiy, A. N. KVANTOVAYA ELEKTRONIKA, 3, 1677 (1976).

5. Bott, J. F.; Cohen, N. J. Chem Phys.,59, 447 (1973).

6. Lucht, R. A.; Cool, T. A. J. Chem. Phys. 60, 1026 (1974).

7. Hinchen, J. J.; Hobbs, R. N. J. Chem Phys., 63, 353 (1975)

8. Lucht, R. A.; Cool, T. A., J. Chem. Phys. 63, 3962 (1975).

9. Rhodes, C. K.; Kelly, M. J.;Javan, A. J. Chem. Phys. 48, 5730 (1962)

10. Marriott, R. Proc. Phys. Soc., 84, 877 (1964).

11. Bridges, T. J. Appl. Phys. Letts, 9, 174 (1966).

12. Cheo, P. K. Appl. Phys., 38, 3563 (1967).

13. Brzhazovskiy, Yu. V.; Vasilenko, L. S.; Chebotayev, V. P. ZhETF, 55, 2095 (1968).

14. Carbone, R. J.; Witteman, W. J. IEEE J QE-5 442 (1969).

15. Rosser, V. A.; Hoag, E.; Gerry, E. T. J. Chem. Phys., 57, 4153 (1972).

16. Bulthuis, K.; Ponsen, G. J. Chem. Phys. Letts, 21, 415 (1973).

17. Garside, B. K.; Reid, J.; Ballik, E. A. IEEE J. QE-11, 264; 583, (1975).

18. Agroskin, V. Ya.; Vasil'yev, G. K.; Kir'yanov, V. I.; Tal'roze, V. L. KVANTOVAYA ELEKTRONIKA, 3, 1932 (1976).

19. Agroskin, V. Ya.; Vasil'yev, G. K., Kir'yanov, V. I.; Tal'roze, V. L. KVANTOVAYA ELEKTRONIKA, 5, 2436 (1978).

20. Jones W. E.; MacKnight, S. D.; Teng, L. Chem. Rev., 73, 407 (1973).

21. Jones, W. E.; Skolnik, E. G. Chem. Rev., 76, 563 (1975).

22. Vasil'yev, G. K.; Makarov, Ye. F.; Chernyshev, Yu. A. KINETIKA I KATALIZ, 2, 320 (1975).

23. Kurylo, M. J. J. Phys. Chem., 76, 3518 (1972)

24. Kondrat'yev, V. N. "Velocity Constants of Gas-Phase Reactions. Moscow "Nauka,"

25. Chegodayev, P. P. Candidate's Dissertation NIFKhI imeni L. Y. Karpov, Moscow, 1974.

26. Arutyunov, V. S.' Popov, L. S.' Chaykin, A. M. "Kinetics and Catalysis," 17, 292 (1976).

27. Kapralova, G.A.; Margolina, Ye. M.; Chaykin, A. M. "Kinetics and Catalysis," 17, 292 (1976).

28. Holtz, D. F.,; Ferrer, J. N. J. Appl. Phys., 39, 1797 (1968).

29. Lachambre, J. L.; Gilbert, J.; Rheault, F.; Fortin, R.; Blanchard, M. IEEE J QE-9, 459 (1973).

30. Biryukov, A. S.; Volkov, A. Yu.; Kudryavtsev, Ye. M.; Serikov, R. I. KVANTOVAYA ELEKTRONIDA, 3, 1748 (1976).

31. Stark, E. E.; Appl. Phys. Letts, 23, 335 (1973).

32. Moore, C. B.; Wood, R. E.; Hu, B. L.' Yardly, J. T. J. Chem. Phys., 46, 4222 (1967)

33. Stephenson, J. C.; Wood, R. E.; Moore, C. B. J. Chem. Phys. 54, 3097 (1971).

34. Stephenson, J. C.; Moore, C. B. J. Chem. Phys. 56, 1295 (1972).

35. Tsuchiya, S.; Inoue, G.' Takahaski, Y. J. Phys. Soc. Japan, 41, 2072 (1976).

36. Agroskin, V. Ya.; Vasil'yev, G. K.; Kir'yanov, V. I. "High Energy Chemistry," 8, 283 (1974).

37. Rosser, W. A.; Wood, A. D.; Gerry, E. T. J. Chem. Phys., 50, 4996 (1969)

38. Stephenson, J. C.; Moore, C. B. J. Chem. Phys., 52, 2333 (1970).

39. Rao, I. V.; Rao, V. S. Chem. Phys. Letts, 17, 531 (1972).

40. Rosser, W. A.; Gerry, E. T. J. Chem. Phys., 51, 2286 (1969).

41. Stephenson, J. C.; Wood, A. D.; Moore, C. B. J. Chem. Phys., 54, 3097 (1971).

42. Simpson, C. J.; Chandler, T. Proc. Roy. Soc. 317A, 265 (1970).

43. Taylor, R. L.; Bitterman, S. Rev. Mod. Phys., 41, 26 (1969).

44. Kerber, R. L.; Cohen, N.; Emanuel, G. IEEE J. QE-9, 94 (1973).

45. Kulakov, L. V. Candidate's Dissertation, FIAN, Moscow, 1974.

46. Osgood, R. M. Appl. Phys. Letts, 28, 342 (1976).

47. Kasner, W. H.; Pleasance, L. D. Appl. Phys. Letts, 31, 82 (1977).

48. Basov, N. G.; Bashkin, A. S.; Grigor'yev, P. G.; Orayefskiy, A. N.; Porodnikov, O. Ye. KVANTOVAYA ELEKTRONIKA, 3, 2067 (1976).

49. Vasil'yev, G. K.; Makarov, Ye. F.; Chernyshev, Yu. A. "Physics of Combustion and Explosion," 15, N3 (1979).

50. Losev, S. A. "physics of Combustion and Explosion," 12, 163 (1976).

51. Shved, G. M. "Optics and Spectroscopy," 41, 882 (1976).

52. Jacobs, R. R.; Pettipiece, K. J.; Thomas, S. J. Phys. Rev., A 11, 54 (1975).

53. Casleton, K. H.; Flynn, G. W. J. Chem. Phys., 63, 3133 (1977).

2291
CSO: 8144/1033

PHYSICS

UDC 621.373.826.038.823

SATURATION IN WAVEGUIDE CO_2 LASERS

Moscow KVANTOVAYA ELEKTRONIKA in Russian Vol 6, No 2, Feb 79 pp 288-294

[Article by V. V. Grigor'yants, B. A. Kuzyakov, A. M. Sinitsyn, Institute of Radioelectronics AN USSR (Moscow), submitted 16 Feb 78]

[Text] A dependence is studied theoretically of the CO_2 waveguide laser active medium gain on the local radiation density in the active volume; a dependence is considered of the saturation parameter on the pressure, pumping current density and laser tube internal diameter. For two compositions of the CO_2-N_2-He mixture, an experimental dependence has been derived of the saturation parameter on the pressure and a comparison has been made of the theoretical and experimental results.

Introduction

Waveguide CO_2 lasers (CO_2-VL) and amplifiers are distinguished by high values of radiation intensity in the active volume. Here stimulated transition plays a noticeable role in evacuating the upper laser level, which it is necessary to take into account in calculating such parameters of the CO_2-VL as population of the CO_2 working levels, the gain, the maximum radiation power etc. Therefore, the investigation of the saturation effects of the CO_2-VL is of great interest.

Experimental investigations [1-5] indicated that the saturation parameter I_s in CO_2-VL (the intensity of radiation at which the gain is halved as compared to the gain of a weak signal) exceeds by about an order of magnitude the saturation of the usual electric discharge CO_2 lasers [6, 7].

This is explained by a considerable difference between the basic working parameters of CO_2-VL (pressure, density of current pumping etc.) and the parameters of a low pressure CO_2 laser.

A comparison of theoretical evaluations of saturation with experimental data for the usual CO_2 lasers indicated [6] that the correct evaluation of I_s requires the taking into account of the diffusion of excited molecules and the shape of the intensity of radiation which passes through the active volume. Moreover, it is necessary to keep in mind that the working system based on CO_2 has a great number of levels [6].

At present, the CO_2-VL investigated in the greatest detail are the ones with a cylindrical waveguide tube, with a working mixture (as a rule, CO_2-N_2-He) which is excited by a longitudinal electric discharge. This paper is dedicated to the investigation of the effects of interaction between the radiation field and the active medium of the waveguide laser of the indicated type. The parameters of the active medium are found by solving a system of kinetic equations for the working levels of CO_2 [6,7], while the radiation field is characterized by the value and shape of local radiation intensity I(r) without specifying methods for obtaining it. Therefore, where this is not specifically indicated, the obtained results are true for the active media of the waveguide laser, as well as for the amplifier.

This paper theoretically investigates the dependence of the gain of the working medium of CO_2-VL on the radiation density in the active volume and considers the dependence of the saturation parameter on the pressure, density of pumping current and the radius of the discharge tube. Moreover, an experimental dependence was obtained of the saturation parameter on pressure for two compositions of the CO_2-N_2-He mixture and a comparison was made of the theoretical and experimental data.

1. Populations of Laser Levels

The populations of CO_2-VL working levels are determined from the system of kinetic equations written for levels 10^00 and 00^01 of CO_2 molecules and the level v=1 of the N_2 molecule [8, 9], taking into account the diffusion of

excited CO_2 and N_2 molecules to the walls and deactivating on them [10]. It may be considered that in a cylindrical laser tube, the radial density distribution of electrons of the discharge n_e is described by Bessel's function of the zero order, i.e., $n_e \sim (2.4r/R)$, where R is the inner radius of the tube; r is the distance from its axis.

Then, in cylindrical coordinates, for the case of stationary molecule distribution along the working levels, it is possible to obtain a partial solution of the kinetic equations system. Then populations n_2 of the upper and n_1 of the lower laser levels may be expressed by Bessel functions of the zero order:

$$n_2 = \sum_{i=1}^{3} H_i I_0(\sqrt{\lambda_i}\, r) + E J_0\left(\frac{2.4r}{R}\right); \qquad (1)$$

$$n_1 = \sum_{i=1}^{3} F_i I_0(\sqrt{\lambda_i}\, r) + G J_0\left(\frac{2.4r}{R}\right), \qquad (2)$$

where $I_0(\sqrt{\lambda_i}\, r)$ are modified Bessel functions; λ_i -- roots of the characteristic cubic equation; H_i and F_i -- coefficients determined from boundary conditions. We will assume that at the gas-wall boundary of the tube

$$n_1(R) = 0; \quad n_2(R) = 0, \qquad (3)$$

and the velocity of the deactivation of excited molecules $CO_2(00^01)$ on the wall may be written in the form

$$\int_S q\,dS = \int_V [A^+ - k_2 n_2 - W(f_2 n_2 - f_1 n_1)]\, dV, \qquad (4)$$

where q -- a stream of quanta of excitations of the upper laser level through the boundary; A^+ -- excitation velocity of the working mixture;

S and V -- area of the inner surface and the internal volume of the laser tube; k_2 -- deactivation velocity of the upper laser level; W -- probability of induced transitions; f_1 and f_2 portions of particles populating levels nm0 and 00v, which are respectively in levels 10^00 and 00^01. It is easy from (1) and (4) to determine coefficients G, E, F_i and H_i (i=1-3). They all depend on the parameters of the working mixture, dimensions of the laser tube, excitation conditions etc.

In this paper, values of basic parameters are used in calculations typical for the first CO_2-VL [1-5]. It is assumed that a laser tube with an inner diameter of about 1 mm and external diameter of $2R_1 \sim 3$ mm, made of quartz or BeO and cooled with water with T_0=290K, is filled with a three-component mixture CO_2-N_2-He. The excitation of the working medium is done by a longitudinal electric discharge. In calculations, the value of the excitation velocity of the working mixture were used, obtained in [11], and data on the velocity of collision deactivation of the excited molecules at various values of the working medium temperature from [12-13].

Temperature distribution over the cross section of the tube is described by formula [14]

$$T = \sqrt{0{,}235\left(\frac{\pi R^2 Q}{A}\right) J_0\left(\frac{2{,}4r}{R}\right) + (T_0 + \Delta T)^2}, \qquad (5)$$

where Q -- unit power of pumping; A -- coefficient of linear dependence of thermal conductivity of the gas mixture on temperature;

$$\Delta T = (R^2 Q / 2k_{TP}) \ln(R_1/R)$$

is the temperature difference on the wall of the tube; k_Tp -- thermal conductivity coefficient of the tube material.

In this paper we will be interested in the effect of laser radiation intensity on the basic parameters of CO_2-VL. The probability of the induced transitions inside the laser tube may be written in the form [15]

$$W = A_{21}c^2F_J I/32\pi^2 h\nu^3\Delta\nu, \qquad (6)$$

where I -- density of laser radiation in the cuvette; F_J -- portion of the molecules of oscillation level $00^0 1$ in rotation level J of the upper level of laser transition; $\Delta\nu$ -- width of CO_2 radiation line.

We will assume that oscillation occurs at optimal transition

$$(J = \sqrt{kT/2hcB} - 1/2)$$

and the number of equivalent rotation levels of CO_2-VL participating in the oscillation is the same as in the usual electric discharge CO_2 laser [6]. Then in the MKS system of units

$$W = 1{,}35 \cdot 10^{-3} I/(\delta_C + 0{,}73\delta_N + 0{,}6\delta_{He})p, \qquad (7)$$

where $\delta_C, \delta_N, \delta_{He}$ -- mole ratios of CO_2, N_2 and He in the working mixture; p -- its pressure. In the general case the probability of induced transitions in CO_2-VL has the form

$$W = \frac{3{,}54 \cdot 10^3 (2J+1) \exp[-(hcB/kT) J(J+1)]}{(\delta_C + 0{,}73\delta_N + 0{,}6\delta_{He})\, p \sqrt{T}}. \qquad (8)$$

Using the cited formulas and data [10-13] on the BESM-6 computer, basic characteristics of the CO_2-VL were calculated.

2. Gain

Using the well known expression for the gain of a CO_2 laser and taking into accountthe Lorentz widening of the radiation line at working pressures typical for CO_2-VL, it is possible to write a calculation formula for the

gain in the center of radiation for a wavelength of 10.6 microns:

$$K=2{,}92\cdot10^{-19}(n_2-n_1)/(\delta_C+0{,}73\delta_N+0{,}66\delta_H)p. \qquad (9)$$

In this formula, unlike in expression (4) of [16], the population of the lower laser level n_1 is taken into account. In the general case, the gain is a function of the local intensity of radiation I and the coordinates. We will note that even at zero intensity of I, the value and radial distribution of density of the stock and gain, as also in the usual electric-discharge CO_2 lasers [17], may change within wide limits depending upon the excitation conditions, composition and pressure of the working mixture, laser tube parameters etc.

Figure 1 shows the radial distribution and the gain for various values of pumping current density J_H and local radiation intensity.

At low densities of pumping current and electrons in the discharge, increases in J_H lead to increases in K. It reaches a maximum on the axis of the laser tube, where the density of discharge electrons is maximum (curves 1, 2). A further increase in J_H leads to a strong heating of the mixture on the axis and equalizing K(r) over the cross section (curve 3). At high pumping current density the maximum of K(r) is reached at a certain distance from the tube axis and a characteristic dip occurs at the axis, due to a temperature increase in the deactivation velocity (curve 4).

When laser radiation is present in the waveguide, there is a reduction in value and a change in the shape of the radial distribution of the gain in the active medium. Curves 5-11 in Fig. 1 were calculated on the assumption of a uniform distribution of radiation intensity over the cross section of the waveguide tube and give a qualitative concept on possible versions of distribution K(r). We will note that in actual laser waveguides the value of intensity and the shape of the passing beam are functions of the

coordinates, therefore, the picture shown in Fig. 1 will, generally speaking, change.

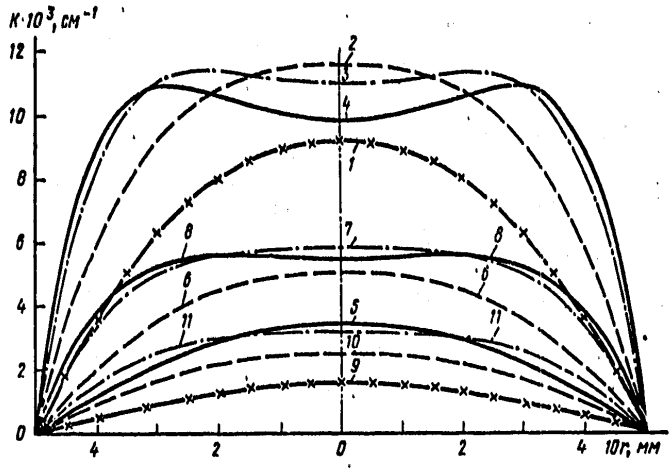

Fig. 1. Radial distribution of the amplification coefficient [Gain] of the working mixture CO_2:N_2:He=1:1:8 in a quartz waveguide tube for values of local intensity of laser radiation I=0(1-4), 1(5-8 and 2 kw/cm^2 (9-11) and density of pumping current J=50 (1, 5, 9), 100 (2, 6, 10), 200 (3, 7, 11) and 250 ma/cm^2 (4, 8) at R=0.5 mm, R_1=1.5 mm p=70 mm of the mercury column, T_o=290K.

We will compare with experimental data the calculated value of the average gain over the cross section of the tube. It may be obtained easily, substituting (1) and (2) into (9) and averaging the obtained expression for corrdinates r, θ :

$$\overline{K} = \frac{2{,}92\cdot 10^{-17}}{(\delta_C + 0{,}73\delta_N + 0{,}65\delta_{11})\,p}\left[\sum_{i=1}^{3}\frac{2}{\sqrt{\lambda_i}\,R}(H_i - F_i)\,I_1(\sqrt{\lambda_i}\,R) + 0{,}433\,(E-G)\right]. \tag{10}$$

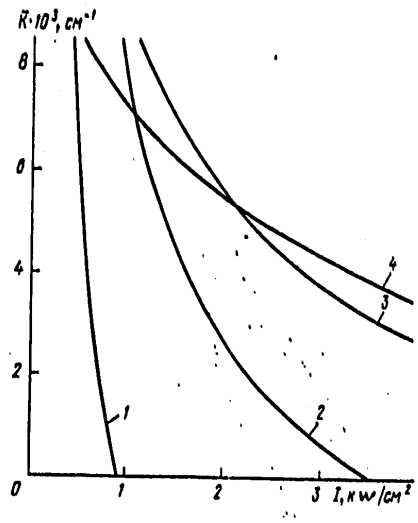

Fig. 2. Relationship between average gain in a quartz waveguide tube and the radiation density for pressures of working mixtures CO_2:N_2:He=1:1:8 p=30(1), 60(2), 100(3) and 140 mm of the mercury column (4) for J=200 ma/cm^2; To=290K, R_1=R+1 mm.

Fig. 2 shows the relationship between the average gain and radiation density, It may be seen that at low pressures of the working mixture (curve 1) a rapid saturation occurs. The gain decreases sharply with an increase in I and drops to zero at a radiation density $\sim$3kw/cm^2. A Pressure increase to 100-140 mm of the mercury column leads to an increase in collision deactivation (and to dropping $K_0=\overline{K}(I=0)$, decreases the relative contribution of forced transitions and the total velocity of evacuating the upper laser level. Therefore, at high pressure, the gain is less sensitive to the value of I.

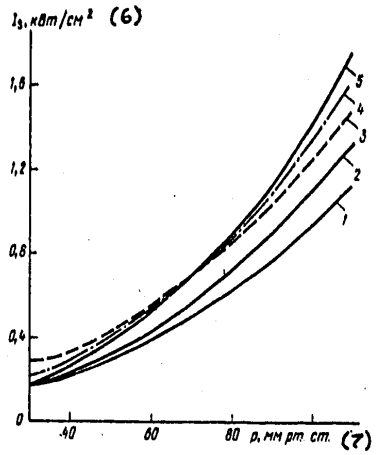

Fig. 3. Calculated relationships between saturation parameters and pressure for mixtures CO_2:N_2:He=1:1:2 (1, 2, 5), 1:1:8 (3) and 1:1:4 (4) (J=50 (1), 100 (2) and 200 ma/cm^2 (3-5).

6. kw/cm^2 7. mm of the mercury column

3. Saturation Parameter

An important characteristic of CO_2-VL is saturation parameter I_S (value of radiation field leading to the disturbance of the active medium condition). The expression for the gain depends in a complex manner on I, therefore, an analytic expression for I_S is very cumbersome. In this paper, I_S is calculated numerically as the value of I at which the gain is halved compared to its value at I=0.

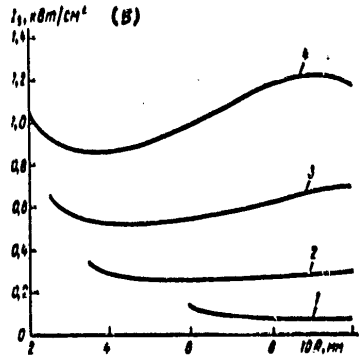

Fig. 4. Relationship between the saturation parameter and inner radius of the laser tube made of BeO for mixture $CO_2:N_2:He=1:1:2$ with pressure p=20 (1), 40 (2), 60 (3) and 80 mm of the mercury column (4) (T_o=200 ma/cm^2, $R_1=R+1$ mm).

5. kw/cm^2

For certain conditions of CO_2-VL operation, the value of the saturation parameter is an entirely defined characteristic of the system. However, the dependence of I_s on some physical parameter X will be different, depending upon the manner of posing the problem or the conditions measuring the relationship I_s (X).

If, in calculating or measuring, the value of gain of a weak signal is preserved, then the behavior of the saturation parameter is similar to the behavior of the deactivation velocity of the upper laser level [6].

This paper considers another important case frequently met with in experiments, namely, the preservation of conditions for excitation (density of pumping current, parameter E/p etc.). Fig. 3 shows changes of I_s with

pressure for several values of density of pumping current in mixture CO_2:N_2:He=1:1:2. An increase in I_s at increasing J_H in the region of high pressure is explained by the heating of the working mixture and the increase in the velocity of collision deactivation. The saturation parameter changes are considerably stronger with pressure. At high pressures $I_s \sim p^2$ corresponds to the formation of linear with respect to p velocity of collision deactivation and width of the radiation line [7]. In the region of low pressures, I_s depends weakly on p because, in this case, the contribution of collision deactivation to total velocity k_2 is not very great [16].

The value of the saturation parameter is also affected by the characteristics of the laser tube: the inner diameter, the wall thickness and the thermal conductivity; in this case, the gas mixture temperature depends on the wall thickness and the thermal conductivity, while relationships $I_s = I_s(R)$ is shown in Fig. 4. For a certain value of R (characteristic for each value of p) the saturation parameter reaches the minimum value, which corresponds to the minimum of the total deactivation velocity of level 00^01 of the CO_2 molecule [16]. A reduction in R leads to an increase in the velocity of deactivation of CO_2 on the wall and to a corresponding increase in I_s. At high values of R, the velocity of deactivation is determined by the value of the mixture pressure and for p=const the value of I_s is also constant (curve 3).

Simultaneously with theoretical calculations, the value of the saturation parameter in CO_2-VL was determined experimentally. It is well known that in the case of small losses, the value of I_s is related to the gain of weak signal K_o and linear power of radiation S by relation

$$I_s = S/\pi b_0^2 K_0, \qquad (11)$$

where b_o -- radius of the beam at intensity level 1/e.

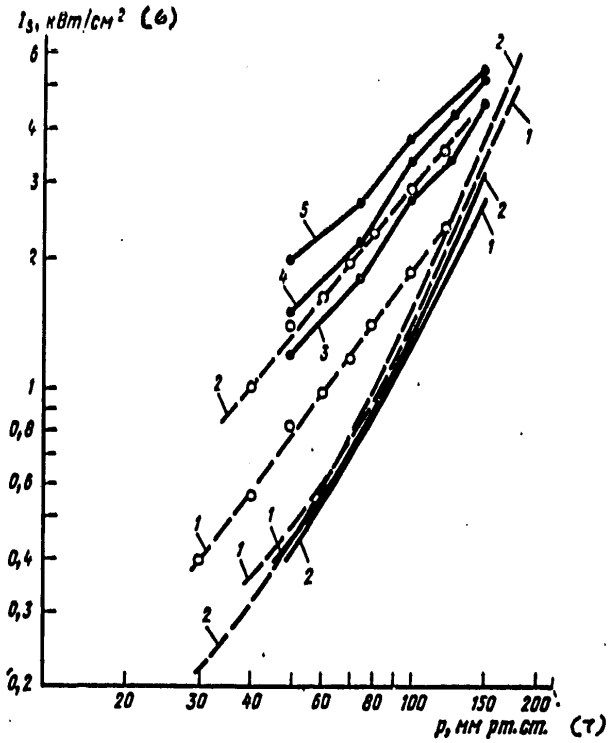

Fig. 5. Experimental (●, ○) and calculated relationships between the saturation parameter and pressure for working mixtures CO_2:N_2:He= 1:1:8 (1) and 1:1:4 (2) in glass waveguide tubes (broken line) and BeO tubes (solid line) (3-5 data from [5] obtained at pumping currents J=2 (3), 3 (4) and 4 ma (5).

6. kw/cm^2

7. mm of the mercury column

Experiments on measuring gain and oscillation power were madeon a glass discharge tube with an inner diameter of 1 mm and 12.5 cm long. NaCl windows at Brewster's angle were installed at the ends of the tube. The resonator of CO_2-VL consisted of two spherical mirrors with a radius of curvature R_o=10 cm, located 9.5 cm from the ends of the waveguide. The radiation was brought out through an internal NaCl plate 2 mm thick. Measurements were

made for compositions of working mixture CO_2:N_2:He=1:1:8 and 1:1:4. The density of the pumping current was 200 mA/cm^2.

The values of the saturation parameter, depending upon the average pressure, are shown in Fig. 5. Three experimental relationships are shown for $I_S=I_S$ (p) for various values of pumping current density in a BeO 1.65 mm tube [5] (velocity of pumping is 200 volumes per second) and two corresponding theoretical curves for mixtures 1:1:8 and 1:1:4. Although experimental and calculated conditions are not quite identical, a fairly good coincidence of results was observed, especially in the high pressure region.

We will note that the experimental value of I_s depends strongly on the chosen value of beam diameter d and may change from 105 w/cm^2 [1] (d=2R, low pressures) to 6.3 kw/cm^2[3] (d=0.91R). The calculated values of I_S, obtained in this paper, fall within the indicated region, although they are somewhat lower than those obtained in [2-5]. This discrepancy may be due to the imprecision of excitation and relaxation velocities used in the calculations, or to the underestimation of the value of d in evaluating the experimental value of I_S. Radial distribution of gain may change strongly depending upon the pumping conditions (see Fig. 1), and the shape of the beam (in particular, in the amplifier tube) may differ from the Gaussian. Therefore, for a reliable evaluation of d (and, therefore, of I_S), it is necessary to record the radial distribution of the radiation intensity in the tube.

Values of I_S obtained for typical operating conditions of CO_2-VL exceed by more than an order of magnitude the corresponding values for the usual electrical-discharge CO_2 lasers [6, 7]. In combination with a higher gain, this makes it possible to obtain in CO_2-VL a unit power density of up to about 30 w/cm^3, which is two orders of magnitude higher than the values of the corresponding parameters for low pressure electric discharge CO_2 lasers [18].

Thus, the calculations cited in this paper indicate a strong dependence of

the population of laser levels and gain on local radiation intensity in the active volume of the CO_2-VL, while the nature of the dependence may change essentially for changes in the composition and pressure of the working mixture, pumping conditions and the material and dimensions of the waveguide tube. The value of the saturation parameter in CO_2-VL exceeds considerably the values of I_s for low pressure CO_2 lasers and is a function of pressure, composition and temperature of the working mixture. A comparison of the theoretical evaluations obtained of the value of I_s for CO_2-VL with experimental data shows a good coincidence, especially in the high pressure region.

BIBLIOGRAPHY

1. Jensen, R. E.; Tobin, M. S. Appl. Phys. Letts. 20, 508 (1972).

2. Bridges, T. J.; Burkhardt, E. G.; Smith, P. W. Appl. Phys. Letts, 20, 403, (1972).

3. Burkhardt, E. G. Bridges, T. J. Smith, P. W. Optics Comms, 6, 193, (1972).

4. Degnan, J. J.; Walker, H. E.; McElroy, J. H.; McAvoy, N. IEEE J QE-9, 489 (1973).

5. Klein, M. B.; Abrams, R. L. IEEE J.QE-11, 609 (1975).

6. Christensen, C. P.; Freed, C.; Hans, H. A. IEEE J. QE-5, 276 (1969).

7. Nachshon, Y.; Oppenheim, U. P. Appl. Optics, 12, 1934 (1973).

8. Moore, C. B.; Wood, R.E.; Hu, B. L.; Yardley, J. T. J. Chem.Phys. 46, 4222 (1967).

9. Tychinskiy, V. P. UFN, 91, 389 (1967).

10. Kovacs, M.; Rao, D. R.; Javan, A. J. Chem. Phys., 48, 3339 (1968).

11. Nighan, W. L. Phys. Rev., 2A, 1989 (1970).

12. Poponin, V. P.; Shanskiy, V. F. "Pulsed CO_2 Lasers with a Nonindependent Discharge." Leningrad, NIIEFA, 1976.

13. Poehler, T. O. ; Pirkle, J. C.; Walker, R. E. IEEE J. QE-9, 83 (1973).

14. Yeletskiy, A. V.; Mishchenko, L. G.; Tychinskiy, V. P. ZhPS, 8, 425 (1968).

15. Tyte, D. C. Adv. Quant Electr., 1, 129 (1970).

16. Grigor'yants, V.V.; Kuzyakov, B.A.; Sinitsyn, A.M. KVANTOVAYA ELEKTRONIKA, 4, 1482 (1977).

17. Weigand, W. J.; Fowler, M.C.; Benda, J. A. Appl. Phys. Letts, 18, 365 (1971).

18. Fowler, M.C. Appl. Phys., 43 (1972).

2291
CSO: 8144/1033

PHYSICS

UDC 621.373.7

PARAMETRIC AMPLIFICATION BASED ON FOUR-WAVE PARAMETRIC PROCESSES IN A TWO-PHOTON RESONANCE

Moscow KVANTOVAYA ELEKTRONIKA in Russian Vol 6, No 2, Feb 79 pp 295-303

[Article by G. M. Krochik, submitted 14 Mar 78]

[Text] Processes are studied of parametric amplification in two-photon absorption (DFP) and stimulated Raman scattering (VKR) of pumping in gaseous media. It is shown that effective amplification takes place provided the DFP cross sections of fields to be amplified is greater than the DFP and VKR cross sections of pump, and at the nonlinear medium thickness a significant DFP of pumping occurs. Noise characteristics of corresponding parametric amplifiers have been investigated. It is shown that processes of the four-photon parametric luminescence make a major contribution to the noise power. The power of the parametric superluminescence under DFP or VKR of the pumping in metal vapors is calculated. It is shown that this luminescence may be observed in sodium vapors exposed to the rhodamine laser radiation. Conditions are analyzed for the triggering of an optical parametric oscillator (PGS) with a wide tuning range in IR and UV bands on the basis of the considered processes in vapors and gases. It is found that high-power laser pulses whose duration is 10^{-5} to 10^{-6} seconds are required to pump PGS.

Introduction

Four-wave parametric processes for two-photon resonance (ChPPDR) in vapors and gases are being investigated intensively from the viewpoint of using them for frequency transformation of laser radiation [1,2]. Of interest is the study of the special features of parametric radiation in such processes, as well as problems closely associated with them -- parametric superluminescence and oscillation. It is not less important to investigate the noise properties of ChPPDR, which will determine the noise characteristics of amplifiers and converters and thresholds of parametric superluminescence. This paper is dedicated to the theoretical analysis of the problems enumerated.

We will cite a brief list of papers concerning the enumerated questions. The possibility of achieving high gains in four-wave parametric processes for two-photon absorption (DFP) of pumping was reported in [3]. In papers [4,5], directional forced radiation for (DFP) laser pumping in rubidium vapors was observed. The four-photon parametric superluminescence plays a considerable role in the formation of this radiation, along with the indicated, in [4,5], mechanism of mixing pumping radiation and infrared laser radiation, originating as a result of the formation of an inversion between level 2, pumped by a two-photon pump, and the intermediate underlying level. The excitation threshold of the parametric oscillator of light (PGS) on the basis of ChPPDR at the given pumping was evaluated in [6]. The effect of the type of resonance transition and polarization of pumping on the value of this threshold was studied [7].

1. Polarization of the Gaseous Medium

We will assume that acting on the medium consisting of freely oriented molecules (atoms) is electromagnetic field

$$\vec{g} = \sum_j e_j E(\omega_j) \exp(i\omega_j t) + \text{kompl. copr. [expansion unknown]}$$

where

$$e_j \left((e_0 = e_z,\ e_\pm = \mp \frac{1}{\sqrt{2}} (e_x + i e_y) \right)$$

are circular unit vectors of the fields, while field frequencies ω_j (j=1,2,3,4) satisfy the condition of two-photon resonance:

$$\omega_1 + \omega_2 = \omega_3 \pm \omega_4 = \omega_{21} + \Delta, \quad \Delta \ll \omega_j. \qquad (1)$$

ω_{21}-- transition frequency between energy states of molecules;

$$|1, j_1, m_1\rangle \text{ and } |2, j_2, m_2\rangle;\ j_{1,2}, m_{1,2}$$

-- quantum numbers of the full moment of the amount of movement and its projection on the direction of the external field.

The nonlinear polarization of such a medium may be obtained by using the expansion of the matrix of density

$$\sigma_{m_1 m_2} = \langle 1, j_1, m_1 | \hat{\sigma} | 2, j_2, m_2 \rangle$$

by irreducible tensor of operators σ_q^x [8]. We will cite as an example an expression for the amplitude of medium polarization at field frequency ω_1,

in the process of parametric amplification at DFP pumping with frequencies ω_3 and ω_4 *:

$$\mathcal{P}_a(\omega_1) = \hbar^{-1} e^{-i\Delta t} \sum_{\varkappa, q} \frac{2\varkappa+1}{2j_1+1} \sigma_q^{\varkappa} \left[\varkappa_{ab\,q}^{\varkappa}(\omega_1)\right]^* E_b^*(\omega_2)(-1)^b, \qquad (2)$$

where the expression for the stationary value of $\sigma_q^{\varkappa}$, obtained on the assumption of the isotropy of relaxation processes, without taking into account Stark shifts and the induced widening of the transition line, has the form

$$\sigma_q^{\varkappa} = -i \frac{\sigma_{m_1 m_1} - \sigma_{m_2 m_2}}{(T^{-1} + i\Delta)\hbar} e^{i\Delta t} \left[\varkappa_{cd\,q}^{\varkappa}(\omega_1) E_c^-(\omega_1) E_d^-(\omega_2) + \varkappa_{cd\,q}(\omega_3) E_c^-(\omega_3) \times E_d^-(\omega_4)\right]. \qquad (3)$$

In these expressions

$$\varkappa_{ab\,q}^{\varkappa}(\omega_1) = \sqrt{2j_1+1} \sum_{m_1 m_2} \begin{pmatrix} j_1 & j_2 & \varkappa \\ m_1 & -m_2 & q \end{pmatrix} (-1)^{j_1 - m_1} \varkappa_{ab}^{m_1 m_2}(\omega_1) = \begin{pmatrix} 1 & 1 & \varkappa \\ -a & -b & -q \end{pmatrix} \varkappa^{\varkappa}(\omega_1), \qquad (4)$$

$$\varkappa^{\varkappa}(\omega_1) = (-1)^{j_1+j_2} \sqrt{2j_1+1}\hbar^{-1} \sum_{j \neq j_1, j_2} d_{j_1 j} d_{j j_2} \begin{Bmatrix} 1 & 1 & \varkappa \\ j_2 & j_1 & j \end{Bmatrix} \left[\frac{1}{\omega_{j j_1} - \omega_1} + \frac{(-1)^{\varkappa}}{\omega_{j j_2} + \omega_1}\right]; \qquad (5)$$

$d_{j_1 j_2}$ -- matrix elements of the dipole moment operator for transition

$$|i, j_1\rangle \to |k, j_2\rangle;$$

$$\varkappa_{ab}^{m_1 m_2}(\omega_1)$$

*Similar expressions for polarization amplitudes were obtained in [9], however, they make it possible to investigate only polarization features of ChPPDR, but do not permit the calculation of the cubic receptivity according to known powers of the oscillators.

is the polarizability of the second order for transition

$$|1,\ j_1,\ m_1\rangle \to |2,\ j_2,\ m_2\rangle;\ \begin{pmatrix} \cdot & \cdot & \cdot \\ \cdot & \cdot & \cdot \end{pmatrix},\ \begin{Bmatrix} \cdot & \cdot & \cdot \\ \cdot & \cdot & \cdot \end{Bmatrix}$$

--3j- and 6j symbols; T -- relaxation time of the nondiagonal element of the density matrix;

$$\sigma_{m_i m_i} = \sigma_i/(2j_i+1)$$

is the population of sublevels m_i of level j_i; rank $\varkappa$ of irreducible spherical tensors $\sigma_q^{\varkappa}$ and $x_q^{\varkappa}(\omega_i)$ satisfy conditions

$$0 \leqslant \varkappa \leqslant 2,\quad |j_1 - j_2| \leqslant \varkappa \leqslant |j_1 + j_2|.$$

In expressions (2) and (3) summation means repeated polarization indices a, b, c, d.

Substituting expressions (3) - (5) into (2), it is easy to reduce the expression for the polarization amplitude of the medium at frequency ω_i to an explicit form

$$\mathcal{P}(\omega_1) = -iN^{-1}\frac{\sigma_{m_1 m_1} - \sigma_{m_2 m_2}}{T^{-1} + i\Delta}\left[G(\omega_1, \omega_1)E(\omega_1)|^2 E(\omega_2)|^2 + G(\omega_1, \omega_3)E^*(\omega_2) \times E(\omega_3)E(\omega_4)\right], \tag{6}$$

where

$$G(\omega_1, \omega_3) = \frac{x^{0*}(\omega_1)x^0(\omega_3)}{3(2j_1+1)}e_2^*(e_3e_4) + \frac{x^{1*}(\omega_1)x^1(\omega_3)}{2(2j_1+1)}\cdot[e_3(e_2e_4) - e_4(e_2^*e_3)] + + \frac{x^{2*}(\omega_1)x^2(\omega_3)}{6(2j_1+1)}[-2e_2^*(e_3e_4) + 3e_3(e_2^*e_4) + 3e_4(e_2^*e_3)]. \tag{7}$$

while an expression for $G(\omega_1, \omega_1)$ may be obtained from (7) by replacing

$$\omega_3 \to \omega_1,\ e_3 \to e_1,\ e_4 \to e_2.$$

Vectors for polarization amplitudes at field frequencies $\omega_2, \omega_3, \omega_4$. have a similar form.

2. Parametric Amplification for DFP Pumping

2.1 Let radiations of fields, with frequencies satisfying condition $\omega_1 + \omega_2 \quad \omega_3 + \omega_4 = \omega_3$, act on the gaseous medium. Equations for complex amplitudes of fields

$$C_j = E(\omega_j)\exp(ik_j z)$$

for their single-dimensional interaction along axis Z may be obtained easily, substituting expressions for amplitudes of field polarization of type (6) into Maxwell's equations:

$$\frac{dC_{1,2}}{dz} = -\alpha_{11,22}\left|C_{2,1}\right|^2 C_{1,2} - \alpha_{12,21} C^*_{2,1} C_3 C_4 e^{i(\delta k)z}, \tag{8a}$$

$$\frac{dC_{3,4}}{dz} = -\alpha_{33,44}\left|C_{4,3}\right|^2 C_{3,4} - \alpha_{34,43} C^*_{4,3} C_1 C_2 e^{-i(\delta k)z}, \tag{8б}$$

where

$$\delta k = (k_1 + k_2) - (k_3 + k_4)$$

is the detuning of the wave vectors of the fields;

$$\alpha_{11,22} = \omega_{1,2}\alpha_0 G(\omega_1, \omega_2);\quad \alpha_{12,21} = \omega_{1,2}\alpha_0 G(\omega_1, \omega_2);$$
$$\alpha_{33,44} = \omega_{3,4}\alpha_0 G(\omega_3, \omega_3);\quad \alpha_{34,43} = \omega_{3,4}\alpha_0 G(\omega_3, \omega_1); \tag{9}$$

$$\alpha_0 = 2\pi\eta N T\hbar^{-1}c^{-1};$$

N -- density of the number of particles; η -- the difference in populations of sublevels 1 and 2.

We will assume that for the considered transition

$$|1, j_1\rangle \rightarrow |2, j_2\rangle$$

the following condition is fulfilled

$$G(\omega_1, \omega_2) = G^{1/2}(\omega_1, \omega_1) G^{1/2}(\omega_2, \omega_2). \tag{10}$$

It follows for (6) and (7) that this condition is fulfilled, for example, for transitions

$$^1S_0 \rightarrow {}^1S_0,\quad {}^2S_{1/2} \rightarrow {}^2S_{1/2},\ {}^2S_{1/2} \rightarrow {}^2D_{3/2}$$

in metal vapors. Let further boundary amplitudes of fields

$$C_j|_{z=0} = C_{j0}$$

satisfy the inequality

$$|C_{30}||C_{40}|G^{1/2}(\omega_3, \omega_4) \gg |C_{10}||C_{20}|G^{1/2}(\omega_1, \omega_1). \tag{11}$$

Then equations describing the process of parametric amplification of weak optical signals C_1 and C_2 at DFP pumping C_3 and C_4 may be simplified considerably:

$$\frac{dC_1}{d\zeta} = -\gamma_1 e^{-i\delta\zeta} f(\zeta) C_2^*, \quad \frac{dC_2^*}{d\zeta} = -\gamma_2 e^{i\delta\zeta} f(\zeta) C_1, \tag{12}$$

where

$$\zeta = M_3 z; \ \delta = \delta k / M_3; \ \gamma_{1,2} = \alpha_{11,33} C_{30} C_{40} / M_3; \tag{13}$$

$$f(\zeta) = M_3 \exp\zeta |\alpha_{33}|C_{40}|^2 \exp 2\zeta - \alpha_{44}|C_{30}|^2]^{-1}; \tag{14}$$

$$M_3 = \alpha_{33}|C_{40}|^2 - \alpha_{44}|C_{30}|^2 = \alpha_{33}|C_4|^2 - \alpha_{44}|C_3|^2. \tag{15}$$

In obtaining equations (12) we neglected the DFP amplified fields and their effect on pumping fields, considering that the pumpings only change due to the DFP.

2.2 In this case of zero wave detuning ($\delta = 0$), the solution of equations (12) has the form

$$C_1 = C_{10} \operatorname{ch} \mathcal{Z} - C_{20}^* \left(\frac{\omega_1}{\omega_2}\right)^{1/2} \operatorname{sh} \mathcal{Z}; \tag{16a}$$

$$C_2^* = -C_{10} \left(\frac{\omega_2}{\omega_1}\right)^{1/2} \operatorname{sh} \mathcal{Z} + C_{20}^* \operatorname{ch} \mathcal{Z}, \tag{16б}$$

where

$$\mathcal{Z} = R \ln \left[\frac{\alpha_{33}^{1/2} A_{40} e^{\zeta} - \alpha_{11}^{1/2} A_{30}}{\alpha_{33}^{1/2} A_{40} e^{\zeta} - \alpha_{44}^{1/2} A_{30}} \frac{\alpha_{33}^{1/2} A_{40} + \alpha_{44}^{1/2} A_{30}}{\alpha_{33}^{1/2} A_{40} - \alpha_{44}^{1/2} A_{30}} \right]; \tag{17}$$

$$R = \left(\frac{\alpha_{11}\alpha_{33}}{\alpha_{33}\alpha_{44}}\right)^{1/2} = \left[\frac{\omega_1\omega_3}{\omega_3\omega_4}\,\frac{G(\omega_1,\ \omega_1)}{G(\omega_3,\ \omega_3)}\right]^{1/2}; \qquad (18)$$

$$A_j = |C_j| = C_j \exp(i\varphi_j)$$

-- actual amplitudes of the fields; it follows from (16) that amplification of the weak radiation proceeds efficiently, if the DFP cross section of the amplified fields is not smaller than the cross section of the DFP of pumping ($R \gtrsim 1$) and there is strong DFP pumping along the length of the nonlinear medium. The latter condition is fulfilled if the limiting intensities of pumping satisfy equation

$$A_{30}^2/A_{40}^2 = \alpha_{33}/\alpha_{44} = \omega_3/\omega_4, \qquad (19)$$

which, in particular, is true for degeneratred DFP pumping ($\omega_3 = \omega_4$). DFP nondegenerated with respect to frequency pumping is used in ChPPDR for providing conditions for spatial synchronism, by retuning pumping frequencies near resonances [10, 11]. When equation (19) is fulfilled, expression (17) has the form

$$\mathcal{Z} = R \ln[1 + 2\zeta_1]^{1/2}, \qquad (20)$$

where

$$\zeta_1 = \alpha_{44} A_{30}^2 z = \alpha_{33} A_{40}^2 z. \qquad (21)$$

2.3. In case of arbitrary wave detuning when fulfilling condition (19), the system of equations (12) may be reduced to the following two differential equations of the second order:

$$\frac{d^2C_{1,2}}{d\zeta_1^2} + \left(\mp i\delta + \frac{2}{1+2\zeta_1}\right)\frac{dC_{1,2}}{d\zeta_1} - R^2(1+2\zeta_1)^{-2}C_{1,2} = 0. \qquad (22)$$

To illustrate the effect of wave detuning, we will consider the case R=2, when equations (22) are equations with full differentials and their solutions for $A_{40}=0$ may be presented in the form

$$C_1 = \frac{C_{10}}{\delta^2(1+2\zeta_1)^2}[(4+\delta^2+2\delta^2\zeta_1-4\cos\delta\zeta_1)^2+(4\sin\delta\zeta_1-4\delta\zeta_1)^2]^{1/2}\times$$

$$\times\exp\left\{i\,\mathrm{arctg}\frac{-4\sin\delta\zeta_1+4\delta\zeta_1}{4+\delta^2+2\delta^2\zeta_1-4\cos\delta\zeta_1}\right\}; \qquad (23a)$$

$$C_2 = -\left(\frac{\omega_2}{\omega_1}\right)^{1/2}\frac{2C_{10}}{\delta^2(1+2\zeta_1)}[(2-2\cos\delta\zeta_1+\delta\sin\delta\zeta_1)^2+(\delta+2\delta\zeta_1-2\sin\delta\zeta_1-$$

$$-\delta\cos\delta\zeta_1)^2]^{1/2}\exp\left\{i\,\mathrm{arctg}\frac{4\delta\zeta_1-4\sin\delta\zeta_1}{4+\delta^2+2\delta^2\zeta_1-4\cos\delta\zeta_1}\right\}. \qquad (23b)$$

For $\zeta_1 \to \infty$ the amplitudes of the amplified fields approach values

$$A_2|_{\zeta_1\to\infty} = \frac{2}{|\delta|}\left(\frac{\omega_2}{\omega_1}\right)^{1/2}A_{10}, \quad A_1|_{\zeta_1\to\infty} = \left[\frac{\delta^2+4}{\delta^2}\right]^{1/2}A_{10},$$

which are determined by the ratio of the value of wave detuning (δk) to the coefficient of the two-photon absorption of pumping

$$L_{DFP}^{-1} = 2\alpha_{33}A_{40}^2.$$

Fig. 1. shows relationships $A_{1,2}(\zeta_1)$ (23), plotted for various values of δ. It may be seen from Fig. 1 that amplified fields reach the maximum values at $z \approx \pi(\delta k)^{-1}$; ; at $\pi(\delta k)^{-1} \leqslant z \leqslant 2\pi(\delta k)^{-1}$, when a reverse parametric conversion of the amplified fields to pumping occurs, the efficiency of wave interaction becomes lower due to the DFP pumping that has occurred on the initial section. Therefore, after reaching the maximum conversion, the amplified fields complete attenuating oscillations with a period of $2\pi(\delta k)^{-1}$ and approach the value near the maximum.

3. Parametric Amplification of VKR Pumping

As is the previous paragraph, we will consider parametric amplification of weak radiation when strong inequality (11) is true for the limiting values of fields. Then the solution of equations for complex amplitudes of fields (8), in which $C_4 \to C_4^*$, should be replaced, for

$$\delta k = (k_1+k_2)-(k_3-k_4)=0$$

has the form (16), where

$$\mathcal{L} = R\,\mathrm{arctg}\,b(e^{\zeta_2}-1); \quad b = A_{40}^2\omega_3/A_{30}^2\omega_4; \qquad \zeta_2 = \alpha_{33}A_{30}^2 z. \qquad (24)$$

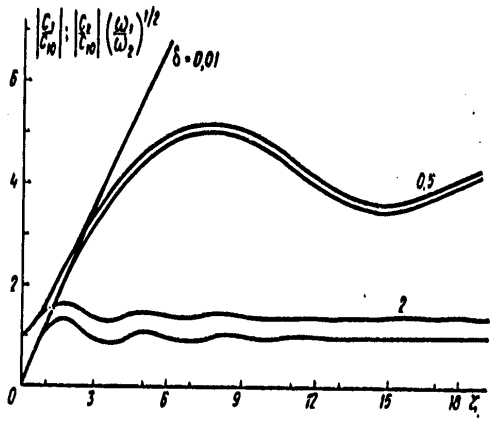

Fig. 1. Relationships between amplified fields and coordinates for various values of wave detuning δ (see (13), (15).

We will assume that $A_{20} \ll A_{10}$, then it follows from (16) and (24) that fields C_1 and C_2 increase monotonically and approach limits

$$\lim_{\zeta_1 \to \infty} A_1^2 \simeq A_{10}^2 \operatorname{ch}^2\left(R\frac{\pi}{2}\right), \quad \lim_{\zeta_1 \to \infty} A_2^2 \simeq A_{10}^2 \frac{\omega_2}{\omega_1} \operatorname{sh}^2\left(R\frac{\pi}{2}\right), \tag{25}$$

determined by the value of parameter R (see (8)). With increasing R, i.e., the ratio of cross section of DFP of amplified fields to the cross section of the VKR pumping, the limiting values of the amplified fields increase. In this case, the length on which the amplified fields reach maximum amplification, is determined by the length of the combination conversion of pumping into its Stokes component.

Thus, for example, for R=3-4, at which is provided at quasiresonance at the frequency of the amplified field, the maximum gain is equal to 10^3-10^5 (see (25)). To attain this gain it is necessary to provide conditions of phase matching (see [2]) on the entire length where almost a full (0.8) conversion occurs of pumping photons into Stokes component photons.

4. Noise Characteristics of ChPPDR Optical Amplifiers

4.1. If the wavelength of resonance transition 1→2 lies in the near infrared, visible or ultraviolet ranges of the spectrum (electronic transitions of atoms and molecules), then the thermal population of level 2, due to its interaction with the thermostat, is immaterial (for metal vapors at

$$300-500\,C\exp[-\hbar\omega_{21}/kT]\approx 10^{-11}-10^{-16}).$$

In this situation, thermal (molecular) noises, due to two-quanta spontaneous radiation, may be neglected. If the wavelength of resonance transition lies in the far infrared region (oscillation-rotation transitions of molecules), for example, at two-photon pumping of SF_6 by a CO_2 laser [12], thermal noises must be taken into account.

We will consider only the first situation, the most interesting from the viewpoint of experimental implementation. We will also assume that the population of level 2, due to DFP or VKR pumping, is small so that spontaneous two-photon radiation from that state can be neglected. In this case, the basic contribution to the noise power of the parametric amplifier is made by vacuum noises, i.e., noises originating as a result of the conversion of zero fluctuations at the frequency of the free wave into radiation at the frequency of the amplified field four-photon parametric luminescence [13]. We will make a calculation of the power of such noises.

As before, we will describe the pumping field classically, considering it quasimonochromatic and assuming that the number of its quanta is large. We will describe amplified fields in quantum language, representing them in the form of superposition of flat waves [14]:

$$\mathcal{E}=\sum_{j=1,2}\frac{i}{2\pi}\int(\hbar\omega_j)^{1/2}\left[a_j(\mathbf{k})\,e^{-i\mathbf{kr}+i\omega_j t}-a_j^{+}(\mathbf{k})\,e^{i\mathbf{kr}-i\omega_j t}\right]\hat{e}_j d\mathbf{k}, \qquad (26)$$

where $a_j^{+}(k)$ and $a_j(k)$ -- operators of origination and destruction for photons of amplified fields. Equations for operators $a_j(k)$ and $a_j^{+}(k)$ have a form, similar to (12), where it is necessary to replace

$$C_1\to a_1(\mathbf{k}),\ C_2^{*}\to a_2^{+}(\mathbf{k}),$$

while their solutions for $\delta\mathbf{k}=0$ have a form similar to (16):

$$a_1=a_{10}\mathrm{ch}\mathcal{L}-a_{20}^{+}\mathrm{sh}\mathcal{L}; \qquad (27a)$$

$$a_2^{+}=-a_{10}\mathrm{sh}\mathcal{L}+a_{20}^{+}\mathrm{ch}\mathcal{L}. \qquad (27б)$$

where $\mathcal{L}$ is, as before, determined in (17), (20) or (24) depending upon the type of process. It is easy to obtain from (27) expressions for the density of the number of photons $N_i = \langle a_i^+ a_i \rangle$:

$$N_1 = N_{10}\mathrm{ch}^2\mathcal{L} + (N_{20}+1)\mathrm{sh}^2\mathcal{L}; \tag{28a}$$
$$N_2 = (N_{10}+1)\mathrm{sh}^2\mathcal{L} + N_{10}\mathrm{ch}^2\mathcal{L}, \tag{28b}$$

where N_{10}, N_{20} -- density of the number of entering photons (z=0)

The power of scattered radiation at frequency ω_i, for collinear wave interaction can be obtained easily from (28), assuming $N_{10}=0$, $N_{20}=0$:

$$P(\omega_1) = A\int_{\omega_1} J^0_{\omega_1}\,\Lambda\,\Omega(\omega_1)\,\mathrm{sh}^2\mathcal{L}(\omega_1)\,d\omega_1, \tag{29}$$

where $J^0_{\omega_1} = \hbar\omega_1 k_1^3/8\pi^3$ is the "spectral brightness of the vacuum" on the left of the nonlinear medium [13]; A -- cross section of beam; $\Delta\Omega(\omega_1)$ -- element of solid angle of scattering; $\mathcal{L}(\omega_1) \sim R(\omega_1)$ (see (18) takes into account dispersion $\zeta_i(\omega_1, \omega_2)$ within the interval of amplified frequencies.

Formula (29) was obtained without taking into account the transverse structure of the beam and is approximately true when inequality $\lambda_{3,4} \ll d \ll L$, exists, where $d \approx \sqrt{A}$ -- diameter of beam; L -- length of interaction. On taking into consideration the transverse structure of the beam, see [13] and papers cited in it. Solid angle $\Delta\Omega(\omega_1)$ and the interval of amplified frequencies are determined from condition

$$\delta k(\omega_1) = |k(\omega_3) + k(\omega_4) - k(\omega_1) - k(\omega_2)| \approx 0.$$

Making simple geometrical plots (Fig.2) we find that at collinear synchronism the dispersion angles do not exceed values

$$\Delta\Omega(\omega_{1,2}) = \theta_{1,2} \approx 8|\delta k/k_{1,2}|, \tag{30}$$

where it is assumed that the length of coherent interaction $L \approx |\delta k|^{-1}$ (see 2.3)

4.2. We will calculate the gain and the noise power of the parametric amplifier if radiations, reduced to the input, with λ_1=14.8 microns,

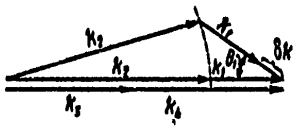

Fig. 2. Vector diagram of parametric luminescence for collinear synchromism.

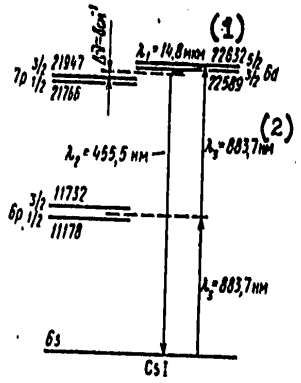

Fig. 3. Arrangement of the process of parametric amplification for wavelengths λ_1=14.8 microns and λ_2=455.5 nm in cesium vapors.

λ_2=455.5 nm for DFP circularly-polarized pumping ($\lambda_3=\lambda_4$=883.7 nm) between levels $6S_{\frac{1}{2}}$ and $6D_{5/2}$ in cesium vapors (Fig. 3). The condition of synchronism $\delta k=0$ is met for the indicated wavelengths, while values $G(\omega_3,\omega_3)$ and R, calculated from formulas (7), (5), (18), are equal to 2.66×10^{-44} SGSE and 7 respectively. (For a degenerated DFP ($\omega_3=\omega_3$) the value of $G(\omega_3,\omega_3)$ is doubled; the strengths of the transition oscillators are taken from [15, 16]. Ata density of cesium atoms

$$N = 4\cdot10^{18}\ \text{см}^{-3}\ (\eta N=2\cdot10^{16}\ \text{см}^{-3}),\ T=3\cdot10^{-10}$$

5. Parametric Superluminescence and Generation

5.1 We will now consider the possibility of four-photon parametric luminescence at two-photon resonance. To observe it, it is necessary to provide a gain of about 10^{10}. This gain, as follows from the above, may be achieved at large parameters of R, i.e., at small frequency detuning of the amplified radiation with respect to the resonance line of the medium. The DFP and inverse conversion of these fields in pumping becomes considerable, in this case, with an increase in the amplified fields. In papers [18, 20] the oscillation processes of the difference frequencies at DFP and VKR of pumping were analyzed taking into account these two effects. It was established in these papers that amplified fields at $\delta k=0$ approach the stationary states in which the power of the amplified fields is maximum.

The values of fields in the stationary state satisfy the following equations, which may easily be obtained from corresponding equations in [18, 20]*

For a process on the basis of DFP pumping $(\omega_3 \approx \omega_4)$

$$J_{30}^2 \exp\left[-\frac{4}{R}\operatorname{arcsh}\left(\frac{J_1}{J_{\omega_1}}\right)^{1/2}\right] \approx \frac{G(\omega_1, \omega_1)}{G(\omega_3, \omega_3)} J_1^2 \frac{\omega_3}{\omega_1}, \quad J_3 \approx \frac{\omega_3}{\omega_1} J_1, \qquad (31)$$

For a process on the basis of VKR pumping

$$J_{30}^2 \sin^2\left[\frac{2}{R}\operatorname{arcsh}\left(\frac{J_1}{J_{\omega_1}}\right)^{1/2}\right] \approx \frac{G(\omega_1, \omega_1)}{G(\omega_3, \omega_3)} \frac{4\omega_3\omega_2}{\omega_4\omega_1} J_1^2. \qquad (32)$$

In (31), (32) by $J_{\omega_{1,2}}$ is meant power density of vacuum noises at the input: $J_{\omega_{1,2}} = \tilde{P}(\omega_{1,2})/A$.

5.2 We will calculate the arrangement of parametric superluminescence in sodium vapors radiated by circularly polarized radiation of a rhodamine laser

*High gains are provided in frequency interval $\Delta\omega_1 = \Delta\omega_2 \lesssim 2\pi T^{-1}$, so that conditions for achieving stationary states may be left approximately the same as for the case of quasimonochromatic fields.

from [17], length of coherent interaction L=5 cm, pumping power* J_{30}=2.5 Mw/cm^2 (5x10^3 SGSE) the reverse length of DFP (DFP coefficient) L^{-1}_{DFP}=0,7 cm^{-1}, the radiation gain on ω_1 and ω_2 is equal to 10^4.

We will calculate noise powers of amplifiers at frequencies ω_1 and ω_2 reduced to the input. Assuming $\delta k = L^{-1} = 0{,}2$ cm, we find from (30) $\Delta\Omega(\omega_1) =$ 3.8 x 10^{-4} steradians, $\Delta\Omega(\omega_2) =$ 1.6x10^{-5} steradians. The range of amplified frequencies is determined from condition $\delta k(\omega_1) \leqslant L$; it is equal to $\Delta\nu = 0.3$ cm^{-1}. For confocal focusing of pumping [19] the cross section area of the beam $A = L\lambda/4 = 10^{-4}$ cm^2, the dispersion aperture does not exceed the value of $\Delta\Omega \leqslant A/L^2 = 4 \cdot 10^{-6}$ steradians $< \Delta\Omega(\omega_1), \Delta\Omega(\omega_2)$. A change in parameter R within the frequency interval $\Delta\nu_1 = 0{,}3$ cm^{-1} is negligibly small, so that it may be assumed in (29) that $\mathcal{X}(\omega_1)$=const.

Then we will find from (29)

$$P(\omega_1) = J^0_{\omega_1} A \, \Delta\Omega 2\pi c \, \Delta\nu_1 = 2{,}1 \cdot 10^{-14} \mathrm{sh}^2 \mathcal{X} \quad \text{watts},$$

$$P(\omega_2) = 10^{-16} \mathrm{sh}^2 \mathcal{X} \quad \text{watts};$$

respective noise powers reduced to the input are equal to

$\tilde{P}(\omega_1) = P(\omega_1)/\mathrm{sh}^2\mathcal{X} = 2{,}1 \cdot 10^{-14}$ watts, $\tilde{P}(\omega_2) = 10^{-16}$ watts.

When using laser pumping with length of pulse τ_H = 30 nanoseconds, the pulse noise power reduced to the input is $\tilde{P}(\omega_1)\tau_H = 6 \cdot 10^{-22}$ joules $< \hbar\omega_1 = 1{,}27 \cdot 10^{-20}$ joules

$\tilde{P}(\omega_2)\tau_H = 3 \cdot 10^{-18}$ joules $> \hbar\omega_2 = 4{,}1 \cdot 10^{-19}$ joules.

Thus, for the indicated parameters, the four-photon parametric luminescence will contribute to the noise power only when the ultraviolet signal becomes stronger and has no effect on noise characteristics of the infrared radiation amplifier. We will note also that noise characteristics of infrared radiation converters (14.7 microns) into visible (455nm) will not be worse, on the basis of the indicated arrangement of the generation of the difference frequency than using for this purpose a process of generation of a total frequency for DFP pumping. In this case, the conversion coefficient in accordance with the number of quanta of such converters will be found to be significantly higher (10^4). (In the process of generation of total frequencies for DFP and VKR pumping, the conversion coefficient in accordance with the number of quanta $\eta \leqslant 1$[2]).

---

*Pumping intensity of the saturating two-photon transition $6S_{1/2} \rightarrow 6D_{3/2}$ $J_{нас} \approx \hbar |4\tau TG(\omega_2, \omega_2)|^{-1} = 10^3$ SGSE [CGSE] for $\tau = T = 3 \times 10^{-10}$ sec (we assume that the relaxations of populations occur due to collisions [17]; at $J_{30} \leqslant J_{sat}$ no considerable increase in the length of conversion occurs [18].

tuned to a 578.9 nm wavelength (Fig. 4). The calculation of wave detuning indicates that the condition for spatial synchronism is fulfilled for $\nu_1 = 427.6$ cm^{-1} ($\lambda_1 = 2.34$ microns), $\nu_2 = 30276$ cm^{-1} ($\lambda_2 = 330.3$ microns),

$G(\omega_1, \omega_2) = 4 \cdot 10^{-44}$ cm^6, $G(\omega_1, \omega_1) = 2.6 \cdot 10^{-41}$ cm^6, $R = 16.8$ ([15, 16]).

For $T = 3 \cdot 10^{-10}$ c, $\eta N = 10^{17}$ cm^{-3}, $J_{30} \approx 3 \cdot 10^3$ SGSE ($J_{max} = 8.5 \times 10^3$ SGSE) reverse length of DFP of pumping $L_{DFP}^{-1} = 4.8$ cm^{-1}.

We will assume that length of interaction L=2 cm. If, on this length, the DFP of the amplified fields and their inverse effect on pumping can be neglected, then gain $\mathrm{sh}^2\mathcal{Z}$ is equal to 4×10^{16}. Obviously this gain will not be provided, since long before it is reached, the amplified fields will become stationary. We will show this.

For $\delta k = L^{-1} = 0.5$ cm^{-1} the frequency width of amplified fields is equal to 0.1 cm^{-1}, while the aperture of the dispersion angles $\Delta\Omega(\omega_1) = 2.3 \cdot 10^{-4}$ steradians, $\Delta\Omega(\omega_2) = 2.1 \cdot 10^{-5}$ steradians. At confocal focusing of pumping in region $L = 2$ cm $A = L\lambda/4 = 2.8 \cdot 10^{-5}$ cm^2, $\Delta\Omega = A/L^2 = 7 \cdot 10^{-6}$ steradians $< \Delta\Omega(\omega_{1,2})$.

Thus, the powers of vacuum noises reduced to the input $\tilde{P}(\omega_2) = 4.6 \cdot 10^{-10}$ watts, $\tilde{P}(\omega_1) = 1.3 \cdot 10^{-12}$ watts,

$$\tilde{J}_{\omega_2} = 1.65 \cdot 10^{-5} \text{ w/cm}^2, \qquad \tilde{J}_{\omega_1} \approx 4.64 \cdot 10^{-6} \text{ w/cm}^2.$$

We will find from (32) that the stationary intensity of amplified fields J_1=SGSE (4.6×10^3 w/cm^2), and $\bar{J}_2$=66 SGSE (33×10^4 w/cm^2).

Thus, the maximum gains do not exceed 10^{10} and the calculation should be made taking into account the DFP of the amplified fields and their effect on pumping.

The length at which values of amplified fields $J'_{1,2} = 0.9\bar{J}_{1,2}$ are achieved is determined by formula [18]

$$L = \frac{1}{2\alpha_{33}} \int_{J_3'(J_1)}^{J_{30}} dJ_3 \frac{1}{J_3 [J_3 - [(G(\omega_1, \omega_1)/G(\omega_2, \omega_2) J_1 J_2]^{1/2}]}, \qquad (33)$$

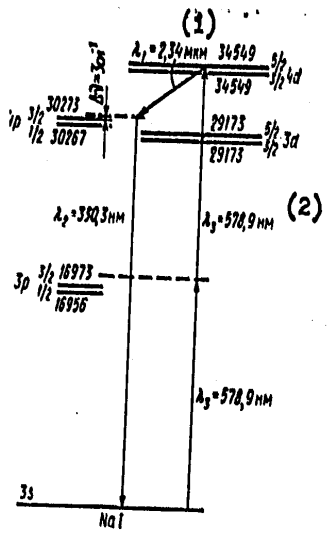

Fig. 4. Arrangement of the process of parametric superluminescence in sodium vapors

1. microns 2. nm [n nometers]

where J_1 and J_2 are expressed through J_3 with the aid of the first integrals of the system of equations (8) for $\delta k=0$. As shown by calculation, this length does not exceed value L=2 cm. Thus, on this length, the following powers of radiation dispersion will be attained. $J_1' \approx 0{,}9 J_1 \approx 4 \cdot 10^3$ w/cm^2, $J_2' \approx 0{,}9 J_2 \approx 2{,}9 \cdot 10^4$ w/cm^2.

We will finally note the following. Above we made the calculation not taking into account field absorption at frequency ω_2. This can be done if, for each value of the two photon-absorbed pumping, the "parametric increment" of the increase in the amplified fields is considerably greater than the linear coefficient of their absorption, i.e., condition

$$\alpha_{33} R' (1 + L_{DFP}^{-1} z) \geqslant \alpha_2/2 \qquad (34)$$

is fulfilled for all of z from the region of interaction of fields. For the considered example

$$\nu_2 - \nu_{3S-4P_{3/2}} = 3\ \text{см}^{-1},\quad \alpha_2 = \frac{2\pi\eta N\omega_2 T^{-1}}{nc\,(T^{-2}+\Delta^2)}\,\frac{d^2_{3S-4P_{3/2}}}{3} = 1{,}2\ \text{см}^{-1},\ \alpha_{33} = 8\cdot10^{-4}\ \text{SGSE},$$

L=2 cm, inequality (34) is fulfilled for all

$$0 \leqslant z \leqslant L = 2\ \text{см}:\ \alpha_{33}R(1+L_{\text{диф}}^{-1}L)^{-1} = 8\ \text{см}^{-1} \gg \alpha_2/2 = 0{,}6\ \text{см}^{-1}$$

and the cited evaluations are true.

5.3. We will dwell here on the possibility of creating PGS on the basis of a ChPPDR. It was shown above that a gain of 10^3 to 10^{10} (for one passage) can be provided near resonance lines. Thus, the creation of PGS with small regions of detuning λ_1 and λ_2 (10cm^{-1}) will not be difficult. It is of interest to evaluate the possibility of creating PGS with a wide range of retuning, spanning the UV, visible and IR ranges.

We will assume that to fulfill self-excitation conditions, it is necessary that the gain for one passage be in the order of 1% which takes place in PGS on nonlinear crystals [21]. We will calculate PGS parameters with a retuning range for wavelengths λ_1=1.4-10 microns, λ_2 =355-455 nm in sodium vapors, radiated by circular-polarized pumping, the wavelength of which satisfies the condition of a two-photon resonance with transition $3S_{1/2} \rightarrow 3D_{5/2}(\lambda_3 = \lambda_1 = 686)$ nm). The wave detuning in the indicated ranges is positive and at sodium vapor densities of $3\text{x}10^{16}$ cm^{-3} changes from 3 to 3.4 cm^{-1}. Calculations for wave detuning for buffer gas Xe, made in accordance with Cox's formula [16] indicates that in this range of wavelengths an Xe pressure in the order of 200 to 600 mm of the mercury column is required to provide the same negative wave detuning. Thus, by changing the Xe pressure, it is possible to achieve condition δk=0 for any wavelength in the indicated intervals.

We will evaluate, at first, the radiation gain with λ_1=1.4 microns, λ_2=455 nm for which $G_1(\omega_1,\omega)=5\times10^{-47}$ SGSE and R=0.1 ($G_1(\omega_3,\omega_3)=4\times10^{-45}$ SGSE. For $T=3\times10^{-10}$ seconds, $J_{30}\approx10^4$ SGSE (5 MW/cm^2) reverse length of DFP L^{-1}_{DFP}=1.4 cm^{-1}. If the condition of spatial synchronism is fulfilled on length L=30 cm., then the gain for one passage is equal to 3.6%. For λ_1=10 microns, λ_2=355 nm parameter R $\approx$ 0.04 and corresponding coefficient is equal to 0.6%. To obtain total gains of 10^{10} requires no less than 10/lg 1.036=650 passages for λ_1=1.4 microns and 3850 passages at λ_1=10 microns; for a resonator length of 40 cm, the time of increasing the oscillation pulses will be 1.7×10^{-6}, 10^{-5} respectively. It follows from here that for pumping such PGS, it is possible to utilize retunable laser sources with long pulses, for example, pigment lasers with tube pumping.

The maximum oscillation power is determined by conditions of fields attaining states, near to stationary ones, and may be 0.1 to 0.3 of the pumping power [18].

Conclusion

1. The ChPPDR in metal vapors and gases may be used for amplifying weak optical signals in a wide spectral range from vacuum UF to the far IR region. Corresponding amplifiers have an extremely low level of internal noises and their gains reach several orders of magnitude.

2. A four-photon parametric luminescence at a two-photon resonance, similar to the three-photon nonresonance luminescence observed in anisotropic nonlinear crystals [22,23] may be observed in metal vapors and gases. Lines of dispersed radiation are shifted with respect to resonance lines of the medium by an order of magnitude of cm^{-1} units and their powers attain values of 10^{-2} to 10^{-3} of the pumping power. These lines must shift in frequency when synchronism conditions change; for example, when a buffer gas is introduced into the cell containing the metal vapor.

3. Apparently, the creation of a PGS on the basis of a ChPPDR in gaseous media with small retuning regions (several cm^{-1}) will not produce great

difficulties. To provide parametric oscillation in wide UV and IR regions of the spectrum, it is necessary to have powerful sources of laser pumping with radiation pulse length of 10^{-5} to 10^{-6}, tuned to two-photon resonance with the corresponding transition of the medium.

The author is grateful to S. A. Bakhramov, D. N. Klyuchko and Yu. G. Khronopulo for the useful discussion of the paper and their valuable remarks.

BIBLIOGRAPHY

1. Hodgson, R. T.; Sorokin, P. P.; Wynne, J. J. Phys. Rev. Letts, 32, 343, (1974).

2. Venkin, G. V.; Krochik, G. M.; Kulyuuk, L. L.; Maleuev, D. I.; Khronopulo, Yu. G. ZhETF, 70, 1674 (1976).

3. Butylkin, V. S.; Krochik, G. M.; Khronopulo, Yu. G. KVANTOVAYA ELEKTRONIKA, 5, 698 (1978).

4. Korolev, F. A.; Bakhramov, S. A.; Odintsov, V. I. "Letters to ZhETF," 12, 131 (1970).

5. Korolev, F. A.; Bakhramov, S. A.; Odintsov,, V. I. OPTIKA I SPEKTROSKOPIYA, 30, 788 (1971).

6. Kirsanov, V. P.; Selivanenko, A. S. OPTIKA I SPEKTROSKOPIYA, 26, 986 (1969).

7. Il'inskiy, Yu. A., Taranukhim, V. S. KVANTOVAYA ELEKTRONIKA, 2, 1575, (1975).

8. D'yakonov, M. I. ZhETF, 47, 2213 (1964).

9. Il'inskiy, Yu. A.; Taranukhin, V. D. KVANTOVAYA ELEKTRONIKA, 2, 1497 (1975).

10. Bjorklund, G. C.; Bjorkholm, J. E.; Liao, P. E.; Storz, P. H. Appl. Phys. Letts, 29, 729 (1976).

11. Bjorklund, G. C.; Bjorkholm, J. E.; Freeman, R. R.; Liao, P.E. Appl. Phys. Letts, 31, 330 (1977).

12. Barch, W. E.; Feetterman, H. R., Schlossberg, H. R. Optics Comms, 15, 358 (1975).

13. Klyshko, D. N. ZhETF, 64, 1160 (1973).

14. Akhiezer, A. I.; Berestetskiy, V.B. "Quantum Electrodynamics, Moscow "Nauka", 1969.

15. Kasabov, G. A.; Yeliseyev, V. V. "Spectroscopic Tables for Low-Temperature Plasma," Moscow, Atomizdat, 1973, 1973.

16. Miles, R. B.; Harris, S. E. IEEE J., QE-9, 470 (1973).

17. Stapperts, E. A., Bekkers, G. W.; Young, J. F.; Harris, S. E. IEEE j., 12, 331 (1976).

18. Butylkin, V. S.; Krochik, G. M.; Khronopulo, Yu. G. ZhETF, 68, 506 (1975).

19. Ward, J. F.; New, H. C. Phys. Rev., 185, 57 (1969).

20. Krochik, G. M.; Krochik, G. M; Khronopulo, Yu. G. KVANTOVAYA ELEKTRONIKA, 2, 1693 (1975).

21. Tsernike, F.; Midvinter, J. "Applied Nonlinear Optics. Moscow, "Mir", 1976.

22. Kilshko, D. N.; "Letters to ZhETF, 6, 490 (1966).

23. Akhmanov, S. A.; Fadeyev, V. V.; Khokhlov, R. V.; Chunayev, O. "letters to ZhETF," 6, 575 (1966).

2291
CSO: 8144/1033

PHYSICS

UDC 66.092

ISOTOPE SEPARATION BY MULTIPHOTON MOLECULAR DISSOCIATION IN THE HIGH-POWER CO_2 LASER FIELD. PROSPECTS OF PRACTICAL REALIZATION

Moscow KVANTOVAYA ELEKTRONIKA in Russian Vol 6, No 2, Feb 79 pp 317-326

[Article by Ye. P. Velkhov, V. S. Letokhov, A. A. Makarov, Ye. A. Ryabov, Spectroscopy Institute, AN USSR (Moscow), submitted to ATOMNAYA ENERGIYA 6 Mar 78, submitted to KVANTOVAYA ELEKTRONIKA 2 Nov 78]

[Text] Consideration is given to the problems encountered in the practical implementation of a process of isotope separation by multiphoton dissociation. The process of optimization is made in order to achieve the maximum utilization of laser power. Estimations are presented of the efficiency of the method.

1. Introduction

In recent years, work was developed intensively on laser separation of isotopes,(see reviews [1,2]). This is related to the fact that laser methods, compared to existing traditional methods of isotope separation, have a number of advantages.

1. High selectivity of the elementary act of separation. In most traditional methods, the coefficient of separation by one step α is very small ($\alpha - 1 \leqslant 1$), therefore, to obtain a high degree of separation q, a great many separation steps, n, are required: $q = \alpha^n \gg 1$. Laser methods provide fundamentally the obtaining of $\alpha \gg 1$, which leads to a multifold reduction in the number of separation steps, reducing their number in many cases to one.

2. The possibility of separating the needed isotope, without affecting the other isotopes. When an element has a number of isotopes intermediate by weight, it is possible by using frequency retunable lasers to tune in on the absorption line of the needed isotope and separate it without practically affecting other isotopes.

3. Low power losses. Cited below are comparative power losses (electron/atom) [1] for various separation methods. It may be seen that for most traditional methods, power losses are greater than for laser losses.

Traditional methods:

1. Electromagnetic separation	10^6-10^7
2. Gas diffusion (for ^{235}U)	3×10^6
3. Gas centrifuge (^{235}U)	4.5×10^5
4. Distillation (for ^{10}B-^{11}B)	10^3
5. Chemical exchange (for ^{10}B-^{11}B)	10^2

Laser methods

1. Dissociation by IR radiation (for laser efficiency of 10%)	10^2
2. Ionization or dissociation by visible or UV radiation (for laser efficiency of 1%)	10^3
Thermodynamic limit	10^{-2}-10^{-1}

4. Low starting period. For the majority of laser methods, the stationary mode of operation is reached almost instantaneously. In traditional methods the starting period may take several months [3].

5. Possibility of carrying out the separation process by using only laser radiation. The absence in laser methods of such separating elements as plates, membranes etc. insures minimal contact between the enriched product and the surface of the apparatus and, therefore, minimum contamination. This is especially important for separating radioactive isotopes.

6. Universality. Laser methods, with rare exceptions, may be used with practically the same success for separating isotopes of any elements -- light, intermediate and heavy -- unlike traditional methods, the efficiency of most of which depend on the weight of the enriched product.

However, not all laser methods used successfully on a laboratory scale for separating isotopes in trace or even significant quantities are promising for isotope separation on a manufacturing scale. A method potentially suitable for manufacturing usage must have at least the following two features: the possibility of generating the radiation required for the laser method with an average power level from 1 kw to 1 Mw (depending upon the needed productivity); simplicity and efficiency of laser equipment in manufacturing and operation. These two requirements limit considerably the number of methods implemented on an industrial scale with the lasers known at present. Most promising from this viewpoint today, apparently, is a method based on the effect of isotopic-selective dissociation of multiatom molecules in a strong IR field. In this method, radiation is used of probably the simplest and cheapest pulsed CO_2 laser with a standard efficiency of 5 to 10%, the average power of which even today is a kw.

Since discovering the effect of isotopic-selective dissociation of molecules [4] and separating sulfur isotopes by this methods [5], a large number of experiments were made on investigating the physical nature of this phenomenon and the possibility of its use for isotope separation [1,2,6]. It was shown that molecule dissociation is a highly selective process, distinguished by high efficiency and, therefore, may be used as a promising method for isotope separation. However, all these experiments were made on laboratory installations with an average radiation power of the pulsed CO_2 lasers no greater than 3 to 5 watts and, usually, with small volume of the dissociation region. As already noted, in creating an industrial process for separating isotopes, it is necessary to use CO_2 lasers with high average radiation power (in the order of a kw and greater).

Naturally, such an increase in the scale of the separation process produces a number of problems. First, of course, it is necessary to obtain maximum productivity of the process. For this, it is necessary to choose an optimal arrangement for the process of obtaining a product with a given enrichment coefficient. The coefficient of utilization of laser radiation must be high. This problem is not so simple if it is considered that the required intensities of radiation may attain values of 10^7 to 10^8 w/cm^2 and the necessary characteristic line of the dissociation region for the full utilization of laser radiation may be several tens of meters. Moreover, using CO_2 lasers with high average power, in principle, may originate difficulties related to the liberation of heat and to a reduction in the selectivity of molecule dissociation due to the heating of the gases. Finally, it is necessary to select an optimal method for chemical bonding and subsequent extraction of molecule dissociation products from the excited isotopic composition after radiation.

Thus, only after solving all these problems will it be possible to create an industrial installation for separating isotopes. Therefore, the aim of this paper is to investigate the indicated problems on the example of separating isotopes of sulfur ^{34}S and ^{32}S when dissociating SF_6 molecules by the radiation of a pulsed CO_2 laser with a high average power.

2. Characteristics of Isotopically-Selective Dissociation (SF_6 Molecule)

Experimental investiaations of the dissociation of a great number of multiatom molecules indicated that the dissociation process independently of the type of molecule, is characterized by a number of general parameters. Using the results of investigations of molecule SF_6 [7,8] dissociation, we will cite briefly its basic characteristics that we will need in the future.

Velocity of dissociation. When irradiating sulfur hexafluorine by the intense pulse of a CO_2 laser, a dissociation of SF_6 occurs and the concentration of the irradiated molecules m decreases exponentially with time t or the number

of irradiation pulses N so that

$$m = m_0 \exp(-\omega N), \qquad (1)$$

where m_0 is the initial concentration of the irradiated molecules. The value of ω in (1) by analogy with chemical kinetics is determined as the velocity of molecule dissociation (during the pulse) in the volume of the strong field V_0 region. Expression (1) is written for the case when the volume of cuvette $V_k = V_0$. If they differ, so that $\Gamma = V_0/V_k < 1$, then for a condition that during the time between pulses the gas moves over the entire volume of the cuvette, it is easy to obtain

$$m = m_0 [1-\Gamma(1-e^{-\omega})]^N = m_0 [1-\Gamma\beta]^N, \qquad (2)$$

where the value of β, follows from (1), is the portion of the molecules dissociating in the volume of the region of strong field V_0 during one pulse.

The molecule dissociation process in a strong IR field has a threshold nature. The dissociation threshold, as well as its velocity in SF_6, is determined by the density of the pulse energy [9] and not by its intensity. This, apparently, takes place until the duration of the radiation time is less than the characteristic time between collisions, i.e., the effect of collisions on the process of multiphoton excitation of molecules and their dissociation may be neglected. In the case of SF_6, this corresponds to pressures p at which $p\tau_{имп} \lesssim 30$ nanoseconds-mm of the mercury column. The characteristic value of threshold energy density for SF_6 is $\Phi_{пор} = 2.0$ joules/cm^2. At energies higher than the threshold, the velocity of dissociation w is proportional to the cube of the energy density Φ and the relationship between w and Φ may be written for SF_6 in the form

$$\begin{cases} w = w_1 + w_2(\Phi/\Phi_{пор} - 1)^3 & \text{at } \Phi \geq \Phi_{пор}, \\ w = 0 & \text{at } \Phi < \Phi_{пор}, \end{cases} \qquad (3)$$

where $w = 10^{-3}$, $w = 5 \times 10^{-3}$ for the P16 line of the CO_2 laser.

Dissociation selectivity. When radiating a mixture of molecules with various sulfur isotopes, a dissociation of molecules occurs of that isotope composition on the absorption region of which is tuned the radiation frequency of the laser. AS a result of this, there is an enrichment of the residual mixture of the SF_6 gas not excited by the isotope molecules due to the "burning out" of the others. In the dissociation products and further chemical reactions, conversely, enrichment occurs of those sulfur isotopes which are in the composition of the SE_6 molecules being excited.

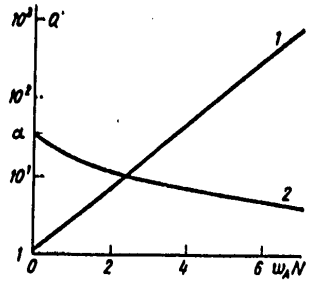

Fig. 1. Relationship between degree of separation Q and duration of radiation (in units of $w_A N$) of gas in cuvette ($\Gamma = 1$) at excitation of isotope A for enrichment in the residual gas (1) and in products of dissociation (2).

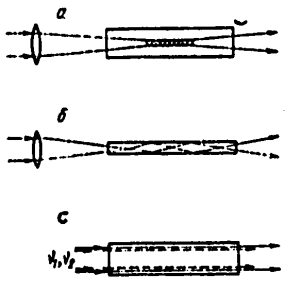

Fig. 2. Geometry of radiation:
a -- focusing by lens (dissociation region cross-hatched); b -- Light-guiding geometry; c -- molecule dissociation at frequencies ν_1 and ν_2 in the direct beam.

Separation coefficient α is the selectivity characteristic of the dissociation process for the excitation of molecules of selected isotope composition A with respect to molecules B of a different kind. The value of α, naturally, determines the ratio of the share of A type molecules, dissociating during one pulse to the share of the B type dissociating molecules.

$$\alpha = \frac{[A]_0 - [A]_1}{[A]_0} : \frac{[B]_0 - [B]_1}{[B]_0} = \frac{\beta_A}{\beta_B} = \frac{1 - \exp(-w_A)}{1 - \exp(-w_B)}. \quad (4)$$

When dissociating molecules with isotope A, there takes place an enrichment of the mixture by isotope B and, in this case, the $q_{ост}$ in the residual gas is determined as

$$q_{ост}(B/A) = \frac{[B]_N}{[A]_N} : \frac{[B]_0}{[A]_0}, \quad (5)$$

where index "0" refers to the unradiated mixture and "N" -- to the radiated mixture. Using (2), we obtain

$$q_{ост} = \left(\frac{1 - \beta_B \Gamma}{1 - \beta_A \Gamma}\right)^N. \quad (6)$$

Enrichment with isotopes A occurs in the products of dissociation and the degree of $q_{пр}$ separation is equal to

$$q_{пр}(A/B) = \frac{\Delta[A]}{\Delta[B]} : \frac{[A]_0}{[B]_0} = \frac{1 - (1 - \beta_A \Gamma)^N}{1 - (1 - \beta_B \Gamma)^N}. \quad (7)$$

The nature of the relationship between the degree of separation in the residual gas and in the products of dissociation when irradiating a portion of gas in the cuvette and the number of the pulse is shown in Fig. 1. As may be seen, the degree of separation in the residual gas increases with the proportion of radiation, and for a large enough number of pulses, it is possible to obtain any previously given value of $q_{ост}$. The degree of separation in dissociation products decreases with the proportion of radiation. For a small degree of molecule dissociation in the cuvette $\beta_A \Gamma N \ll 1$, the value $q_{пр}$ attains the maximum value equal to the separation coefficient $q_{пр} \approx \beta_A / \beta_B = \alpha$, and thus is the selectivity characteristic of the dissociation process.

The investigation of enrichment in products of dissociation of SF_6 indicated that when dissociating $^{32}SF_6$ and a gas pressure of 0.1 mm of the mercury column $\alpha \approx 25$ to 30. The selectivity of the dissociation process decreases

exponentially with an increase in SF_6 and a reduction of the value of α by e times occurs when the SF_6 pressure increases by about 0.6 mm of the mercury column. Therefore, when separating isotopes it is necessary to work at pressures less than 1 mm of the mercury column.

3. Geometry of Radiation and the Coefficient of Utilization of Laser Radiation

Molecule dissociation in a strong IR field has a threshold nature and the dissociation velocity depends very strongly on exceeding the radiation energy density above the threshold $w \sim (\Phi/\Phi_{пор})^n$. . The density of radiation energy at the output of the presently available periodic-pulse CO_2 lasers does not usually exceed 1 to 1.5 joules/cm^2 and is basically determined by the beam strength of the optical elements. Thus, in order to provide an efficient dissociation of molecules in the volume of the laser beam, it is necessary to compress it. At the same time, the characteristic dimensions of the strong field region must be large enough to provide simultaneously the maximum utilization of laser radiation.

Since it is necessary to work at gas pressures less than 1 mm of the mercury column, the coefficient of nonlinear radiation absorption $\varkappa_r$ is very small. For SF_6 at p= 0.1 mm of mercury column $\varkappa_r \approx 10^{-4}$ cm^{-1} [7]. In this case, the characteristic length of the strong field region may be several tens of meters.

The efficiency of laser radiation utilization is characterized by coefficient

$$\eta = D_0 N_д / E_0. \qquad (8)$$

where D_0 -- energy of molecule dissociation; $N_д$ -- number of molecules dissociating in the volume of strong field V_0; E_0 -- energy of the radiation pulse.

The maximum value of the coefficient of radiation utilization $\eta_{max} = 1$ is attained when all the energy of the laser pulse goes to molecule dissociation. However, due to the fact that not all excited molecules have energy greater than the dissociation energy, as well as because of difficulties in creating a volume of dissociation region sufficient for the absorption of the entire pulse, $\eta < 1$ is realistic. To obtain high productivity, it is necessary to attain η as large as possible. We will consider the available possibilities.

Focused geometry of radiation. In the simplest case, the region of a strong field may be created by focusing radiation by a lens (Fig. 2a). Let the diameter of the radiation beam on the surface of the lens with a focal distance f be $2r_0$, the divergence of radiation φ, then, considering laser

radiation in the form of a set of plane waves with a full aperture angle 2φ, we will obtain a radius of the spot in the focus $r_1 = f\varphi$. The density of the pulse energy in the focus $\Phi_1 = E_0/(\pi f^2\varphi^2)$, , from which the focal distance of lens $f = \varphi^{-1}|E_0/(\pi\Phi_1)|^{1/2}$. The length of the region in which the radiation density $\Phi \geqslant \Phi_1/\gamma$ $(\gamma > 1)$, and its volume V_0 are equal

$$l \approx 2\frac{f^2\varphi(\sqrt{\gamma}-1)}{r_0 - r_1} = \frac{2}{\pi}\frac{E_0(\sqrt{\gamma}-1)}{\varphi\Phi_1(r_0 - r_1)}, \tag{9}$$

$$V_0 \approx \frac{2}{3\pi}\frac{(\gamma\sqrt{\gamma}-1)}{(r_0 - r_1)}\left(\frac{E_0}{\Phi_1}\right)^2. \tag{10}$$

We will evaluate the efficiency of laser radiation utilization for typical parameters of the laser pulse $E_0 = 10$ joules, $\varphi = 10^{-3}$ radians, $2r_0 = 3$ cm. We will select for SF_6 the energy density at the focus from the condition that $w = 1$, which corresponds to $\Phi_1 = 14$ joules/cm^2. It was not beneficial to select a greater value of w because then, as follows from (4), the dissociation selectivity decreases. We will determine the volume of the strong field region from the condition that on its boundary $w = 0.1$, which corresponds to $\gamma = 1.9$ (it is easy to show, using (3), that the greatest part of the molecules are dissociated in this region).

Using (10), we will determine the volume of the region of the strong field $V_0 \approx 135$ cm^3. Energy of the SF_6 dissociation on $SF_6 + F$ is equal to 3.3 electron volts. Using (3), it is easy to obtain $\beta = N_д/N_0 = 0{,}3$. . Finally, from (8) we obtain that the coefficient of radiation utilization in the considered case is $\eta \approx 0.8\%$.

It follows from here that a single focusing of radiation by a lens is inefficient. The radiation must be focused several times in sequence. However, it is more efficient to utilize a wavebeam guide [10] for creating a strong field in a large volume.

Wavebeam guide geometry of radiation. The wavebeam guide (Fig. 2b) is a metal tube with a well-polished inner surface. Laser radiation is focused within the tube and if its radius r_1 is smaller than $r_{пор} = (E_0/\pi\Phi_{пор})^{1/2}$, then the gas within the wavebeam guide is dissociated. Due to the absorption of radiation by molecules and walls of the guide by reflections, the density of energy radiation is decreased along the length of the guide. Therefore, it is natural to select a length of the guide on the basis of the condition of equality of the energy density at its exit and the threshold energy for dissociation. We have from here

$$\exp(\varkappa L) = \Phi_1/\Phi_{пор}, \tag{11}$$

where Φ_1 -- energy density at the wavebeam guide entrance. It was assumed here that the radius of the guide is approximately equal to the radius of the light beam at its entrance $r_1 \approx f\varphi$. The absorption coefficient per unit length $\varkappa = \varkappa_r + \varkappa_c$ is written in the general form. The contribution to absorption by molecules $\varkappa_r$ and walls $\varkappa_c$ will be evaluated below. For simplicity, we will assume that the radiation energy distribution is uniform over the cross section of the guide. Then, using (3), we obtain

$$N_{\text{д}} \approx \pi m_0 r_1^2 \int_0^L \left\{ w_1 + w_2 \left[\frac{\Phi_1 \exp(-\varkappa x)}{\Phi_{\text{пор}}} - 1 \right]^3 \right\} dx, \qquad (12)$$

where m_0 -- density of molecules excited by the laser, while the length of the guide L is determined from (11).

We will introduce a nondimensional parameter $z = \Phi_{\text{пор}}/\Phi_1$. . Integrating 12, we obtain

$$N_{\text{д}} \approx (\pi m_0 r_1^2/\varkappa) h(z), \qquad (13)$$

where function h(z) has the form

$$h(z) = w_2 [1/3 (z^{-3}-1) - 3/2 (z^{-2}-1) + 3 (z^{-1}-1)] + (w_2 - w_1) \ln z. \qquad (14)$$

Parameter z changes from $z = 1$, which corresponds to the dissociation threshold, to $z = 0.14$, which corresponds to the dissociation velocity of the wavebeam guide $w = 1$ at the guide entrance.

From (13) it is easy to obtain the expression for the coefficient of radiation utilization:

$$\eta \quad D_0 N_{\text{д}}/E_0 \approx (D_0 m_0/\varkappa \Phi_1) h(z). \qquad (15)$$

It follows from (15) that the situation is optimal when the absorption by the walls of guide $\varkappa_c$ is less than the absorption by molecules $\varkappa_r$.

We will evaluate the absorption coefficient for reflected $\varkappa_c$, using known metal optics formulas [11]. At incidence angles ψ , near $\pi/2$, the absorption coefficient is proportional to angle $\pi/2 - \psi$ and it may be presented in the form

$$R_{\parallel} \approx a_{\parallel} \quad (\pi/2 - \psi) \qquad (16)$$

for a wave, polarized in the incidence plane, and

$$R_{\perp} \approx a_{\perp} (\pi/2 - \psi) \qquad (17)$$

for polarization in the plane perpendicular to the incidence plant. Values

of $a_{\parallel}$ and $a_{\perp}$ are determined by the properties of metal, and for copper $a_{\parallel} = 12.7$, $a_{\perp} = 1.4$. Knowing $a_{\parallel}$ and $a_{\perp}$, we will evaluate $\varkappa_c$. The characteristic incidence angle for the guide wall $\psi_x \approx \pi/2 - r_0/f$, where r_0 is the radius of the beam in the plane of the focusing lens; f is its focal distance. Characteristic distance x_x from the entrance of the guide on which the greater part of the radiation encounters the first reflection $x_x \approx 2r_1 (\pi/2 - \psi_x)^{-1}$. Since, when reflecting from the cylindrical surface of the guide, both polarizations are probable, then for $\varkappa_c$ it may be written approximately

$$\varkappa_c \approx \frac{a_{\parallel} + a_{\perp}}{2} \frac{\pi/2 - \psi_x}{x_x} = \frac{a_{\parallel} + a_{\perp}}{2x_x} \frac{r_0^2}{2\varphi f^3} = \frac{a_{\parallel} + a_{\perp}}{4} r_0^2 \varphi^2 \left(\frac{\pi \Phi_1}{E_0}\right)^{4/3}. \quad (18)$$

We will consider now numerical examples for dissociation of $^{32}SF_6$ and pressure of gas p = 0.1 mm of the mercury column for the case of a copper wavebeam guide. As before, we will assume for the parameters of the laser beam $r_0 = 1.5$ cm, $\varphi = 10^{-3}$ radians. The table for various energies of the laser pulse and parameters z shows $\varkappa_c$, η and the calculated length of guide L at pressure SF_6 0.1 mm of the mercury column, $\varkappa = 10^{-4}$ cm^{-1}.

It may be seen that at relatively low energies $E_0 \leq 5$ joules losses in the guide are basically related to absorption when reflected on walls, since the small amount of energy requires more rigid focusing of radiation in the guide and increasing the number of reflections. In this case, a strong dependence of pulse energy on values of $N_{\text{д}} \sim E_0^{5/2}$, $\eta \sim E^{3/2}$ is observed. For pulse energies $E_0 > 5$ the basic role is played by SF_6 molecules and, in this case, $N_{\text{д}} \sim E_0$ and η depend very little on E_0. Evaluations done show the wavebeam guide geometry permits raising considerably the utilization coefficient of radiation by a lens. Thus, for $E_0 = 10$ joules in wavebeam guide geometry $\eta = 17\%$ instead of 0.8% for focusing. The shortcomings of guide geometry include rather rigid requirements for the quality of the inner surface of the guide. However, as follows from the table, even at $\varkappa_c > \varkappa_r$ the guide geometry insures a considerably greater value of η compared to focusing.

Two-frequency dissociation of molecules. Another approach to the problem of increasing the efficiency of the separation process is using a two-frequency excitation of molecules [12].

For two-frequency excitation (Fig. 2c) the "weaker"field at frequency ν_1, produces isotope-selection excitation of molecules at several oscillating levels. Further excitation and dissociation of molecules is done by the "strong" field at frequency ν_2, tuned usually to the red side from the molecule absorption band. As shown by the first experiments [13, 14], in this case, velocity of dissociation w increases sharply, while the dissociation

threshold decreases to several tens of joules per square centimeter. This important circumstance makes it possible to work with direct beams without focusing the radiation. At the same time, at two-frequency excitation, there is an increase in the dissociation selectivity, especially in the case of molecules with a small isotope shift in the oscillating spectrum, typical for heavy elements.

Calcualtion of Wavebeam Guide

(1) E_0, Дж	z	$\frac{\delta}{x_0}$	L, м	η, %
1	0,16	19	9,2	1,4
	0,25	9	13,9	0,7
	0,36	5,8	15	0,27
2	0,16	6,9	23	3,6
	0,25	3,5	30	1,6
	0,36	2,0	34	0,59
4	0,16	2,4	54	7,8
	0,25	1,2	63	3,3
	0,36	0,7	60	1,1
7	0,16	1,0	92	14
	0,25	0,5	92	4,7
	0,36	0,3	79	1,4
10	0,16	0,6	115	17
	0,25	0,3	107	5,5
	0,36	0,2	85	1,6

1. E_0, joules.

Thus, when retunable lasers are available, which provide the necessary detuning between frequencies of excitation ν_1 and dissociation ν_2, the use of the two-frequency method solves the problem of utilizing radiation and providing high productivity of the separation process.

4. Selection of the Optimal Arrangement of the Isotope Separation Process

An important parameter, which characterizes the separation process, is productivity -- the amount of product with a given content of the desired isotope, obtained per unit time. Its value, naturally, depends on the required degree of separation and the initial concentration of the desired isotope x_0 and, for fixed parameters of the laser, is determined primarily

by coefficient η , dissociation selectivity α and the selection of the separation arrangement.

Let there be a mixture of two isotopes. Usually it is necessary to obtain a strong increase at the exit in the content of the "poor" isotope. As mentioned in section 2, this may be achieved in two ways. The "rich" isotope may be dissociated and enrichment of the desired isotope in the residual gas may be obtained. However, for an equal coefficient of utilization of laser radiation, more beneficial is a process in which dissociation of the desired isotope and the enrichment of it with products of dissociation are produced directly. Actually, energy required for the dissociation of one molecule is equal for both isotopes, however, the initial product contains in $(1-x_0)/x_0$ more of the rich isotope compared to the poor, desired one. Therefore, even at optimal (see below) dissociation of the rich isotope, the radiation increases by $(1-x_0)/x_0$ times. Thus, for equal utilization of laser radiation when dissociating the desired isotope

$$j_{\text{п}} \quad |(1-x_0)/x_0|j_{\text{б}}, \tag{19}$$

where $j_{\text{б}}$ -- productivity when dissociating the rich isotope. However, this gain is realized only for $\alpha \gg x_0^{-1}$, when all the absorbed energy of laser radiation goes for dissociating the desired isotope. In the converse case, when $\alpha \ll x_0^{-1}$, basic energy expenditures when radiating the desired isotope are related to the dissociation of the rich isotope and the gain in productivity will be considerably less than follows from (19). This case is realized, for example, in concentrating heavy water, whose content in nature is $x_0 = 0.01\%$ and it is difficult to expect that $\alpha \gg 7000$ can be attained. It may be shown that in the general case for an arbitrary relationship between α and x_0, $(x_0 \ll 1)$,

$$\frac{j_{\text{п}}}{j_{\text{б}}} = \frac{1-x_0}{x_0} \frac{\alpha x_0}{1+x_0(\alpha-1)}. \tag{20}$$

In the case where $\alpha \ll x_0^{-1}$ we obtain from (20)

$$j_{\text{п}} = \alpha j_{\text{б}}. \tag{21}$$

We will now evaluate the productivity of the enriching process in cases where the desired isotope, or the rich isotope are dissociated. Let the region

of strong field V_o in cuvette V_k be created by one of the methods in section 3 and, for simplicity, we will assume that $\Gamma = V_o/V_k = 1$. We will consider that the portion of molecules of the excited isotope, dissociating in this volume furing a pulse, is equal to β, and of the nonexcited (due to finite selectivity) -- $\beta_s = \beta/\alpha$.

4.1. Dissociation of the desired isotope. In this case, as follows from (7), for a single radiation the degree of separation in dissociation products $q_1 = \alpha$. If it is necessary to obtain $q > \alpha$, then the products of the dissociation can be restored anew in the initial molecule and the radiation repeated. In each such step the degree of separation $q_1 = \alpha$ and after n steps

$$q = (\beta/\beta_s)^n = \alpha^n. \tag{22}$$

Since, in the considered method, $\alpha \gg 1$ ($\alpha = 25$ to 30 for SD_6), then compared to traditional methods, the number of steps is reduced sharply and in case of $q \leqslant \alpha$ is reduced to one.

Let there be an initial mixture M containing quantity M_o of the desired isotope and m_o of the rich isotope. We will assume that an equal portion of the excited molecules is dissociated at each step. Then, after n steps we will have $M_n = M_o \beta^n$ of the desired isotope. We will determine the minimum number of pulses required for carrying out this process. We will assume that at each step, the total number of molecules in the volume of the strong field is constant, i.e., $p = M_i^* + m_i^* = \text{const}$. It is then easy to show that at the i-th step the number of pulses at $\alpha \gg 1$

$$N_i = \frac{M_o \beta^{i-1}}{p}\left(1 + \frac{1}{\alpha^{i-1} x_o}\right). \tag{23}$$

The total number of pulses for n steps

$$N_n = \Sigma N_i = \frac{M_o}{p}\left[\beta \frac{1-\beta^{n-1}}{1-\beta} + \frac{1}{x_o}\frac{1-(\beta/\alpha)^n}{1-\beta/\alpha}\right] = \frac{M_o}{p} y. \tag{24}$$

For $\beta < 1$, $x_o \ll 1$, $\alpha \gg 1$, value of $y \approx x_o^{-1}$ and the radiation time are

determined in the basic time of the first step because $N_1 = (M_o/p)\ x_o^{-1}$.

Finally we have that the productivity of the process when reaching the separation degree $q = \alpha^n$ is

$$I_n = (M_n + m_n)\theta/N_n \approx (x_0/x)\beta^n p\theta = (x_0/x)\beta^n L_n, \qquad (25)$$

where x -- the final content of the desired isotope; θ -- frequency of pulse repetition; L_n -- flow of initial raw material, while the number of steps is equal to $n = \ln q/\ln\alpha$.

Realistically, apparently, it is difficult to obtain $\beta > 0.5$ to 0.6, therefore, at smaller values of β, since the time of the entire process is determined basically by the length of the radiation time in the first step, it is necessary to increase the radiation time in the following steps in such a way that when the gas passes through the radiated cuvette, it would be subjected to several radiation pulses (their number $l > 1$). In this case, the portion of dissociated molecules of the desired isotope will increase:

$$\delta = [1-(1-\beta)^l]. \qquad (26)$$

For such a separation process the productivity will be

$$I_n \approx (x_0/x)\beta\delta^{n-1}L_n, \qquad (27)$$

and the separation degree after n steps $q = \prod_{i=1}^{n} q_i$. Comparing (25) and (27), we see that the productivity in the latter case may be considerably higher, especially at small β . If the laser can excite the desired isotope as well as the rich one, then the optimal process will appear as follows. The dissociation of the desired isotope is done in the first step and dissociation degree $q \approx \alpha$ is attained. Since $\alpha \gg 1$, isotope concentration becomes comparable, and in the second step (after chemical conversion) the already

unneeded rich isotope is dissociated up to obtaining the required concentration x of the desired isotope in the residual gas. The duration of the second step is considerably smaller than the time of the second step for $\alpha \gg 1$: $\tau_2 \ll \tau_1 \beta (x_0 - 1/\alpha)$. Therefore, productivity is determined only by the duration of the first step, and for the entire process it may be written:

$$I_{опт} \approx (x_0/x)\beta I_{\text{п}}. \qquad (28)$$

4.2. Dissociation of the rich isotope. If, for some reason, the dissociation of the desired poor isotope is impossible, the enrichment process may be done also by the dissociation of the rich isotope, although the productivity in this case, as mentioned before, is smaller. Such a situation is realized, for example, when enriching isotope ^{34}S, since the region of the retuning of existing CO_2 lasers does not provide for the possiblilty of efficient dissociation of $^{34}SF_6$ and the process of enrichment may be carried out only by dissociating $^{32}SF_6$. In this case, two possibilities for carrying out the process are available which in simplified form, appear as follows.

Mode of "deep burn-out." In this mode, the gas in the cuvette is irradiated up to the obtainment of the given enrichment of the desired isotope in the remaining initial product. After that, a new portion of gas is passed into the cuvette. Thus, at the output we have at once a product with a given degree of separation q. If the initial amount of the desired isotope in the cuvette is M_0^* and the rich one m_0^*, then after N pulses

$$M_N^* = M_0^*(1-\beta_*)^N = M_0^* \exp(-\omega_* N) \text{ и } m_N^* = m_0^*(1-\beta)^N = m_0^* \exp(-\omega N),$$

and

$$m_N^* = m_0^*(1-\beta)^N = m_0^* \exp(-\omega N),$$

from where the degree of separation is

$$q = \frac{M_N^*}{m_N^*} : \frac{M_0^*}{m_0^*} = \exp[(w - w_s)N].$$

the number of radiation pulses to obtain the given q

$$N = \ln q/(w - w_s). \tag{29}$$

For $w < 1$, the separation coefficient $\alpha \approx w/w_s$. Taking into account (29) we obtain

$$M_N^* = M_0^* q^{-w_s/(w-w_s)} = M_0^* q^{-1/(\alpha-1)}, \tag{30}$$
$$m_N^* = m_0^* q^{-w/(w-w_s)} = m_0^* q^{-\alpha/(\alpha-1)}, \tag{31}$$

and content x of the desired isotope after radiation is

$$x = \frac{M_N^*}{M_N^* + m_N^*} = \frac{1}{1 + (m_0/M_0)\, q^{-1}}. \tag{32}$$

In this case, the productivity of obtaining product $M_N^* + m_N^*$ with enrichment q and content x at a frequency of pulse repetition θ is equal to

$$j_r = \frac{(M_N^* + m_N^*)\,\theta}{N} = \frac{M_0^*\theta\,(w - w_s)\,q^{-1/(\alpha-1)}}{x \ln q} = \frac{x_0 L_r\,(w - w_s)\,q^{-1/(\alpha-1)}}{x \ln q}, \tag{33}$$

where x_0 -- initial concentration of the desired isotope; L_r -- flow of initial raw material at the entrance of the cuvette.

However, such an arrangement of the enrichment process when obtaining a sufficiently high value of q is not optimal from the viewpoint of obtaining maximum productivity. This is due to the fact that the quantity of dissociated mulecules $N_\mu = m_0^* w e^{-\omega N}$ during one pulse decreases with the time of radiation as the excited molecules burn out. This leads to a reduction in coefficient η (8) and to a reduction of the process productivity as a whole, therefore, the separation process must be done differently.

Mode of constant partial pressure of dissociated rich isotope. To attain maximum productivity, it is necessary to provide a constant maximum N_μ during the entire enrichment process. This condition is met by maintaining constant pressure of the excited rich isotope in the cuvette. As an illustration, we will consider the following simplified arrangement of the process.

Let there be a certain amount of initial product so that the mass of the desired isotope is M_0 and the mass of the rich isotope is m_0. The gas is pumped through the irradiated cuvette and at any moment of time it contains m_0^* of the rich isotope being dissociated at partial pressure p. To obtain high productivity, it is necessary to have such a speed of gas pumping that during its passage through the cuvette $\Delta m^*/m_0^* \leq$ of the amount of irradiated molecules succeed in being dissociated. In our case, the cuvette volume is equal to the volume of the strong field, which corresponds to a single gas radiation in the cuvette, so that $\Delta m^*/m_0^* \leq \beta$. After irradiating all the gas, it is cleaned of the dissociation products. This radiation cycle is repeated at the same partial pressure of the excited isotope etc. In this case, during the entire enrichment time, the values of N_μ, and, therefore, η are maintained constant.

In each repeated cycle, the total gas pressure will increase due to an increase in the partial pressure of the desired isotope. Such cycles must be repeated up to the attainment of the given degree of q enrichment. Since, in each cycle there is produced $\Delta m/m = \beta$ of the rich isotope being dissociated

and because of finalselectivity $\Delta M/M \simeq \beta_s$ of the desired one, after n cycles we will have

$$q = [(1-\beta_s)/(1-\beta)]^n. \qquad (34)$$

Comparing (22) and (34), it is apparent that for dissociation of the rich isotope, the number of cycles and enrichment steps increases considerably.

It is easy to show that the number of pulses in the i-th cycle is

$$N_i = (1-\beta)^{i-1} m_0/m_0^*. \qquad (35)$$

From here, the total number of pulses for enriching the initial amount of gas is

$$N_n = \frac{m_0}{m_0^*} \sum_{i=1}^{n} (1-\beta)^{i-1} = \frac{m_0}{m_0^*} \frac{[1-(1-\beta)^n]}{\beta}. \qquad (36)$$

After n cycles, the remaining quantities of q are: the desired isotope $M_n \simeq M_0(1-\beta_s)^n$ and of the rich isotope $m_n = m_0(1-\beta)^n$. From here, we obtain for productivity in the mode of constant partial pressure

$$j_n = \frac{\theta (M_n + m_n)}{N_n} = \frac{x_0 \beta q L_n}{x[(1-\beta]^{-n} - 1]}, \qquad (37)$$

where L_n --- flow of initial raw material; x -- final content of desired isotope. Since

$$(1-\beta)^{-n} = q^{w/(w-w_s)} \approx q^{\alpha/(\alpha-1)}$$

at $\alpha < 1$, we obtain from (37)

$$j_n = \frac{x_0}{x} \frac{q\beta L_n}{(q^{\alpha/(\alpha-1)}-1)}. \qquad (38)$$

At low values of q, the value of j_n approach j_r (35) and at

$$q=(1-\beta_0)/(1-\beta),$$

i.e., for one cycle of radiation $j_n=j_r$.

From (33) and (37), it is easy to determine the ratio of productivities in these separation arrangements for dissociation of a rich isotope:

$$\chi = \frac{j_n}{j_r} = \frac{\alpha}{\alpha-1} \frac{\ln q}{(1-q^{-\alpha/(\alpha-1)})}. \qquad (39)$$

Fig. 3 shows a result of calculating the value of χ depending on q for $\alpha=30$. As may be seen, the mode of constant partial pressure of the isotope being dissociated is considerably more beneficial compared to the mode of deep burnout.

It should be noted, however, that while a gain of 3 to 4 times in productivity is entirely attainable, it is unrealistic to obtain a 10-fold gain. This is due to the fact that in calculating j_n, it was assumed that the selectivity of α during the entire process is constant. However, due to an increase in the partial pressure of the desired isotope, as it is being enriched, α decreases. Thus, for example, when enriching sulfur isotope ^{34}S to $x=0.999$ (natural content is 4.2%), as a result of dissociation of $^{32}SF_6$ (content of ^{32}S -- 95%), in the last cycles the pressure of $^{34}SF_6$ will be $p(^{34}SF_6)\approx 1000$, $p_0(^{32}SF_6)=100$ mm of the mercury column for $p_0(^{32}SF_6)$ 0.1 mm of the mercury column. At such a pressure the value of α will drop sharply. At the same time, for $x=0.8 (q=96)$, when $\chi=5$, at the end of

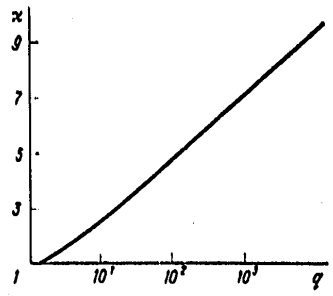

Fig. 3. Relationship between the productivity ratio in modes of constant partial pressure and "deep burn-out" $\chi = j_n / j_r$ for the dissociation of the rich isotope.

process p ($^{34}SF_6$) $\approx 3.6p_0 = 0.36$ mm of the mercury column and, in this case, the selectivity is still high ($\alpha \gg 1$).

5. Calculation of Productivity (on Example of SF_6)

We will evaluate the productivity of the enrichment process of an isotope for a natural content of ^{34}S and ^{32}S isotopes in the initial raw material. The enrichment will be done in a wavebeam guide geometry of radiation in the mode of constant partial pressure of the rich $^{32}SF_6$ isotope being dissociated. From (13) and (14) it is easy to determine the portion β of $^{32}SF_6$ molecules being dissociated in the volume of the wavebeam guide during a pulse:

$$\beta = \ln^{-1}(1/z)h(z). \qquad (40)$$

In particular, for $z = 0.14$, $\beta = 0.16$. Therefore, it is necessary to renew the gas in the wavebeam guide fully during the time between pulses. This may be acheved by pumping gas, for example, through longitudinal side slots in

in the guide. The size of the slot is sensibly selected on the condition that radiation losses on it do not exceed absorption losses in the guide. Evaluations show that for $r_0 = 1.5$ cm, $\varphi = 10^{-3}$ radians, $z = 0.14$ the width of the slot changes in the interval $(6.5 \text{ to } 60)\times10^{-3}$ cm at $1 \leqslant E_0 \leqslant 10$ joules. For these slot sizes the condition for the speed of pumping is fulfilled with a reserve: total gas changes during the time between pulses up to $\theta = 100$ Hz.

Let laser pulse energy be E_0 10 joules, frequency of pulse repetition $\theta = 100$ Hz, partial pressure of $^{32}SF_6$ 0.1 mm of the mercury column. We will determine the productivity of j_η for 96-fold enrichment of ^{34}S isotope (final content $x = 0.8$). Under these conditions, the average selectivity during the entire process is $\bar{\alpha} = 15$. Utilizing (38), we find that for an average laser power of q,1 kw, a coefficient of radiation utilization $\eta = 17\%$ (see Table), the productivity is $j_\eta \approx 7$ grams/hour of sulfur with a content of ^{34}S $x = 0.8$. As has been shown before, the process of ^{34}S enrichment by dissociating molecules with the desired $^{34}SF_6$ molecules would be considerably more beneficial. In this case, for the same value of $\eta = 17\%$, the productivity may reach

$$j_u \approx \frac{1-x_0}{x_0}\,\frac{\alpha x_0}{1+x_0(\alpha-1)} \approx 9\eta.$$

An important feature of the considered laser method for separating isotopes compared to the traditional ones is the considerably lower flow of raw material at the entrance to the installation for an equal degree of separation and productivity. Actually, as shown in [3], in traditional methods for obtaining at the exit a product with content x for an initial content x_0, the required minimal flow of raw material will be L_T, so that

$$j_T \approx (x_0/x)\varepsilon L_T. \qquad (41)$$

where $\varepsilon = \alpha - 1$ -- coefficient of enrichment.

In the mode of constant partial pressure, we obtain from (38) at $\alpha \gg 1$

$$j_{\Pi} \approx (x_0/x)\beta L_{\Pi}. \qquad (42)$$

From (41) and (42), we find that at $j_T = j_{\Pi}$

$$L_{\Pi} = (\varepsilon/\beta) L_T. \qquad (43)$$

Since, in traditional methods $\varepsilon = 10^{-2}$ to 10^{3}, the flow reduction is quite considerable. This is due to a considerably greater selectivity of the laser method of separation.

Thus, the evaluations cited above of the productivity of an isotope separation method based on the dissociation of molecules in a strong IR field, taking into account the available prospects for further development (the utilization of two-frequency excitation) show that this method may be used successfully for separating isotopes on an industrial scale.

BIBLIOGRAPHY

1. Letokhov, V. S.; Moore, C. B. KVANTOVAYA ELEKTRONIKA, 3, 248, 485 (1976).

2. Letokhov, V. S.; Moore, C. B. In: "Chemical and Biochemical Applications of Lasers," vol 3, New York, Acad. Press. 1977.

3. Rozen, A. M. "Theory of Separating Isotopes in Columns, Moscow, Atomizdat, 1960.

4. Ambartsumyan, R. V.; Letokhov, V. S.; Ryabov, Ye. A.; Chekalin, N. V. "Letters to ZhETF," 20, 597 (1974).

5. Ambartsumyan, R. V.; Gorokhov, Yu. A.; Letokhov, V. S.; Makarov, G. N. "Letters to ZhETF,: 21, 375 (1975).

6. Ambartsumyan, R. V.; Letokhov, V. S. In "Chemical and Biochemical Applications of Lasers," Acad. Press. N. Y., 1977, v 3.

7. Ambartsumyan, R. V.; Gorokhov, Yu. A.; Letokhov, V. S.; Makarov, G. N. ZhETF, 69, 1956 (1975).

8. Ambartsumyan, R. V.; Gorokhov, Yu. A.; Letokhov, V. S.; Makarov, G. N.; Puretskiy, A. A. ZhETF, 71, 440 (1976).

9. Kolodner, P.; Winterfeld, C.; Yablonovitch, E. Optics Comms, 20, 119 (1977).

10. Grasyuk, A. Z.; Zubarev, I. G.; Kotov, A. V.; Mikhaylov, S. I.; Smirnov, V. G. KVANTOVAYA ELEKTRONIKA, 3, 1062 (1976).

1. Born, M.; Vol'f, E. "Principles of Optics," Moscow, "Nauka", 1973, paragraph 13.2.

12. Ambartsumyan, R. V.; Gorokhov, Yu. A.; Letokhov, V. S.; Makarov, G. N. Puretskiy, A. A. "Letters to ZhETF," 23, 217 (1976).

13. Ambartsumyan, R. V.; Gorokhov, Yu. A.; Makarov, G. N.; Puretskiy, A. A.; Furizikov, N. P. KVANTOVAYA ELEKTRONIKA, 4, 1589 (1977).

14. Akulin, V. M.; Alimpiyev, S. S.; Karlov, N. V., Prokhorov, A. M.; Sartakov, V. G.; Khokhlov, E. M. "Letters to ZhETF," 25, 428 (1977).

2291
CSO: 8144/1033

PHYSICS

UDC 535.212

ESTIMATION OF THE INTENSITY OF SOUND WHICH ARISES UPON LASER LIGHT PROPAGATION IN THE ATMOSPHERE AND ITS EFFECTS ON THERMAL BLOOMING OF THE BEAMS

Moscow KVANTOVAYA ELEKTRONIKA in Russian Vol 6, No 2, Feb 79 pp 327-330

[Article by V. V. Vorob'yev. Institute of Atmosphere Physics (Moscow), submitted 20 Mar 78]

[Text] The intensity and shape of sound pulses which arise upon propagation of laser beams in the atmosphere are calculated. The feasibility of measuring these pulses is estimated. Changes are considered in focusing the properties of the refractive index inhomogeneities that are formed in the atmosphere under the thermal effect of modulated laser radiation. It is shown that with spatial-temporal modulation, self-focusing of a portion of the beam is possible.

Many papers have appeared recently (see, for example, [1-5]), dedicated to theoretical and experimental investigations of the generation of sound, time modulated by laser radiation in liquids with a high absorption coefficient ($\alpha \geqslant 0.1\text{cm}^{-1}$). It should be expected that a similar phenomenon may also be found when powerful laser beams are propagated in the atmosphere. Although, due to the small absorption coefficient of air which, in the visible and near IR bands, will be small, changes in the pressure and density of the medium in the beam may exceed those that are caused by electrostriction. Therefore, in calculating the self-action of beams, they must be taken into account first. Moreover, the intensity of these sound waves is high enough to be measured, which may be found to be useful for the remote determination of the power and dimensions of the laser beam.

1. If the duration of the laser pulse is small so that heat transfer from the beam, due to molecular heat conductivity and convection, may be neglected, the change in pressure p and of refractive index n of air may be described by equations

$$\partial^2 P/\partial t^2 - u^2 \Delta_\perp P = -\alpha(\gamma-1)\partial J/\partial t; \qquad (1)$$

$$\frac{\partial^2 n}{\partial t^2} - u^2 \Delta_\perp n = \frac{\alpha(\gamma-1)(n_0-1)}{\rho_0} \int_0^t \Delta_\perp J dt, \qquad (2)$$

where $\gamma = c_p/c_v$; u -- speed of sound; n_0, ρ_0 -- undisturbed refractive index and density; J(x, y, z, t) -- power density of laser radiation.

Special features of sound radiation in a weakly-absorbing medium is that intensity J changes weakly along axis Z, along which the beam is propagated; therefore, the sound source is cylindrical and is not a point source as in strongly absorbing media.

We will consider first how pressure varies with time at distance r away from the center of the beam, assuming that the distribution in it is Gaussian along the transverse coordinates and step-shaped with respect to time

$$J(x, y, z, t) = (W/\pi a^2)\exp[-(x^2+y^2)/a^2]\theta(t), \qquad (3)$$

(W-- power of beam). The solution of equation (1) may be written in the form

$$P(r, t) = \frac{\alpha(\gamma-1)W}{2\pi^2 u a^2} \int_{r-ut}^{r} d\xi \times$$
$$\times \int_{-\sqrt{u^2t^2-(r-\xi)^2}}^{\sqrt{u^2t^2-(r-\xi)^2}} \exp\left(-\frac{\xi^2+\eta^2}{a^2}\right)[u^2t^2-(r-\xi)^2-\eta^2]^{-1/2} d\eta. \qquad (4)$$

For $r \gg a$ integration boundaries for η may be replaced by $\mp\infty$ and values of ξ and η^2 may be neglected as compared to $r\xi$ in the denominator of the subintegral expression. As a result of integration we will obtain

$$P(r, t) = \frac{\alpha(\gamma-1)W}{u\sqrt{ar}(2\pi)^{3/2}} f\left(\frac{r-ut}{a}\right), \qquad (5)$$

where

$$f(\xi) = e^{-\xi^2} \int_0^\infty t^{-1/2} e^{-(t^2+2\xi t)} dt = \sqrt{\frac{\pi}{\sqrt{2}}} e^{-\xi^2} D_{-1/2}(\sqrt{2}\xi);$$

D_ν -- function of a parabolic cylinder. The curve of function $f(\xi)$ is shown in Fig. 1. Its asymptotic behavior $f \to (\pi/2\xi)^{1/2}\exp(-\xi^2)$ for $\xi \to \infty$, $f(\xi) \to |\pi/(-\xi)|^{1/2}$ for $\xi \to -\infty$.

To determine the change in pressure in the region of beam propagation $r \lesssim a$, it is convenient for the solution of equation (1) to use Fourier's transformation along transverse coordinates x and y. For the more general case than (3) of harmonic modulation of intensity with time

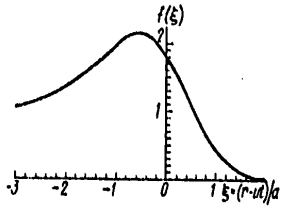

Fig. 1

$$J = \frac{W}{\pi a^2} \exp\left(-\frac{x^2+y^2}{a^2}\right) \cos \Omega t\, 0\,(t) \qquad (6)$$

we will obtain

$$P(r,\ t) = \frac{\alpha(\gamma-1)\,W}{2\pi} \int_0^\infty \frac{\exp\left(\frac{-\varkappa^2 a^2}{4}\right) J_0(\varkappa r)\,\varkappa}{\Omega^2 - u^2\varkappa^2} \times$$
$$\times\ (\Omega \sin \Omega t - u\varkappa \sin u\varkappa t)\, d\varkappa. \qquad (7)$$

In the center of the beam (for r=o)

$$P(0,\ t) = \frac{\alpha(\gamma-1)\,W}{2\pi} \int_0^\infty \frac{\exp\left(-\frac{\varkappa^2 a^2}{4}\right)\varkappa}{\Omega^2 - u^2\varkappa^2} (\Omega \sin \Omega t - u\varkappa \sin u\varkappa t)\, d\varkappa. \qquad (8)$$

For long intervals of time ut $\gg a$, the integral of the second addend is approaching asymptotically to zero:

$$\int_0^\infty \frac{\varkappa^2 \exp(-\varkappa^2 a^2/4) \sin u\varkappa t}{\Omega^2 - u^2\varkappa^2}\, d\varkappa \sim -\frac{2}{\Omega^2 (ut)^3}, \quad \text{for } \Omega t \gg 1. \qquad (9)$$

The harmonic member is equal to

$$P(0,\ t) = P_0 g\left(\frac{a\Omega}{2u}\right) \sin \Omega t, \quad \text{where} \quad P_0 = \frac{\alpha(\gamma-1)\,W}{2\pi a u}, \qquad (10)$$
$$g(x) = x E_1^*(x^2)\, e^{-x^2}\ ;\ E_1^* \text{ -- integral exponential function}$$

equal to the value of integral $\int_{-\infty}^{x} \exp t\,dt/t$.
The pressure amplitude has a maximum at frequency $\Omega \approx 2{,}82u/a$, which corresponds to the length of the sound wave $\lambda_{зв} \approx 2{,}23\,a$. In this case, $g = 0.95$.

We will compare, first, the change in pressure for a thermal effect of radiation with a change in pressure due to electrostriction $P_{стр} \approx \frac{1}{2}(n_0 - 1)W/(\pi c a^2)$, where c is the velocity of light. For air parameters $n_0 - 1 \approx 2{,}5 \cdot 10^{-4}$, $\gamma - 1 \approx 0{,}4$, $\alpha = 10^{-6}$ см$^{-1}$, we will have $P_{стр}/P_0 = 8 \times 10^{-5}$ m/a, i.e., change in pressure due to absorption of laser radiation is usually much greater than due to electrostriction.

We will estimate the possibilities of measuring sound pulses generated by laser radiation. The minimum measurable level of sound signals when using capacitor microphones is determined by the level of thermal acoustic noises,* which may be evaluated [8] by formula $P_{ак} = 16\dot{m}vp_0\Delta f/S$, where m -- mass; v -- average velocity of molecules; S --area of membrane; p_0 -- air pressure; Δf -- width of frequency band.

For normal atmospheric conditions and $S = 1$ cm^2 $P_{ak} = 3.4 \times 10^{-12}(\Delta f)^{\frac{1}{2}}$ bar/Hz$^{\frac{1}{2}}$. the pressure in the sound pulse will exceed this level at

$$W[\text{Вт}] > 20[a[\text{м}]r[\text{м}]\Delta f[\text{Hz}]]^{1/2}. \qquad (11)$$

2. In [7], it was shown that for uniform distribution of intensity in the transverse cross section of the beam and its sharp drop at the edge, self-focusing of the beam is possible during the time, while changes in pressure, due to weak absorption, do not succeed in equalizing, i.e., for $ut \ll a$. It is shown in this paper that in the case of beams with Gaussian distribution of intensity, absorption always leads to blooming. In the presence of the small-scale spatial structure, however, besides temporal modulation, a self-focusing of a part of the beam is possible. In this case condition $ut \ll a$ is not necessary.

On the basis of equation (2), we will consider the change with time of focal distance F of thermal lens, determined by relationship

$$F = \pm|\Delta_\perp n(0)|^{-1/2}.$$

*Minimum measureble level of sound pressure, corresponding to an electronic arrangement of amplifying $P_{эл}$ at high enough modulation frequencies may be smaller than P_{ak}. According to [6], for example, for an arrangement of optical-acoustic measurements with a microphone and preamplifier by the firm of Bruel and Kjaer: $P_{эл}/P_{ak} = 160/f(\text{Hz})$.

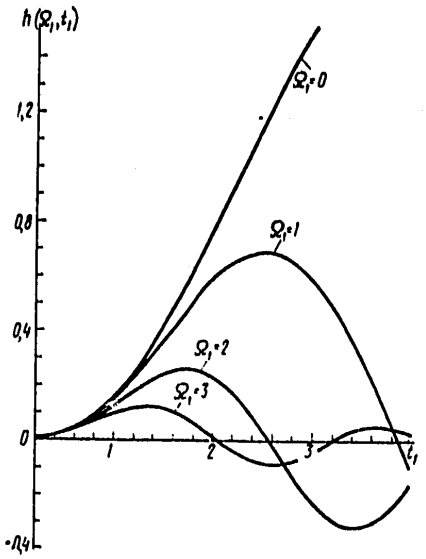

Fig. 2

with sign $F = \operatorname{sign} \Delta_\perp n$, i.e., that inhomogeneities of the refractive index forming in the medium will focus the beam for $\Delta n_\perp < 0$ and defocus for $\Delta_\perp n > 0$. Using Fourier's transformations for solving equation (2) for an intensity distribution $J(x,y,t)$ in the form (6), we will obtain for function $\Delta_\perp n$ expression

$$\Delta_\perp n(t) = Ah(\Omega_1, t_1), \quad h = \int_0^\infty \frac{\xi^4 \exp(-\xi^2)(\xi \sin \Omega_1 t_1 - \Omega_1 \sin \xi t_1)}{\Omega_1(\xi^2 - \Omega_1^2)} d\xi; \qquad (12)$$

$$A = \frac{8(\gamma-1)(n_0-1)\alpha W}{\pi \rho_0 u^3 a^3}; \quad \Omega_1 = \frac{a\Omega}{2u}; \quad t_1 = 2ut/a. \qquad (13)$$

The curve for function h (Ω_1, t_1) for values Ω_1, $t_1 \sim 1$ is shown in Fig. 2 for large times $t_1 \gg 1$, $\Omega t_1 \gg 1$, function $h(\Omega_1, t_1)$ is equal to

$$h(\Omega_1, t_1) = h_0(\Omega_1) \sin \Omega_1 t_1, \tag{14}$$

$$h_0(\Omega_1) = [1/(2\Omega_1)](1 + \Omega_1^2 - \Omega_1^4 E_1^2(\Omega_1^2)), \tag{15}$$

$$h_0(\Omega_1) = \begin{cases} -1/\Omega_1^3 & \text{for } \Omega_1 \gg 1, \\ 1/(2\Omega_1) & \text{for } \Omega_1 \ll 1. \end{cases}$$

The relationship between function h_o and frequency of modulation Ω_1 for $\Omega_1 \sim 1$ is shown in Fig. 3.

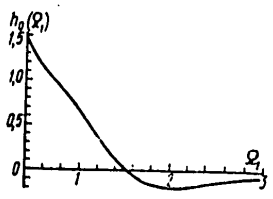

Fig. 3

It may be seen from Fig. 2 that the modulus of function h decreases with an increase in frequency Ω_1, therefore, in the case of temporal modulation in the intensity in the form $J(t)\sim(1+m\cos\Omega t)\theta(t)$ $(m\leq 1)$ formed in the medium, the thermal lens is always a defocusing one.

The temporal intensity modulation, however, may lead to focusing a part of the beam when there is a small-scale spatial structure, for example, for an intensity distribution in the form

$$J=J_0\left[\exp\left(-\frac{x^2+y^2}{a^2}\right)+m\cos\Omega t\exp\left(-\frac{x^2+y^2}{l^2}\right)\right]\theta(t);$$

$$\Delta_\perp n(0,\ t)=\frac{8(\gamma-1)(n_0-1)\alpha J_0}{\rho_0 u^3 a}\left[h\left(0,\ \frac{2ut}{a}\right)+\frac{ma}{l}h\left(\frac{\Omega l}{2u},\ \frac{2ut}{l}\right)\right], \qquad (16)$$

where $h(\Omega,\ t)$ -- function determined by formula (12). For dimensions of disturbances l, less than the width of beam a, expression (16) as may be seen from Fig. 2, may be negative, i.e., self-focusing may originate. For $a\gg 1$, when the first addend in (16) can be neglected, time intervals, during which focusing and defocusing occur, are determined respectively by condition $h(\Omega,t)<0$ and $h(\Omega,\ t)>0$. The characteristic length of the self-action of modulated radiation at $ut\gg 1$ may be evaluated by formula

$$F^{-1}=\frac{8(\gamma-1)(n_0-1)\alpha J_0 m}{\rho_0 u^3 l}\left|h_0\left(\frac{l\Omega}{2u}\right)\right|.$$

BIBLIOGRAPHY

1. Bunkin, F. V.; Komissarov, V. M. AKUSTICHESKIY ZHURNAL, 19, 305 (1973).
2. Westervelt, P. J; Larsen R. S. J. Ac. Soc. Amer., 54, 121 (1973).
3. Bozhkov, A. I.; Bunkin, F. V. KVANTOVAYA ELEKTRONIKA, 2, 1963 (1975)
4. Bunkin, F. V.; Mikhalevich, V. G. Shipulo, R. P. KVANTOVAYA ELEKTRONIKA, 3, 441 (1976).
5. Kasoyev, S. G.; Lyamshev, L. M. AKUSTICHESKIY ZHURNAL, 23, 891 (1977).
6. Rosengren, L. G. Applied Optics, 14, 1960 (1975).
7. Payzer, Yu. P. "Letters to ZhETF," 4, 124 (1966).
8. Van der Zil, A.; "Fluctuations in Radio Engineering and Physics," Moscow-Leningrad. Energoizdat, 1958, p 22.

2291
CSO: 8144/1033

PHYSICS

UDC 351.41 621.375.826

FORMATION OF LASER BEAMS WITH IMPROVED SPACE-ANGULAR CHARACTERISTICS

Moscow KVANTOVAYA ELEKTRONIKA in Russian Vol 6, No 2, Feb 79 pp 331-336

[Article by A. V. Gnatovskiy, A. P. Loginov, N. V. Medved', M. V. Nikolayev, M. T. Shpak, Institute of Physics AN Ukrainian SSR (Kiev), submitted 20 Mar 78]

[Text] The possible transformation of laser fields by means of the two-component optical system is considered. An insignificant dependence of the transformation results on the transverse-mode structure of the initial field is established. Experimental results are presented which illustrate an improvement in the space-angular characteristics of transformed beams.

It is well known that the complex transverse-mode structure of laser radiation causes a large divergence and a comparatively low spatial coherence of the light beam. This frequently limits the use of lasers with such beams when solving a number of scientific and application problems. Therefore, the development of efficient methods for the transformation of complex laser fields into beams with a spatial-angular structure remains an urgent problem.

In using nonresonance correction methods for this purpose it is possible to apply a holographic method in which a hologram compensates for the distortion of the wavefront of the transverse-mode and, therefore, forms a beam with a plane wavefront and a reduced divergence [1,2]. However, the efficient use of such a method requires a high spatial coherence of the mode being corrected (for a quality record of the hologram) and its stability (for precise compensation of the wavefront). Laser radiation does not always meet these requirements. Moreover, materials which make it possible to record holograms efficiently have still not been developed for all wavelengths.

This leads to the necessity of creating arrangements of the nonresonance correction of laser fields which would make it possible to avoid the enumerated difficulties. We consider it promising to use for this purpose a two-element optical system, which first splits the laser field into a series of secondary beams and then makes it possible to synthesize from them, by means of a forming

element, a beam with the desired spatial-angular characteristics practically independent of the structure of the initial radiation [3].

1. Formation of Coherent Light Beam by a Two-Element System

We will consider the optical system shown in Fig. 1a. Radiation of laser 1 that generates transverse-mode TEM_{00} with wavelength λ_0, is expanded by telescope 2 andis split by light-separator 3 into two beams. One of them serves as a reference beam and is directed to the hologram at angle θ_0, while the second beam is passed through a spatial wavefront modulator 4 (a phase transparency with a transmission coefficient $t(x, y,)$, x_1, y_1 -- spatial coordinates in the modulator plane). Radiation diffracted by the modulator interferes with the reference wave in the plane of hologram 5, located at distance d_0 from the modulator. The signal beam field may be represented in the following form with an accuracy to a complex constant:

$$U_0(x_0, y_0) \sim \int_{-\infty}^{\infty}\int t_0(x_1, y_1) \exp\left\{i \frac{\pi}{\lambda_0 d_0}[(x_1 - x_0)^2 + (y_1 - y_0)^2]\right\} dx_1 dy_1. \qquad (1)$$

where x_0, y_0 -- spatial coordinates in the plane of the hologram.

Thus, according to (1) Fresnel spectrum of modulator 4 is recorded on the hologram. We will now transmit, through the modulator-hologram system, laser radiation of a long wavelength λ and an arbitrary wavefront L (x_1, y_1) Fig. 1b), with parameter d and $t(x_1, y_1)$, generally speaking, that can differ from d_0 and $t_0(x_1 y_1)$, used at the recording stage. The field incident on the hologram in this case, like (1) we will record in the form

$$U(x_0, y_0) \sim \int_{-\infty}^{\infty}\int t(x_1, y_1) L(x_1, y_1) \exp\left\{i \frac{\pi}{\lambda d}[(x_1 - x_0)^2 + (y_1 - y_0)^2]\right\} dx_1 dy_1. \qquad (2)$$

Immediately beyond the hologram, in its first diffraction order, will form field

$$W_1(x_0, y_0) \sim U_0^*(x_0, y_0) U(x_0, y_0). \qquad (3)$$

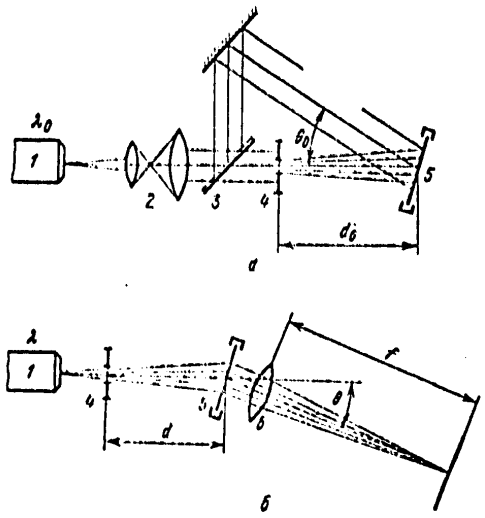

Fig. 1. Optical arrangement of transformation.

Its angular spectrum is observed in the focal plane of lens 6 with focal distance f and is described by an expression, representing the transformation of Fourier field $W_r(x_0, y_0)$:

$$W(x, y) \sim \int\int_{-\infty}^{\infty} W_r(x_0, y_0) \exp\left[i \frac{2\pi}{\lambda f}(xx_0 + yy_0)\right] dx_0 dy_0. \qquad (4)$$

where x, y -- spatial coordinates in the focal plane of lens 6.

Substituting the expression for $W_r(x_0, y_0)$ in (4), and taking into account (1) and (2), we obtain the expression for the angular spectrum of the field, formed by the modualtor-hologram system:

$$W(x, y) \sim \int\int\int\int\int\int t_0^*(x_1, y_1)\, t(\tilde{x}_1, \tilde{y}_1)\, L(\tilde{x}_1, \tilde{y}_1) \exp\left\{i \frac{\pi}{\lambda_0 d_0}[(x_1 - x_0)^2 + (y_1 - y_0)^2]\right\} \exp\left[i \frac{2\pi}{\lambda f}(xx_0 + yy_0)\right] \exp\left\{i \frac{\pi}{\lambda d}[(\tilde{x}_1 - x_0)^2 + (\tilde{y}_1 - y_0)^2]\right\} \times dx_1 dy_1 d\tilde{x}_1 d\tilde{y}_1 dx_0 dy_0. \quad (5)$$

In case $\lambda_0 = \lambda$, it is necessary to equate $d_0 = d$ and $t_0(x_1, y_1) = t(x_1, y_1)$. Expression (5) may be reduced to the form

$$W(x, y) \sim \iint_{-\infty}^{\infty} t_0^*[(x_1 + \beta x), (y_1 + \beta y)]\, t_0(x_1, y_1)\, L(x_1, y_1) \exp\left[-i \frac{2\pi}{\lambda_0 f} \times (x_1 x + y_1 y)\right] dx_1 dy_1, \quad (6)$$

where $\beta = d_0/f$. Expression (6) was obtained in [4] for the case of correcting the radiation of a helium-neon laser. Its analysis indicates that under certain conditions the structure of the transformed field W(x, y) will be determined to a great extent by the transmission coefficient of the modulator rather than the structure of the initial field of the laser. In the limiting case (when the Fourier spectrum of the modulator is recorded on the hologram) the angualr structure of the transformed field will be determined only by the spatial autocorrelation function of the modulator or by the spatial function of modulators used when recording the hologram and its restoration. The insignificant dependence of the angular spectrum of the transformed beam on the field structureof the initial laser is achieved by using modulators with such transmission characteristics that function $L(x_1, y_1)$ may be assumed to be smooth enough compared to $t(x_1, y_1)$. This makes it possible to increase the universality of the correlating arrangement described.

We will consider the case where $\lambda_0 \neq \lambda$. Expressions for purely phase molulators may be presented in the most general form

$$t_0(x_1, y_1) = \exp\left[i \frac{\pi}{\lambda_0} \delta_0 n x(x_1, y_1)\right] \operatorname{rect}\left(\frac{x_1}{X}\right) \operatorname{rect}\left(\frac{y_1}{Y}\right), \quad (7a)$$

$$t(x_1, y_1) = \exp\left[i \frac{\pi}{\lambda} \delta n x(x_1, y_1)\right] \operatorname{rect}\left(\frac{x_1}{X}\right) \operatorname{rect}\left(\frac{y_1}{Y}\right), \quad (7б)$$

where comultiplier $\operatorname{rect}(x_1/X)\operatorname{rect}(y_1/Y)$ determines the aperture of the

modulator; δ_0 and δ -- geometrical depth of the relief; n -- refractive index of the modulator material; function $\varkappa(x_1, y_1)$ we consider to be arbitrary.

By comparing (5) and (6) and taking into account (7), the conclusion can be drawn that in the case of meeting relationships $d=\varepsilon d_0$ and $\delta=\delta_0/\varepsilon$ (where $\varepsilon=\lambda_0/\lambda$) expression (5) leads to form (6), as also in case $\lambda_0=\lambda$. Thus, the two-element system may be simply retuned for the correction of laser beams with various wavelengths, preserving the function form of the angular spectrum of the corrected beam.

2. Field Transformation of Gas Lasers

We will use the results obtained above for forming beams with synthesized angular spectrum of gas laser fields. Fields of these lasers are described by comparatively simple functions and may be reduced to Gaussian beams [5] which makes the necessary computations easier.

Beam multiplication. We will dwell first on case $\lambda_0=\lambda$. As a modulator, we will select a phase diffraction grate with transmission coefficient

$$t(x)=\exp(i^1/_2\mu\cos 2\pi\nu x_1)\operatorname{rect}(x_1/X), \qquad (8)$$

where $\mu=(2\pi/\lambda_0)\delta_0 n$; ; ν -- grate frequency (a single-dimensional problem is considered for simplicity). This case is of special interest because it allows an analytical solution. Moreover, such a modulator is attractive by its simplicity and ease of manufacture.

By substituting (8) into (6) and integrating, we obtain an expression for the intensity of the transformed beam

$$I(x) \sim \sum_{p=-\infty}^{\infty} J_p^2(\mu \sin \pi\nu\beta x)\,|L(x-\pi p\nu)|^2, \qquad (9)$$

where J_p -- Bessel's function of the 1st kind and the p-th order; in this case we select the field of laser $E(x_1)$ in the form of single-dimensional transverse modes, type TEM_{0m} [5] and neglect the finiteness of the aperture of the correcting system, which is true for beams with a cross section smaller than the modulator aperture. Expression (9) describes the energy distribution in the form of a set of orders displaced with respect to each other by value $d=\pi\nu$ along axis X and modulated by corresponding multiplier $J_p^2(\mu\sin\pi\nu\beta x)$. The intensity of these orders attenuate quickly with an increase in p. In the most intensive zero order, due to comultiplier $J_0^2(\mu\sin\pi\nu\beta x)$, which represents an autocorrelation function of a sinusoidal phase grating [6], and energy redistribution in the angular spectrum of the initial beam $L(x)$ is observed and several sharp maximums are formed within its limits with a period $\Delta x=2/(\nu\beta)$. Their angular dimensions and disposition are determined

by parameters ν, β, μ and practically do not depend on the structure of the beam being corrected. By varying parameters ν and β, it is possible to control the maximums, while parameter μ determines the angle size of each one of them. Thus, the system consisting of modulator (8) and a hologram corresponding to it, can be used for multiplying laser beams with a standardized angular spectrum.

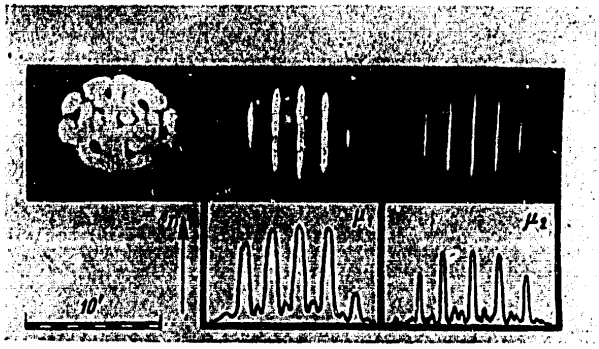

Fig. 2. Multiplication of corrected laser beams ($\mu_1=4.8$; $\mu_2=7.8$).

Fig. 2. shows the results of the transformation of a complex mode of a helium-neon laser ($\lambda=0.63$ microns) into five beams by means of two periodic modulators with equal periods, but various values of μ. A reduction in the size of the angle of each maximum with an increase in μ is observed. The problem can be generalized for the case of a two-dimensional transformation for which it is natural to use two-dimensional periodic modulators. In this case, it is possible to obtain fields with a spatial structure consisting of equal periodically arranged groups with a bell-shaped distribution in each one of them.

Reduction in the beam divergence. In a number of practical problems, a laser beam with a low divergence and a high axis brightness is required for this. The use for this purpose of periodic modulators with parameters for forming only one beam, is not always feasible, inasmuch as in this case, the contribution of the zero member in expression (9) falls sharply (according to estimates, to 12-15% of the total energy of the transformed beam).

In such cases, it is necessary to use modulators that form only one beam (i.e., modulators, the autocorrelation function of which has a δ-shaped nature [3, 4, 7]. In particular, it is possible to use a zone plate with transmission as such a modulator of:

$$t(x) = \exp\left(i\frac{\mu}{2}\cos\frac{x^2}{2\sigma^2}\right) \qquad (10)$$

(as before, we will limit ourselves to the consideration of a single-dimensional problem), where parameter σ determines its focusing properties. Taking into account (10), calculation of integral (6) presents certain difficulties and may be done on a computer. The results of the calculation in the form of curves are shown in Fig. 3.

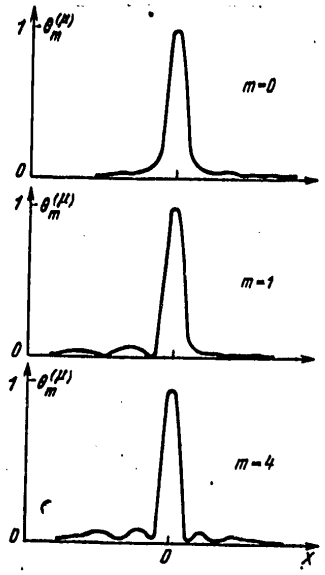

Fig. 3. Calculated distribution of energy $\theta_m^{(\mu)}(x)$ in corrected beams for transverse modes TEM_{00}, TEM_{01}, TEM_{04}.

Fig. 4 shows experimental results confirming the calculation made. Photographs are shown in the far zone of a series of simple and complex transverse modes before (a) and after (b) corrections. Intensity distribution was measured by means of a photoelectric attachment with a scanning slot. The results of these measurements are shown in Fig. 4c. The measurements cited make it possible to conclude that in the order of 25 to 35% of the energy of the transformed field is concentrated in the central maximum.

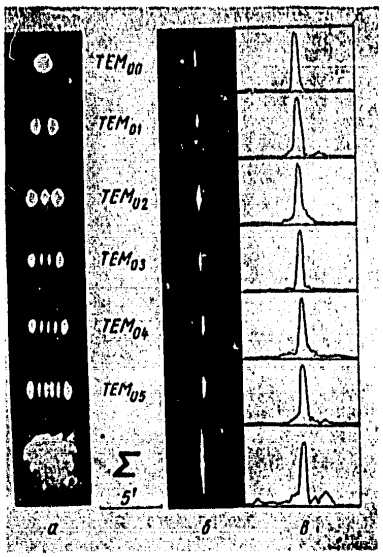

Fig. 4. Correction of transverse modes of a helium-neon laser.

The use of modulators that have maximum symmetry or are obtained by superimposing two type (10) modulators at an angle of 90°, makes it possible to obtain a corrected beam with a cross section in the shape of a point. The same distribution may be provided by modulators with a stochastic phase modulation diffuse-dispersing objects [7].

Change of wavelength of radiation being corrected. We will consider the case where the wavelength of the laser field being corrected differs from the radiation wavelength used for recording a hologram ($\lambda_0 \neq \lambda$). According to the analysis shown above, it is necessary to utilize a correcting system for this, in which parameters d and δ may be changed. To change the distance between the modulator and the hologram, they are mounted on small tables with microfeeds, providing precise motion of these elements along the direction of the laser beam.

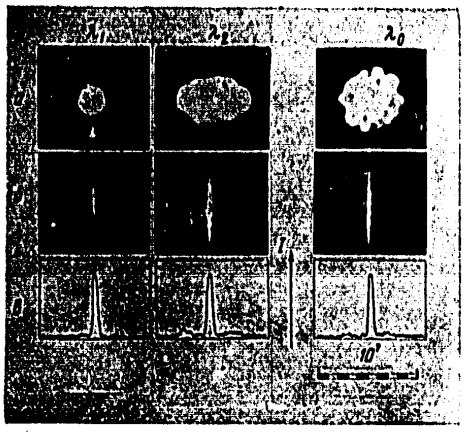

Fig. 5. Correction of laser beams with various wavelengths

The change in the depth of the contour of the modulator, while preserving its spatial structure, may be achieved by the precise replacement of modulators of the same type with different parameters δ . For the case of a single-dimensional correction, difficulties arising due to such replacement may be reduced. For this purpose, it is necessary to make a modulator considerably elongated in the direction perpendicular to the direction of the correction, with a changeable contour and to change modulators by shifting this modulator along this direction.

A single-dimensional zone plate 35x5 mm was made in which the contour depth was changed linearly in the direction of the larger dimension. The working section of the modulator was separated by a 4x5 mm diaphragm within the limits of which δ could be considered constant. By moving the modulator in the vertical direction by means of a microfeed, it was possible to achieve easily the required change in parameter δ preserving the spatial structure of the modulator.

The correction results of laser beams with various wavelengths by means of one retunable system are shown in Fig. 5. Radiation of a helium-neon laser

(λ_0=0.63 microns) was used for recording the hologram. Also shown here are the results of the transformation of beams of helium-cadmium (λ_0= 0.44 μm) and helium-neon (λ_2=1.15 microns) lasers. Photographs taken before (a) and after (b) correction and photometry results (c) show that the proposed two-element correction arrangement is universal enough also with respect to changing the wavelength along with changing the transverse structure of the laser field. The obtained results open up possibilities for transforming wavelengths of laser beams lying in the near IR band, for which proper holographic materials are lacking so far.

3. Discussion of Results and Conclusions

The investigations made show that the problem of forming laser beams with the required spatial-angular characteristics can be solved to a considerable extent by using the described modulator-hologram system. The independence, within a wide range, of correction results from the transverse mode structure of laser radiation provides all the bases to assume that the proposed approach to forming laser beams is not limited to fields of gas lasers. Actually, from the analysis of expressions (5) and (6), it follows that for a sufficiently frequent spatial modulation of the initial field, the structure of the latter has small effect on the final result of transformation. Therefore, with proper selection of modulator parameters, the class of transformed fields may be broadened considerably. In particular, radiations of solid and semiconductor lasers may serve as such fields as well as fields at the exit of fiber optics systems. Preliminary investigations made in this direction gave promising results and made it possible to reduce considerably the divergence of the discussed fields (see, for example, [8]).

Obviously, possibilities of the method are not exhausted by the modulators described in this paper. A development of new modulator types, most fully responsive to the requirement of synthesizing a beam with concrete characteristics represents an important problem. For example, a stochastic modulation of the phase of the transverse mode being corrected makes it possible to control the energy distribution over the cross section of the beam formed [7]. The approach described makes it possible to vary the structure of the transformed beam to a greater extent than by using a purely holographic method [1, 2]. This is explained by the fact that the transformed beam is determined by the transmission of the modulator used, the selection of which may vary within wide limits based on these or those requirements, presented to the structure of the beam being synthesized. In the most general case, posing a converse problem is possible -- given the required structure of the light beam, select a corresponding modulator which would satisfy this requirement. This problem may be formulated mathematically as finding the solution of integral equation (6) for function $t(x_1, y_1)$ assuming $W(x, y)$ to be the given value.

The results of the investigation show that in the considered method, the direction of the propagation and the energy of distribution in the transformed beam depend weakly on the index and orientation of the mode being

corrected. This makes it possible to depend on increasing the spatial coherence in beams, formed of modal structures compared to relatively low spatial coherence, represented by incoherent superimposition of several components. The maximums of corrected beams for various components may coincide. The effect of increasing the spatial coherence in the transformed beam was observed in [9]. As shown by measurements, it was comparable to the coherence of mode TEM_{00}. This result makes it possible to broaden the class of laser sources used for problems of holography, coherent optics etc.

BIBLIOGRAPHY

1. Gnatovskiy, A. V.; Seleznev, V. V.; Shpak, M. T. In handbook KVANTOVAYA ELEKTRONIKA, Kiev, "Naukovaya dumka", 1977, issue 13, p 36.

2. Bondarenko, M. S.; Gnatovskiy, A. V.; Soskin, M. S. DAN USSR, 187 538 (1969).

3. Gnatovskiy, A.V.; Loginov, A. P. Seleznev, V. V.;Shpak, M. T. Ukr. fiz. zhurnal, 22, 1418 (1977).

4. Gnatovskiy, A. V.; Loginov, A. P. Nikolayev, M. V.; Shpak, M. T. Ukr. fiz zhurnal, 23, 311 (1978).

5. Boyd, J.; Gordon, J. In handbook "Lasers," Moscow, IL, 1963, p 363.

6. Malov, A. N.; Morozov, V. V.; Kompanets, I. N.; Popov, Yu. M. KVANTOVAYA ELEKTRONIKA, 4, 1608 (1977).

7. Gnatovskiy, A. V.; Zubrilin, N. G.; Loginov, A. P.; Medved', N. V.; Nikolayev, M. V.; Shpak, M. T. Ukr. fiz. zhurnal, 23, 525 (1978)

8. Volyar, A. V.; Gnatovskiy, A. V.; Kuchikyan, M. G.; Loginov, A. P; Medved', N. V.; Shpak, M. T. DAN Ukrainian SSR, No 4, 329 (1978).

9. Gnatovskiy, A. V.; Loginov, A. P.; Shpak, M. T. DAN Ukrainian SSR,No 11, 1026 (1977).

2291
CSO: 8144/1033

PHYSICS

UDC 621.378

TEMPERATURE DEPENDENCE OF THE OPTICAL GLASS ABSORPTION COEFFICIENT ON EXPOSURE TO THE LASER RADIATION

Moscow KVANTOVAYA ELEKTRONIKA in Russian Vol 6, No 2, Feb 79 pp 337-346

[Article by N. Ye. Kask, V. V. Radchenko, G. M. Fedorov, D. B. Chopornyak, Institute of Nuclear Physics MGU imeni M. V. Lomonosov, submitted 25 Mar 78]

[Text] Results are reported of an interferometric study of variations of the refractive index of K8, I47 glasses and laser glasses on exposure to neodymium laser radiation. It is found that in laser glasses, thermal instability occurs which is related to thermal excitation of ions to the $^4I_{11/2}$ level and the nonradiative channel of the metastable level decay through the higher-lying level of $^2G_{9/2}$. The $^4F_{3/2} \rightarrow {}^2G_{9/2}$ transition cross section is determined.

In transparent solid dielectrics, high temperatures are developed by laser radiation action which lead to melting, boiling, an appearance of plasma and mechanical destruction. Material heating may occur due to linear and nonlinear absorption of incident radiation energy. In the case of high intensity of optical radiation ($> 10^{10} w/cm^2$), avalanche ionization [1-3] is the mechanism of nonlinear absorption, Temperature dependence of foreign inclusions [4] must lead to an increase in laser radiation absorption in the process of radiation, as a result of which an absorption wave may appear, propagated within the dielectric from the inclusion surface [5-7]. In [8] there is considered the heating of a coagulum of admixture centers in a transparent dielectric in the presence of nonradiating transitions, and it has been shown that the temperature in such a coagulum is a nonlinear function of the number of particles and the intensity of laser radiation. Of interest are the role and mechanism of nonradiational transitions when heating dielectrics, activated by Nd^{3+} ions, by radiation of a neodymium laser.

This paper studied the dynamics of temperature development in optical glasses, in particular, those activated by neodymium ions, acted upon by comparatively low power laser radiation.

1. Experimental Installation and Method of Processing

Fig. 1. shows the arrangement of the experimental installation. Laser radiation of the neodymium glass was focused in all cases by a spherical lens with f = 80 mm into the volume of the sample studied.

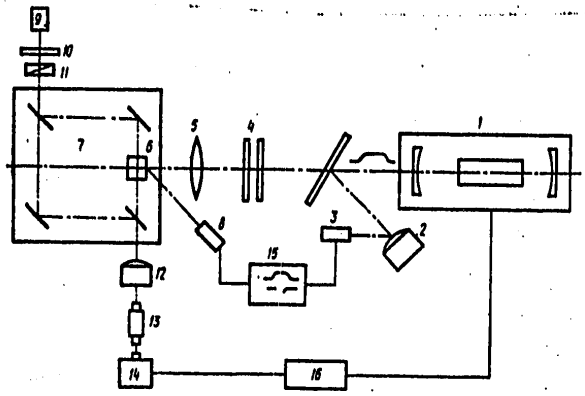

Fig. 1. Arrangement of experimental installation.

1. Neodymium laser
2. Calorimeter
3. FEU-28
4. Neutral light filters
5. Focusing lens
6. Investigated glass sample
7. Mach-Tsender interferometer
8. FEU-16 for recording destruction
9. LG-106M argon laser
10. Quarter-wave quartz plate
11. Polarizer
12. Lens
13. Microscope
14. SKS-IM movie camera
15. S8-2 oscilloscope
16. Arrangement for synchronizing start-up of SKS-IM and firing neodymium laser

The radius of constriction at e^{-1} level is 2×10^{-2} cm. A quasicontinuous pulse generation mode was used with a radiation modulation of less than 10%. Laser parameters were cited before in [9, 10]. The sample was placed in one of the arms of the Mach-Tsender interferometer. The probing radiation of the continuous argon laser (λ_0=488 nm) was directed perpendicularly to the radiation of the neodymium laser. The image of the irradiated region of the glass was projected by means of the lens and microscope on the film of an SKS-IM high-speed camera. During the action of the pulse, the generation of the neodymium laser up to 50 frames of the interference picture were recorded. The time tie-in was implemented with respect either to the moment of destruction (if it occurs), recorded on the film or oscilloscope, or the moment of pulse generation finish. In this case, a maximum shift of the

interference band occurs in the unsoftened region of glass. Samples made of unactivated K8 and L47 glasses and GLS1,GLS4, LGS247-1, 2, 3 and YeD2 glasses, made in the form of 20x20x20 cm cubes were investigated. All the faces of the cubes were thoroughly polished and checked for parallelism and flatness.

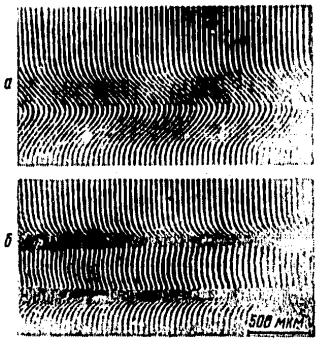

Fig. 2. Interference pictures for K2 glass up to the moment of the formation t=3.5 ms (a) and after the coagulum formation t = 7 msec (b). Duration of laser pulse 10 msec.

Fig. 2 shows interference pictures of the focal region of the glass up to and after the formation of a coagulum produced by the laser pulse action. For K8 and L47 glasses to to the moment of a coagulum formation, as well as for laser glasses at the initial section of heating, the band shift agrees well with the Gaussian distribution (Fig. 3), and formula (П.3) (see appendix) for the determination of refractive index Δn. The formation of a coagulum leads to a distorted Gaussian distribution in the region near the axis of the interference picture, due to the change of the sign of dn/dT because of the structural change in the process of glass softening. (We will note that the authors of [11], using interferometry, could not detect distortions when the coagulum was formed,apparently, due to imperfection in the method they used). The behavior of dn/dT in the softening region for pulse heating is unknown and, therefore, quantitative processing of the interference pictures was done only up to the moment of structural changes. The measurement of the relative shifts of the interference bands was made by an IZA-2 comparator with a precision of up to 1/20 of a band. On the end heating section of

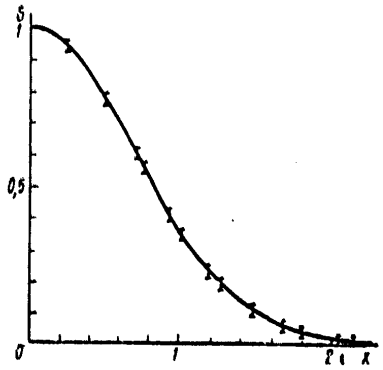

Fig. 3. Gaussian distribution exp (x^2).

Vertical segments characterize the experimental spread data for E|| Z and for E ⊥ Z; axis Z is directed along the axis of the neodymium laser.

the focal region of laser glasses (up to melting) the shift of interference bands already cannot be described by a Gaussian curve and to calculate using formula (П.2) an approximation method was used with an S polynomial of the m-th degree for l points. m=8-10 and l=20-30 were usually used. Integral

$$I(W) = 2\pi \int_0^\infty \Delta n r dr,$$

was used to determine absorption coefficient K, which characterizes the portion of laser radiation energy transformed into heat:

$$K = \frac{c\rho}{dn/dT} \frac{dI}{dW}, \qquad (1)$$

where c -- specific heat; ρ-- density; W -- incident energy. The expression for the total change dn/dT through material constants are shown in the appendix. Numerical values for the glass constants were taken from [12-15]. With such a method for determining the absorption coefficient, it is not necessary to take into account thermal diffusion and the possible effects of self-focusing are taken into account by integral I. The truth of this statement for absorption coefficient K, not depending on temperature, is obvious, while for nonlinear absorption, this may be shown directly by solving the corresponding heat conduction problem, for example, for a contour of a source function of the type $\exp(-\Delta/kT)\exp(-r^2/a_0^2)$.

Experimental Results

Unactivated glasses. Fig. 4 shows the relationship between integral I(W) and incident energy in the case of K8 optical glass.

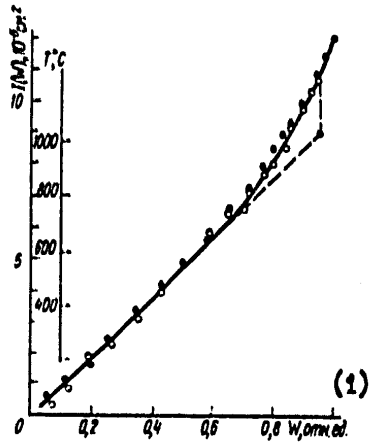

Fig. 4. Relationship $I(W) \approx \Delta n_0 \pi a_0^2$ and energy W(a unit along the abscissa axis is assumed to be threshold energy for the formation of a melted region in K8 glass, equal to 490 joules) for focal plane (O) and a distance of 575 microns ahead of focal point (●).

K8 glass, E∥Z. Temperature scale refers to the coagulum axis for the case of focal plane (r=o, z=o).

1. Relative units.

An indirect method based on the relationship between the thresholds for K8 glass and various absorption coefficients [10], established that almost up to the threshold of mechanical destruction the absorption coefficient does not depend on temperature and, therefore, the deviation from the linear dependence of I as a function of W on Fig. 4 is obviously due to the dependence of dn/dT on the temperature. Deviation from linear dependence is also observed in L47 glass. This dependence should be expected, since the coefficient of linear expansion α, when approaching the region of softening, begins to increase and in the region of softening exceeds its value for hard glass by several times.

If an extrapolation is made of the straight initial section of the curve in Fig. 4, up to the temperature of the formation of the melted region, we will obtain a value of 1000-1100°C. This coincides with the temperature for the formation of a melted region in the K8 glass obtained by a different method [16], which confirms the conclusion made above.

We will note that the experimentally determined value of the radius of distribution shape Δn at the level 1/e of unactivated glasses does not change in the process of being acted upon by laser radiation.

This situation is possible in the investigated range of laser pulse durations, if the starting process of thermodiffusion is "compensated" by the self-focusing of the beam. Characteristic thermodiffusion time $\tau_x = a^2/4\varkappa$ is at least double the time of action while the passed energy is one half to one third of the critical energy of nonstationary thermal self-focusing for unactivated K8 and L47 glasses.

The value of $K = 5.7 \times 10^{-3}$ cm^{-1} ($\pm 10\%$) was obtained for K8 glass and $K = 5.0 \times 10^{-3}$ cm^{-1} -- for L47 glass while, within the measurement accuracy of about 10%, the local absorption coefficient in various points of glass has the same value. The case of the radiation effect on visually observed inclusions was not investigated.

Glass activated by neodymium. Fig. 5a shows relationship I(W) for GLS1 laser glass. Relationships for other laser glasses have similar shapes. As may be seen from comparing Figs. 4 and 5a, the temperature development in the irradiated region of laser glass differs radically from the case of unactivated K8 glass (we will note other facts of different behavior of the GLS1 laser glass and K8 optial glass . Although the absorption coefficient at 300K of GLS1 glass is only a third of that of K8 glass, the threshold of mechanical destruction of GLS1 is 2/3 to 1/2 that of the K8 threshold. The mechanical destruction threshold of K8 glass is 1.5 to 2 times higher than the threshold of the appearance of melting, while in GLS1 glass, the corresponding excess is 10 to 20%. These facts confirm the existence of a temperature dependence of laser glass absorption). Beginning with temperatures of about 150°C there occurs a noticeable nonlinear increase in the temperature of heated glass, while additional absorption, shown in Fig. 5b, has a characteristic exponential temperature dependence of form $\Delta K = K - K_0 = A\exp(-\Delta/kT)$, where K_0 is determined from the initial slope of curve (W) in Fig. 5a. Activation energy Δ, determined from the slope of the straight line in Fig. 5b, is equal to 2000-2100 cm^{-1}. This value agrees well with the energy gap between the basic state and the lower level of working laser transition $^4I_{11/2}$ of ion Nd^{3+} . In Fig. 5b, the temperature for the axis of the laser beam is taken and, since the spatial contour of the beam does not have a rectangular shape, it is necessary to take into account the temperature distribution contour to find coefficient A. Based on the expression for an increase in $\delta(\Delta n)$ during time δt

$$\frac{c\rho}{dn/dT}\delta(\Delta n) = \frac{I_0}{\pi r_0^2}\exp\left(-\frac{r^2}{r_0^2}\right) A\exp\left(-\frac{\Delta}{kT}\right)\delta t, \qquad (2)$$

substituting temperature in form $T = T_H + T_0\exp(-r^2/a_0^2)$ (where T_H -- initial temperature of sample) which describes an actual case of laser heating to an accuracy of 10-15% and replacing

$$x = \frac{T_0 + T_H}{T_H + T_0 \exp\left(-r^2/a_0^2\right)},$$

after integrating with respect to $rdrd\varphi$ we obtain at the limit $\beta t \to 0$

$$A = \frac{cp}{dn/dT} \frac{dI(W)}{dW} e^{\beta} Q. \qquad (3)$$

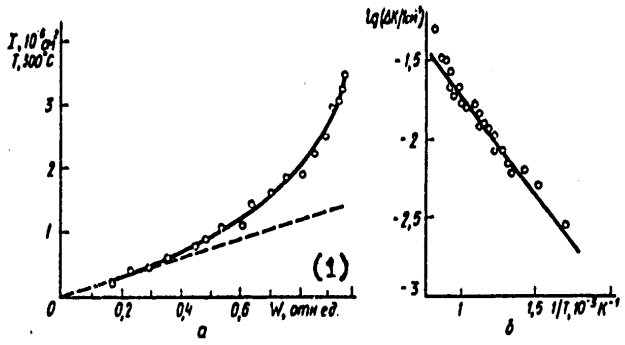

Fig. 5. Relationship between $I(W) = 2\pi \int_0^{\infty} \Delta n(r) r dr$ and energy W for GLS1 laser glass for E // Z (a) and temperature dependence of the additional absorption coefficient of GLS1 glass (b).

1. relative units.

Here

$$Q^{-1} = \frac{\alpha_0 \gamma}{\gamma - 1} \int_1^{\gamma} \left[\frac{\gamma - x}{x(\gamma - 1)}\right]^{\alpha_0 - 1} x^{-2} e^{-\beta_0 \frac{x-1}{\gamma}} dx;$$

$$\gamma = (T_0 + T_H)/T_H;\ \beta_0 = \Delta/kT_H;\ \beta = \Delta/[k(T_H + T_0)];$$

a_0-- radius of the temperature contour; r_0 -- radius of the intensity contour; f_0 -- power of laser radiation. Coefficient $\alpha_0 = (a_0/r_0)^2$ takes into account the effect of self-focusing. For a range of W from 0.5 to 1 ((W=1) corresponds to the moment of appearance of melting) the value of $W \leq W_{кр}$, where

где

$$W_{кр} = \frac{\pi c \rho r^2 \theta^2}{2 n_0 K (dn/dT)_c} \qquad (4)$$

-- critical energy of nonstationary thermal self-focusing; θ -- divergence of laser radiation at the entrance to the medium. At $W = W_{кр}$ the cross section of the beam is halved with respect to the initial area due to the fact that the radius of the temperature contour narrows to 5/6 in the process of development of thermal instability, and α is in the interval from 1 to 1.5. Fig. 6 shows the relationship between correcting multiplier Q and parameter γ for limiting values $\alpha_0 = 1$ and 1.5.

The expression for $(dn/dT)_c$ has the form

$$\left(\frac{dn}{dT}\right)_c \approx \left(\frac{\partial n}{\partial T}\right)_{\sigma=0} - \frac{\alpha E}{1-\nu} \frac{C_1 + 3C_2}{2},$$

where α -- coefficient of linear expansion; E -- Young's modulus; ν --Poisson's coefficient; C_1 and C_2 -- elastic-optical constants. For temperature region $T_H = 300K$, $T_0 \sim 400K$ of interest to us, a weak dependence is observed of multiplier Q on temperature, i.e., the temperature contour has almost no effect on the accuracy of Δ determination. To determine A, the central value q Q was taken designated by a broken line curve (see Fig. 6). In two experiments done on YeD2 glass, the initial temperature of sample T_H was raised to 700K and the increased nonlinear absorption made it possible to find A in initial section γ when $Q \approx 1$. The values of A determined by these two methods coincided with a precision of up to 15%.

For laser glasses LGS247-1, LGS247-2, LGS247-3, GLS1, GLS4 and Ed2, experimentally determined values of A are correspondingly 0.11, 0.32; 0.66; 0.30; 0.58 and 0.23^{-1} cm, while values of absorption coefficient K_0 at wavelength $\lambda = 1.06$ microns are equal to 2.0×10^{-3}, 2.1×10^{-3}, 1.3×10^{-3}; 1.8×10^{-3}; 3.3×10^{-3} and 4.0×10^{-4} cm^{-1}. L47 glass is the basis for brand LGS247 laser glasses.

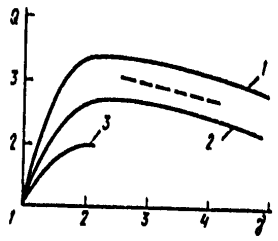

Fig. 6. Relationship between correcting multiplier Q and parameter $\gamma = 1 + T_0/T_H$ for $\beta_0 = 9.6$ (1,2) and 4.1 (3) and $\alpha_0 = 1$ (1), 1.5 (2), 1 (3).

3. Discussion of Results

Thus, additional nonlinear absorption originates as a result of the thermal population of the lower laser level of ion Nd^{3+} and is due to the presence of a nonradiational channel of decomposition of the metastable state $^4F_{3/2}$. Level $^4F_{3/2}$ is populated by the resonance field of laser radiation. The difference in populations of levels $^4I_{11/2}$ (N_2) and $^4F_{3/2}$ (N_3) in the field of laser pumping is determined by expression [16].

$$N_3 - N_2 = \frac{N_0 \exp(-\Delta/kT)}{1 + \exp(-\Delta/kT) + W_{32}\tau_0 q(1 + 2\exp(-\Delta/kT))}. \qquad (5)$$

where N_0 -- total number of ions in unit volume; τ_0 -- spontaneous life of metastable state $^4F_{3/2}$; q -- quantum output of luminescence of level $^4F_{3/2}$; k -- Boltzman's constant; $W_{32} = \sigma_л J$; $\sigma_л$ -- cross section of laser transition (numerical values cited in [18, 19]; J -- radiation intensity.

For $J \sim (1\text{-}3)\cdot 10^{27}$ quanta (sec-cm^2) the value of additional absorption $\Delta K \sim 10^{-4} \exp(-\Delta/kT)$ is insufficient for explaining experimental results. In this connection, we will consider the possible channels of nonradiational decomposition of the $^4F_{3/2}$ metastable state leading to the transformation of all or part of the excitation energy into heat:

1) intracentral multiphonon relaxation from the metastable condition (the value of the energy gap between levels $^4F_{3/2}$ and $^4I_{15/2}$ is about 4700 cm^{-1} and at high temperatures the multiphonon relaxation may be the probable mechanism of nonradiational decomposition);

2) interaction of activator ions between themselves and foreign impurities on the assumption of the uniformity of ion distribution in the matrix, leading to the nonradiational loss of excitation;

3) dissipation of the excitation energy in oscillations of hydroxyl OH [20];

4) nonuniform entrance of activator ions into the glass matrix which leads to concentrated attenuation in regions with higher concentrations of neodymium [21, 22].

At higher excitation levels, the following are also possible:

5) mechanism of excitation relaxation, including two neodymium ions, in which transition $^4F_{3/2} \rightarrow {}^2G_{7/2}$ occurs in one ion and transition $^4F_{3/2} \rightarrow {}^4I_{15/2}$ [23] occurs in the other ion;

6) transition of 1.06 microns by action of radiation from level $^4F_{3/2}$ to a higher lying level $^2G_{9/2}$ with a following nonradiational relaxation.

First of all, we will note that the slope constancy of the relationship between the logarithm of the additional absorption and the reverse temperature (see Fig. 5b) up to 1100K indicates that at least, up to this temperature, some new mechanism of nonradiational relaxation does not enter the game. Previously, such a conclusion was made only up to 720K [24]. Obviously, this eliminated the mechanism of multiphonon relaxation [25] up to 1100K and makes the fifth mechanism imporbable by virtue of its quadratic dependence on the number of electrons in the metastable level. Deviation of dependence lg (Δ K) on 1/T still is silent about including an additional channel of nonradiational composition, since at such temperatures, preceding the formation of a melted area, a relationship between the glass constant and temperature (see Fig. 4) must be manifest. In this connection, it is interesting to apply the given method to crystals activated by neodymium. Regrettably, the problem of strongly-absorbing inclusions in crystals is more acute than in glass and in crystals of yttrium-aluminum garnet with neodymium

available to us, the destruction always occurred in the inclusions at power levels more than an order of magnitude smaller than power densities needed for heating the entire focal region. This type of destruction was investigated in [26] for the case of the effect of laser radiation on organic glass, when destruction is easily observed in local nonuniformities under conditions of dissociation, which leads to the thermal instability of the medium.

It follows from (2) that for mechanisms 2 and 3 to work, it is necessary to have $q \lesssim 10^{-3}$, while for laser glasses $q = 0.5...1$ [14].

To realize the fourth mechanism of the nonradiational decomposition of the metastable state requires the presence of regions with a higher concentration of neodymium ions (clusters) which concentrate $\gtrsim$ 10% of all ions and where almost total attenuation of luminescence occurs. The existence of such regions was postulated in [15, 17] for explaining the deviation of the quanta output of luminescence from level $^4F_{3/2}$ from unity. At small (1-2%) neodymium concentrations in glass, the portion of totally nonradiational ions of neodymium is small ($\sim$1%), but it increases with an increase in concentration [20], and in ED2 glass, where $q \approx 1$, there is almost none.

Thus, the main contribution to the nonlinear increase of the absorption coefficient with temperature at small concentrations of neodymium is given by nonradiational transitions from level $^2G_{9/2}$ into which electrons are thrown by the radiation of laser pumping. This makes it possible to determine the cross section of transition $^4F_{3/2} \rightarrow {}^2G_{9/2}$ $\sigma_{34} = A/N_0$. We will cite the following experimental values of σ_{34} for the investigated laser glasses; σ_{34} (LGS247) $= 0.11 \times 10^{-20}$ cm^2; σ_{34}(GLS1) $= 0.15 \times 10^{-20}$ cm^2; σ_{34} (GLS4) $= 0.12 \times 10^{-20}$ cm^2; σ_{34}(ED2) $= 0.25 \times 10^{-20}$ cm^2. The ratio of the value of this transition to the cross section of laser transition $\sigma_л$ is (10 ± 2)% for all laser glasses which, within the limits of experimental error, coincides with the theoretical value of ratio

$$\sigma(^4F_{3/2} \rightarrow {}^2G_{9/2})/\sigma(^4I_{11/2} \rightarrow {}^4F_{3/2})$$ [27].

The value of the error takes into account the possible contribution of the nonradiating ions. The disproportional increase in coefficient A with an increase in concentration of the concentration series for LGS247 laser glass is explained by increasing the share of neodymium ions in clusters with an increase in concentration.

The authors are grateful to I. M. Buzhinskiy, Ye. M. Dianov and I. A. Shcherbakov for furnishing samples for investigation and useful discussions.

APPENDIX

Determination of Δn from Shift of the Interference Band

To an approximation of geometrical optics and due to the low refraction for an axis-symmetrical distribution of refractive index Δn, the relative shift of interference band S is expressed as follows [28]:

$$S = \frac{2}{\lambda_0} \int_y^\infty \frac{\Delta n r dr}{\sqrt{r^2 - y^2}}. \qquad (\Pi.1)$$

from ($\Pi.1$) for Δn follows integral equation

$$\Delta n = -\frac{\lambda_0}{\pi} \int_r^\infty \frac{dS}{dy} \frac{dy}{\sqrt{y^2 - r^2}}, \qquad (\Pi.2)$$

which for Gaussian contour $S = S_0 \exp(-y^2/a_0^2)$ has solution

$$\Delta n = \frac{\lambda_0 S}{\sqrt{\pi} a_0} e^{-r^2/a_0^2}. \qquad (\Pi.3)$$

Here λ_0 -- wavelength of the probing light.

Determination of dp/dT for E $\parallel$ Z and E $\perp$ Z

The appearance of mechanical stresses in a solid leads to a change in the refractive index which for an isotropic medium is determined by piezo-optical coefficients q_{11} and q_{12} [29]:

$$\begin{bmatrix} \Delta B_1 \\ \Delta B_2 \\ \Delta B_3 \\ \Delta B_4 \\ \Delta B_5 \\ \Delta B_6 \end{bmatrix} = \begin{bmatrix} q_{11} & q_{12} & q_{12} & 0 & 0 & 0 \\ q_{12} & q_{11} & q_{12} & 0 & 0 & 0 \\ q_{12} & q_{12} & q_{11} & 0 & 0 & 0 \\ 0 & 0 & 0 & q_{11}-q_{12} & 0 & 0 \\ 0 & 0 & 0 & 0 & q_{11}-q_{12} & 0 \\ 0 & 0 & 0 & 0 & 0 & q_{11}-q_{12} \end{bmatrix} \begin{bmatrix} \sigma_{xx} \\ \sigma_{yy} \\ \sigma_{zz} \\ \sigma_{zy} \\ \sigma_{zx} \\ \sigma_{xy} \end{bmatrix} \qquad (\Pi.4)$$

$\Delta n^{(\sigma)} = {}^1/_4 n_0^3 \Delta B_i$

For the problem of plane deformations at $z = 0$, the diagonal tensor of stresses in cylindrical coordinates, becomes nondiagonal when a transformation is made to Descartes coordinates

$$\begin{vmatrix} \sigma_{rr}\cos^2\varphi + \sigma_{\varphi\varphi}\sin^2\varphi & (\sigma_{rr}-\sigma_{\varphi\varphi})\frac{\sin 2\varphi}{2} & 0 \\ (\sigma_{rr}-\sigma_{\varphi\varphi})\frac{\sin 2\varphi}{2} & \sigma_{rr}\sin^2\varphi + \sigma_{\varphi\varphi}\cos^2\varphi & 0 \\ 0 & 0 & \sigma_{zz} \end{vmatrix} \qquad (\Pi.5)$$

For radiation with E || Z polarization

$$\Delta n_{\parallel}^{(\sigma)} \equiv \Delta n_3^{(\sigma)} = C_2(\sigma_{rr}+\sigma_{\varphi\varphi})+C_1\sigma_{zz} \qquad (\Pi.6)$$

and for E⊥Z

$$\Delta n_{\perp}^{(\sigma)} = \Delta n_{\parallel}^{(\sigma)} = \frac{C_1+C_2}{2}(\sigma_{rr}+\sigma_{\varphi\varphi}) + C_2\sigma_{zz} + \frac{C_1-C_2}{2}(\sigma_{rr}-\sigma_{\varphi\varphi})\cos 2\varphi, \qquad (\Pi.7)$$

where elastic-optical constants are

$$C_1 = -2q_{11}/n_0^3;\ C_2 = -2q_{12}/n_0^3.$$

In our case

$$\sigma_{zz} = \sigma_{rr} + \sigma_{\varphi\varphi} = -[\alpha E/(1-\nu)]\Delta T \ [30].$$

The total change in dp/dT consists of two members (in our case, the contribution of electrostriction may be neglected):

$$\frac{dn}{dT} = \left(\frac{\partial n}{\partial T}\right)_{\sigma=0} + \left(\frac{\partial n}{\partial T}\right)_T. \qquad (\Pi.8)$$

in case E || Z

$$\left(\frac{dn}{dT}\right)_{\parallel} = \left(\frac{\partial n}{\partial T}\right)_{\sigma} - \frac{\alpha E}{1-\nu}(C_1+C_2). \qquad (\Pi.9)$$

When comparing the experimental shifts of the band for E || Z and E⊥ Z for K8 glass using expressions (П.1), (П.6), (П.7), it was found that for our geometry of the experiment, the member in (П.7), dependent on angle φ may be neglected compared to the first two members in (П.7) for all r. As a result

$$\left(\frac{dn}{dT}\right)_{\perp} = \left(\frac{\partial n}{\partial T}\right)_{\sigma} - \frac{\alpha E}{1-\nu}\,\frac{C_1+3C_2}{2}.$$

The use of polarization E ⊥ Z leads to greater shifts of the interference band, and increases the sensitivity and accuracy of the experiment.

BIBLIOGRAPHY

1. Bloembergen, N. KVANTOVAYA ELEKTRONIKA, 1, 786 (1974).

2. Lee Smith, W.; Bechtel, J. H.; Bloembergen, N. Phys. Rev., B 12, 706 (1975); Optics Comms. 18, 592 (1976).

3. Gorshkov, B. G.; Danileyko, Yu. K; Yepifanov, A. S.; Lobachev, V. A.; Manenkov, A. A.; Sidorin, A. V. ZhETF, 72, 1171 (1977).

4. Danileyko, Yu. K.; Manenkov, A. A.; Nechitaylo, V. S.; Prokhorov, A. M.; Khaimov-Mal'kov, V. Ya. ZhETF, 63, 1030 (1972).

5. Anisimov, S. I.; Makshantsev, B. I. FTT, 15, 1090 (1973).

6. Kovalev, A. A.; Makshantsev, B. I. FTT, 17, 188 (1975).

7. Kondratenko, P. S.; Makshantsev, V. I. ZhETF, 66, 1734, (1974).

8. Makshantsev, V. I.; Kovalev, A. A.; Leonov, R. K.; Yampol'skiy, P. A; ZhTF,, 44, 164 (1974).

9. Kask, N. Ye.; Korniyenko, L. S.; Fedorov, G. M. ZhTF, 43, 2388 (1973).

10. Kask, N. Ye.; Korniyenko, L.S.; Radchenko, V. V.; Fedorov, G. M.; Chopornyak, D. B. KVANTOVAYA ELEKTRONIKA, 3, 1570 (1976).

11. Bonch-Bruyevich, A. M.; Imas, Ya. A.; Komalov, V. L.; Salyadinov, V. S., Smirnov, V. N. ZhTF,45, 1117 (1975).

12. "Colorless Optical Glass. Physio-Chemical Properties. Parameters." GOST 13659-68, Moscow, 1968.

13. Berezina, Ye. Ye. "Opt.-mekh. prom," No 2, 38 (1970).

14. Buzhinskiy, I. M.; Dianov, Ye. M.; Mamonov, S. K. ; Mikhaylova, L. M.; Prokhorov, A. M. DAN USSR, 190, 558 (1970).

15. Buzhinskiy, I. M.; Mamonov, S. K.; Trudy MVTU, No 184, 181 (1974).

16. Kask, N. Ye.; Radchenko, V. V.; Fedorov, G. M.; Chopornyak, D. B. KVANTOVAYA ELEKTRONIKA, 4, 464 (1977).

17. Mikaelyan, A. L.; Ter-Mikaelyan, M. L.; Turkov, B. G. "Optical Oscillators in Solids." Moscow, Sov. radio, " 1967.

18. Dianov, Ye. M.; Karasik, A. Ya.; Korniyenko, L. S.; Prokhorov, A. M.; Shcherbakov, I. A. KVANTOVAYA ELEKTRONIKA, 2, 1665, (1975).

19. Dianov, Ye. M.; Karasik, A. Ya.; Kut'yenkov, A. A.; Neustruyev, V. B.; Shcherbakov, I. A. KVANTOVAYA ELEKTRONIKA, 3, 168 (1976).

20. Alekseyev, N. Ye.; Izyneyev, A. A.; Kravchenko, V. B.; Rudnitskiy, Yu. P. KVANTOVAYA ELEKTRONIKA, 1, 2002 (1974).

21. Basiyev, T. T.; Mamedov, T. G.; Shcherbakov, I. A. KVANTOVAYA ELEKTRONIKA, 2, 1269 (1975).

22. Dianov, Ye. M.; Kut'yenkov, A. A.; Manenkov, A. A.; Osiko, V. V.; Prokhorov, A. M.; Ritus, A. I.; Shcherbakov, I. A. ZhETF, 69, 540 (1975).

23. Tolstoy, N. A.; Abramov, A. P. "Optika i spektroskopiya," 20, 496 (1966).

24. Karpik, J. T.; Di Bartolo, B.; Birang, F. Bull. Amer. Phys. Soc., Ser. II, 15, 800 (1970).

25. Riseberg, L. A.; Moos, N. W. Phys. Rev., 174, 429 (1968).

26. Kovalev, A. A.; Makshantsev, V. I.; Mul'chenko, B. F.; Pilipetskiy, N. F. ZhETF, 70, 132 (1976).

27. Kruppke, W. F. IEEE J. QE-10, 450 (1974).

28. Ladenburg, R. U. "Physical Measurements in Gas Dynamics and in Combustion." Moscow IL., 1957.

29. Hay, Dzh. "Physical Properties of Crystals," Moscow, "Mir", 1967.

30. Boli, F.; Veyner, Dzh. "Theory of Temperature Stresses," Moscow, "Mir", 1964.

2291
CSO: 8144/1033

PHYSICS

UDC 621.378

THIRD ORDER NONLINEAR SUSCEPTIBILITY OF IONIC CRYSTALS NEAR RAMAN AND TWO-PHOTON RESONANCES

Moscow KVANTOVAYA ELEKTRONIKA in Russian Vol 6, No 2, Feb 79 pp 345-348

[Article by L. B. Meysner, N. G. Khadzhiskiy, Moscow Government University imeni M. V. Lomonosov, submitted 28 Mar 78]

[Text] The purpose of this paper is to state the results of theoretical work in which, for the first time, a quantitative description of experimental results on measuring resonance combinational and two-photon susceptibilities of ionic crystals is given.

If the following electric field acts on the ions of the lattice

$$E(t)=E(\omega_1)e^{-i\omega_1 t}+E(\omega_2)e^{-i\omega_2 t}$$

(ω_1 and ω_2 -- frequency of pumping waves introduced into the medium, lying in the transparency region of the crystals), then the polarization induced in the medium at frequency $\omega_3=2\omega_1-\omega_2$ (when difference frequency $\omega_1-\omega_2$ is near frequency ω_T of transverse combinational modes and $2\omega_1$ is close to frequency ω_0 of two-photon resonance) is conveniently written in the form

$$P_\alpha^{(3)}(\omega_3)=3\left[\chi_{\alpha\beta\gamma\theta}^{(3)e}(\omega_3)+\chi_{\alpha\beta\gamma\theta}^{(3)R}(\omega_3)+\chi_{\alpha\beta\gamma\theta}^{(3)tp}(\omega_3)\right]E_\beta(\omega_1)E_\gamma(\omega_1)E_\theta^*(\omega_2)=$$
$$=\sum_{i=1}^{m}a^iN^iW_\alpha^i(\tilde{\omega}_3). \qquad (1)$$

Here $\chi^{(3)e}$, $\chi^{(3)R}$ and $\chi^{(3)tp}$ -- respectively nonresonance electronic, resonance Raman and resonance two-photon susceptibilities of the crystal; W^i -- shift of the charge of the shell of the a^i i-th ion with respect to its equilibrium position; N^i -- number of ions of the i-th kind per unit volume.

In this paper, $\chi^{(3)R}$ and $\chi^{(3)tp}$ are calculated for ionic crystals. The electronic nonresonance susceptibility of the third order for crystals was investigated in great detail in [1].

2. Following [1, 2], of all the causes of the nonlinearity of susceptibility, we will take into account only the one that is related to the nonlinear dependence of the local field on shifts of electronic shells W^i:

$$e_\alpha^l = E_\alpha(t) + \sum_{\beta,\ k} a^k g_{\alpha\beta}^{lk} W_\beta^k + \frac{1}{2} \sum_{\beta\gamma,\ k} a^k f_{\alpha\beta\gamma}^{lk} W_\beta^k W_\gamma^k, \qquad (2)$$

where coefficients g^{ik} and f^{ik} (coefficients of the internal field) are determined only by the lattice structure [3].

Although the external field acts directly on the electronic shells of ions, however, some part of the energy, due to the motion of the electronic cloud, is transmitted to the nuclei. The nuclei begin to oscillate which leads to a change in the local field (of coefficients g^{ik} and f^{ik}). Mathematically this can be written, expanding coefficients g^{ik} and f^{ik} into a series according to shifts of nuclei u^k. We will limit ourselves to taking into account the linear addend according to u^k in expanding coefficient g^{ik}:

$$g_{\alpha\beta}^{lk} = (g_{\alpha\beta}^{lk})_0 + \sum_q \left(\frac{\partial g_{\alpha\beta}^{lk}}{\partial u_q^k} \right)_0 u_q^k. \qquad (3)$$

Computation of derivative $\partial g_{\alpha\beta}^{lk}/\partial u_q^k$ in a balanced configuration is reduced to calculating $f_{\alpha\beta q}^{lk}$.

3. We will write the Hamiltonian system consisting of electrons and ions in the presence of the light wave field

$$H = T + \Delta\Phi^R - \sum_l \mu^l \vec{\mathcal{E}}^l - \sum_l \mu^l E(t). \qquad (4)$$

Here T -- kinetic energy of the system

$$\Delta\Phi^R = \frac{1}{2}\sum_{\alpha,\beta}\sum_{i,k}\left(R^{ik}_{\alpha\beta}\,u^i_\alpha\,u^k_\beta + C^{ik}_{\alpha\beta}\,w^i_\alpha\,w^k_\beta\right)$$

-- increment of the non-coulomb part of the lattice energy to harmonic approximation where R^{ik} and C^{ik} -- force constants representing interaction forces between irons and electrons. Addends $\mu\vec{\mathcal{E}}'$ in (4) describe coulomb's interaction and leads to anharmonic members in (4) of coulomb origin, because $\vec{\mathcal{E}}' = \vec{\mathcal{E}} - E(t)\vec{\mathcal{E}}'$ -- internal field in the lattice), is given by equations (2) and (3) and the dipole moment $\mathcal{M}^i = a^i w^i$. The last addend in (4) takes into account the interaction between the electrons and the external field. The external field is high-frequency and, therefore, acts only on the electron shells.

We will stress that in the general case (4) must also include anharmonic corrections of non-coulomb origin, i.e., corrections representing the following members of expanding $\Delta\Phi^R$ into a series according to the shifts of electrons and ions. Thus, for example, a change in electronic dipole moment $\mathcal{M}^i$, due to nuclei shift at frequency $\omega_1 - \omega_2 = \omega$, is determined not only by a member proportional to $\frac{\partial g^{ik}}{\partial u^k}u^k$, but also member $\frac{\partial C^{ik}}{\partial u^k}u^k$.

However, the calculation of C^{ik} is problematic [3]. Therefore, here will neglect the anharmonism of short-range forces, which is the basic approximation of the so-called model of coulomb anharmonism [1, 2]. It is at least important to discuss qualitatively the possible role of short-range forces, i.e., estimate the degree of approximation of the model.

It follows from the calculation of energy of two-atom crystals that harmonic short-range and long-range force constants have opposite signs and differ 2 to 3 times numerically [3], while in ferroelectrics, as is well known, there is almost full compensation of near-range and far-range forces. If this is also true for anharmonic force constants, then calculation of to a coulomb anharmonism approximation may differ from the experimental data by only 2 to 3 times and the calculated sign should not correspond to the one experimentally measured in all cases.

It may be asserted from these positions that if the calculated sign does not correspond to the one experimentally measured, the anharmonism of the near-range forces dominates and conversely, if the signs coincide, the basic contribution is made by coulomb anharmonism. The values of $\chi^{(3)}$ calculated according to the modulus must differ from experimental data by not more than 2 to 3 times.

The results in [1], in general, confirm everything stated above. In this paper, the equation obtained for $\chi^{(3)R}$ does not contain free parameters and, therefore, calculations of $\chi^{(3)R}$ must give additional important data on the mechanism of nonlinear polarization in various types of crystals.

4. Motion equations for electrons and ions are obtained from relationships

$$m^l \ddot{W}_\alpha^l = -\frac{\partial H}{\partial W_\alpha^l};$$
$$M^l \ddot{u}_\alpha^l = -\frac{\partial H}{\partial u_\alpha^l}, \qquad (5)$$

where m^l and M^l -- masses of an electron and ion.

As shown in [1], in solving a type (5) system, it is convenient to consider all electronic oscillators to a harmonic approximation equivalent, i.e.,

$$a^l = a^k = a, \quad W_\alpha^l(\omega) = W_\alpha^k(\omega) = W_\alpha(\omega) = \frac{\chi_{\alpha\alpha}^{(1)}(\omega)}{aN_0} E_\alpha(\omega),$$

where $\chi^{(1)}$ -- linear macroscopic susceptibility of the crystal; N_0 -- number of ions per unit volume. Since the procedure for solving system (5) is very similar to that considered in [1, 2], we will omit it. We will only note that in solving equations for ions (nuclei) a crystal with one combinational-active oscillation is considered.

The equations obtained for $\chi^{(3)R}$ and $\chi^{(3)tp}$ to a coulomb anharmonism approximation have the form

$$\chi_{\alpha\beta\gamma 0}^{(3)R}(\omega_3) = \frac{\chi_{\alpha\alpha}^{(1)}(\omega_3)\chi_{\beta\beta}^{(1)}(\omega_1)\chi_{\gamma\gamma}^{(1)}(\omega_1)\chi_{00}^{(1)}(\omega_3)}{3N_0^l\left[\omega_T^2 - (\omega_1 - \omega_2)^2 - i\gamma(\omega_1 - \omega_2)\right]} \sum_{\theta,\varepsilon,k,k'} \frac{N^l}{M^k} I_{\alpha\beta\gamma}^{lk} I_{\gamma\theta\varepsilon}^{kk'}; \qquad (6)$$

$$\chi^{(3)R}_{\alpha\beta\gamma\theta}(\omega_3) = \frac{\chi^{(1)}_{\alpha\alpha}(\omega_3)\,\chi^{(1)}_{\beta\beta}(\omega_1)\,\chi^{(1)}_{\gamma\gamma}(\omega_1)\,\chi^{(1)}_{\theta\theta}(\omega_3)}{3N_0^4\left[\omega_0^2 - 4\omega_1^2 - 2i\Gamma\omega_1\right]} \sum_{\rho,l,k,k'} \frac{N^l}{m^k}\, f^{lk}_{\alpha\beta\rho}\, f^{kk'}_{\alpha\theta\rho}. \qquad (7)$$

5. We will dwell separately on expressions (6) and (7). The equation for Raman susceptibility contains no free parameter which makes the procedure of calculating $\chi^{(3)R}$ simple and, what is most important, makes it possible to estimate the role of non-coulomb anharmonism.

In calculating $\chi^{(3)R}$ by (6) linear susceptibility $\chi^{(1)}$, resonance frequency ω_T and attenuation coefficient γ are assumed to be equal to their experimental values, while coefficients of internal field f^{ik} are calculated exactly by known ion coordinates. In the given case, the known difficulty does not arise with series convergence, which was solved by Ewald [3] for a dipole lattice (for g^{ik}). Thus, an error permitted when calculating $\chi^{(3)R}$ by (6) is related only to an experimental error in determining $\chi^{(1)}$, ω_T, γ and the coordinates of the ions.

We calculated $\chi^{(3)R}$ by (6) for a covalent diamond crystal and ionic crystals with a fluorspar structure. The necessary experimental data for these crystals are available [4]. According to (6), for all considered crystals, only component

$$\chi^{(3)R}_{1221}$$

is different from zero which agrees with symmetry requirements. Numerical values of

$$\chi^{(3)R}_{1221}$$

are shown in Table 1. It may be seen that for the case of ionic crystals, the theory agrees almost precisely with the experiment, but gives a considerably higher (five-fold) value of

$$\chi^{(3)R}_{1221}$$

for a covalent diamond crystal.

Table 1

Raman susceptibility in a diamond and crystals with a fluorspar structure

(1) Кристалл	ω, $см^{-1}$	γ, $см^{-1}$	n	$\mathrm{Im}\,\chi^{(3)R}_{1221}(\omega_3)$, 10^{-14} ед. СГСЭ (2)	
				(3) расчет	эксперимент [4]* (4)
CaF_2	322	7	1,43	1,3	1,14±0,28
SrF_2	285	7	1,44	1,7	2,00±0,26
CdF_2	322	14	1,55	2,0	1,54±0,27
BaF_2	240	7	1,47	3,0	5,34±0,57
Алмаз	1332	2,04	2,42	2490	576

* Модуль экспериментальной величины. (5)

1. Crystal
2. SGSE [CGSE system of units]
3. Calculation
4. Experiment
5. Modulus of the experimental value

From the viewpoint of the considered model, the results obtained for $\chi^{(3)R}$ may be understood if it is assumed that in ionic crystals the change in near-range forces is negligibly small, i.e., the anharmonism of near-range forces may be neglected in estimating $\chi^{(3)R}$, which is impermissible in covalent crystals.

We will now turn to (7). Formally, (7) does not contain free parameters, however, experimental data on the value of Γ is lacking. To estimate the denominator in (7), we will assume it to be one and the same for the susceptibilities of various orders. This assumption is used in alll calculations of nonlinear susceptibilities (see, for example, [1, 5-7]), although it is difficult to justify it, but in this case, not too bad an agreement is obtained with experimental values of nonlinear susceptibilities. On the assumption of a single denominator, the denominator in (7) may be expressed in terms of real ε' and imaginary ε'' parts of the high-frequency specific inductive capacitance.

Assuming that electronic oscillators are equivalent to linear approximation and using the tie equation

$$\varepsilon(\omega)=1+4\pi P/E,$$

We will find immediately that

$$D(\omega)=(4\pi N_0 a^2)^2\,[[(\varepsilon'(\omega)-1)^2-\varepsilon''(\omega)^2]\,m^2)^{-1}, \quad (8)$$
$$D(\omega)=\omega_0^2-\omega^2-i\omega\gamma.$$

Table 2

Two-photon susceptibility in crystals with a sphalerite structure

(1) Кристаллы	$\mathrm{Im}\,\chi^{(3)tp}_{1221}$, 10^{-14} ед. СГСЭ (2)	
	(3) расчет	эксперимент* (4)
GaAs	24	23 [9]
GaP	4,2	0,83 [10]
CdTe	5,2	8,7 [11]
CdSe	1,2	1,2 [12]
ZnTe	3,0	2,0 [9]
ZnSe	0,90	1,2 [13]
ZnS	0,33	0,2 [14]

* Модуль экспериментальной величины. (5)

1. Crystals
2. SGSE [CGSE system of units]
3. Calculation
4. Experiment
5. Modulus of experimental value

The calculation of $\chi^{(3)tp}$ according to (7) using (8) agreed well with experimental results. Calculation data for $\chi^{(3)tp}$ in precise resonance for crystals with a sphalerite structure and experimental data are shown in Table 2. Free parameter a in (8) was determined as in [1]. The degree of the ionic character of compounds was assumed according to Phillips [8].

The presence of free parameters always makes the calculation of substance constants non-single-valued. However, for the crystals considered here,

the degree of the ionic character was determined on the basis of various approaches and the results of various authors are found to be in satisfactory agreement. Therefore, we assume that the obtained correspondence between calculation and experiment for $\chi^{(3)tp}$ reflects primarily the applicability of the coulomb's anharmonism to the quantitative (with a precision of up to 2-4 times) description of the two-photon susceptibility of ionic crystals and is not the result of a lucky fit of the free parameter.

6. In spite of certain shortcomings of the considered theory of cubic resonance of susceptibility of ionic crystals, nevertheless, it made it possible to describe quantitatively experimental results for Raman and two-photon susceptibilities of ionic crystals. The results obtained indicate the applicability in principle of lattice dynamics conceptions to the description of dispersion of cubic susceptibility. It is possible to expect that the accumulation of experimental data on $\chi^{(3)tp}$ and $\chi^{(3)R}$ will make it possible to define more concretely the area of applicability of the proposed method for calculating $\chi^{(3)R}$ and $\chi^{(3)tp}$.

The authors consider it their pleasant duty to express their gratitude to S. A. Akhmanov, N. I. Koroteyev and A. P. Levanyuk for their interest in this paper and the discussion of its results.

BIBLIOGRAPHY

1. Akhmanov, S. S.; Meysner, L. B.; Parinov, S. G; Saltiyel, S. M.; Tunkin, V. G. ZhETF, 71, 1710 (1977).

2. Meysner, L. B. ZhETF, 69, 2101 (1975).

3. Born, M.; Kun', Kh. "Dynamic Theory of Crystal Lattices." Moscow, IL, 1958.

4. Levenson, M. S.; Bloembergen, N. Phys. Rev. B, 10, 4447 (1974).

5. Levine, B. F. Phys. Rev. Letts, 22, 787 (1968).

6. Tha, S.; Bloembergen, N. Phys. Rev. 171, 891 (1968).

7. Tang, C. L. IEEE J. QE-9, 755 (1973).

8. Van Vechten, J. A. Phys. Rev., 187, 1007 (1969).

9. Leo, C. C.; Fan, H. Y. Phys. Rev., B, 9, 3505 (1974).

10. Catalano, I. M.; Cingolani, A.; Minafra, A. Solid States. Comms, 16, 417 (1975).

11. Berko, S. T. Phys. Rev., B, 12, 669 (1975).

12. Bechtel, T. N.; Smith, W. L. Phys Rev., B, 13, 3515 (1976).

13. Arsen'yev, V. V.; Dneprovskiy, V. S., Klyshko, D. N.; Penin, A. N. ZhETF, 56, 760 (1969).

14. Panizza, E. Appl. Phys. Letts, 10, 265 (1967).

2291
CSO: 8144/1033

PHYSICS

UDC 621.373.826.038.823

POSSIBLE STABILIZATION OF THE CO_2 LASER FREQUENCY BY AN EXTERNAL STARK CELL WITH 1-1 DIFLUORETHANE ($C_2 H_4 F_2$)

Moscow KVANTOVAYA ELEKTRONIKA in Russian Vol. 6, No 2, Feb 79 pp 351-354

[Article by V. P. Avtonomov, R. Aleksandresku, D. Dumitrush, D. Dutsu, Physical Institute imeni P. N. Lebedev AN USSR (Moscow); Institute of Physics and Technology of Radiation Apparatus (Bucharest) Socialist Republic of Romania, submitted 11 Apr 78]

[Text] Results are presented of the Stark modulation index and coefficient of the absorption of CO_2 laser radiation at the P (24) line by 1-1 difluorethane ($C_2 H_4 F_2$). Possible stabilization of the CO_2 laser frequency by a stark cell is shown and the efficiency is determined of laser frequency tuning within the P (24) line of the $00^0 1 - 10^0 0$ transition.

After modulation of the output beam of a CO_2 laser by means of the Stark effect in molecular gases was achieved [1], a number of papers on this subject appeared [3, 4]. Useful applications of this phenomenon were demonstrated on the examples of deuterated ammonia (NH_2D). In [2] is shown how it is possible to stabilize and retune the CO_2 laser frequency by means of a Stark cell on the P20 line of the $00^0 1 - 10^0 0$ transition. The theoretical aspects of Stark modulation were considered in [5, 6]. It has already been established that at least 11 various gases are suitable for modulating CO_2 laser oscillation lines [7, 8], however, to recommend their use will be possible only after additional investigations.

It was shown in [7] that using 1-1 difluorethane can provide a CO_2 laser amplitude modulation on eight P10-P26 lines of $00^0 1 - 10^0 0$ transition. However, the authors of [7] did not succeed in observing absorption lines with good resolution, which is necessary to solve the problem of stabilizing the laser frequency by using the Stark effect.

This paper gives the results of using 1-1 difluorethane ($C_2 H_4 F_2$) for stabilizing a CO_2 laser in the P24 line of $00^01\text{-}10^00$ transition.

The arrangement of the experimental installation is shown in Fig. 1. CO_2 laser 1 with a resonator 58cm long may be retuned by a diffraction grating in the resonator (75 lines/mm) from the P8 to the P34 and from the R8 to the R34 10.4 micron band, as well as from the P14 to the P34 9.4 micron band [9]. Stabilized power supply circuit 2 and an APCh [Automatic frequency control] system according to the discharge impedance 3[10] made it possible to obtain a stabilized mode of laser operation at any of the indicated lines. The Invar alloy resonator provided amplitude stability of laser operation at a level of 0.5 to 1% at the full output power of the laser of 3.5 watts on line P20. We did not use laser radiation in the direction of the zero-th order of the grating (about 2.5 watts).

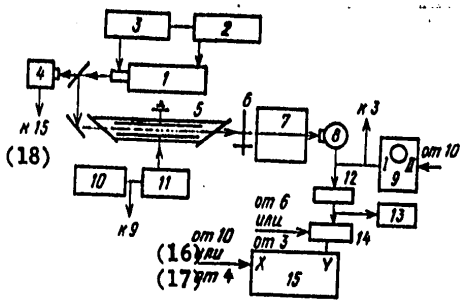

Fig. 1. Arrangement of experimental installation

16. or
17. from
18. to

The output radiation beam was divided into approximately two parts equal in intensity, one of which was directed to calorimeter 4, while the second passed through a Stark cell 5. The 64cm long cell had Brewster windows and flat internal polished aluminum electrodes 55cm long with a 5.0± 0.1mm distance between them. Gas pressure in the cell was measured by an oil manometer. The radiation was modulated by interrupter 6, was passed through monochromator 7 and recorded by a Ge-Au receiver at 77K, 8. The receiver signal was observed on the screen of a two-beam oscillograph 9 and after the amplifier was recorded by either a digital voltmeter 13, or, passing through a synchronous detector, was recorded by a two-coordinate automatic recorder 15.

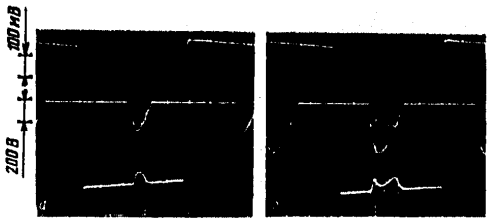

Fig. 2. Oscillograms of a CO_2 laser radiation signals after passing through cell (upper beams) and voltages across electrodes of cell (lower beams) for various voltages and a cell gas pressure of 1.5mm of the mercury column.

Voltages applied to electrodes of cell 5 (DC or AC) were provided by functional oscillator 10 and operational amplifier 1. The laser was tuned in sequence to all possible oscillation lines and was stabilized in frequency. The radiation signal that passed through the cell to the receiver was observed on one of the osvillograph beams. The signal of functional oscillator 10 was sent simultaneously to the second osbillograph input, which determined the voltage change on the electrode of cell 5.

Thus, it was possible to observe modulation on lines cited in [7], as well as five other CO_2 laser lines. The modulation index for lines P28, P32 and P22 of the $00^01\text{-}10^00$ transition was negative and for R18 and R20 of the same transition -- positive (we call modulation index ratio $m = (I_s - I)/I$, where I_s -- radiation power after passing the cell with the field applied; I -- radiation power after passing the cell without a field.

Fig. 2 shows oscillograms of the receiver signals for line $00^01\text{-}10^00$ and the signal from the functional oscillator. It was established that for 240 volts across the cell electrodes, absorptions in the gas has its greatest value at maximum field amplitude (Fig. 2a). If the field amplitude is increased, a clear-cut peak appears in the absorption (Fig. 2b). A breakdown occurs at about 470 volts.

A digital voltmeter was used for a more accurate measurement of the modulation index and absorption coefficients as functions of pressure. Measurement of absorption indices in 1-1 difluorethane indicated an absence of a saturation effect. The values of absorption indices in gas without a field and at the maximum of the absorption peak are equal to $(4.7 \pm 0.1) \times 10^{-3}$ cm^{-1} - mm of mercury column $^{-1}$ respectively.

Fig. 3 shows the dependence of modulation index m on the pressure in the cell. As may be seen from this figure, the maximum value of the modulation index is 9% which agrees with data in [7]. It should be noted that the modulation index reaches its maximum value with increasing pressure at an increasing voltage (250 to 260 volts).

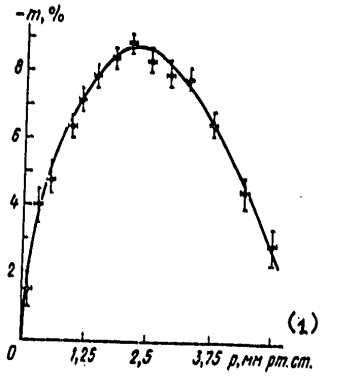

Fig. 3. Relationship between modulation index m and pressure in a 1-1 difluorethane cell at constant voltage across the electrodes.

1. mm of mercury column.

Fig. 4 shows the relationship between m and voltage across the cell electrodes obtained by means of a two-coordinate automatic recorder and synchronous detector (see Fig. 1). It may be seen from Fig. 4 that the absorption peak shifts to the side of higher voltages with an increase in pressure. In our opinion, this is due to the fact that the absorption peak is not the only Stark component line in 1-1 - difluorethane, since an analysis of the dependence of derivative $\partial I / \partial U$ on the absorption contour at low pressure (about 0.6 mm of the mercury column) indicated that the given peak consists of at least two lines. Even at a pressure of 1mm of the mercury column, under our conditions, it was impossible to notice their superimposition. This does not interfere with using the relationship shown in Fig. 4 for stabilizing the CO_2 laser frequency at line P24.

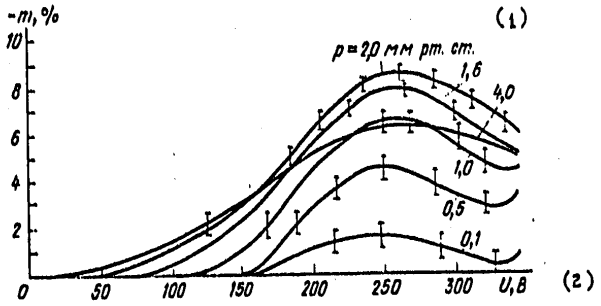

Fig. 4. Relationship between modulation index m and voltage across cell electrodes for various gas pressures.

1. mm of mercury column 2. volts

A semisoidal 8-volt signal was sent from unit 3 (see Fig. 1) to the electrodes of the cell. The constant voltage applied to the electrodes was 240 volts. The signal from receiver 8 was sent to unit 3 and the APCh mode was connected. The investigation of the discriminator contour indicated that its half-width was somewhat smaller, but of the same order of magnitude as the amplification line contour of the laser. This circumstance makes it possible to hope to obtain a level of frequency stability no worse than when using the usual stabilization arrangement [10].

Changing the constant voltage across the cell electrodes made it possible to change the oscillation frequency within the limits of the line without disturbing the operation of the APCh circuit. The lack of a reference stabilized laser did not permit the measurement of the tuning frequency band, therefore, we will cite only the relative estimate of the tuning efficiency, obtained by recording the signal from power meter 4 on automatic recorder 15 (the time constant of the channel was less than 1 second). The scanning voltage was sent from unit 3 to the piezo-ceramic resonator of the laser and to the X-coordinate of the automatic recorder.

It was noted that besides line P24 adjacent to it, lines P22 and P26 could also participate in oscillation without retuning the grating. By changing the constant voltage across the cell electrodes, it would be possible to record the part of line P24 on which the operation of the APCh circuit was stable. The change in voltage was about 50 volts. Since such a determination of the frequency band may lead to large errors, due to stretching the frequency, we measured the relative value of retuning the laser frequency within the limits of line P24. It depends on gas pressure in the cell and is 80% in the 2 to 3.5mm of the mercury column region.

It should be noted that the main limitations in this case were competition points between line P24 and adjacent lines P22 and P26. We consider the optimal pressure in the cell 2mm of the mercury column. It may well be seen from Fig. 4 that the widening of the absorption peak increases with an increase in pressure which may lead to the deterioration of the stability of the system.

BIBLIOGRAPHY

1. Landman, A.; Marantz, H.; Early, V. Appl. Phys. Letts, 15, 357 (1969).

2. Nussmeier, T. A.; Abrams, R. L.; Appl. Phys. Letts, 25, 615 (1974).

3. Asama, C. K.; Plaht, T. K. Appl. Phys. Letts, 30, 96 (1977).

4. Abrams, R. L.; Asama, S. K., IEEE J. QE-12, 646 (1976).

5. Claspy, R. C.; Yoh-HanPao. IEEE J. QE-7, 512 (1971).

6. Lugovoy, V. N. ZhETF, 72, 1283 (1977).

7. Jensen, R. E.; Tobin, M. S. IEEE J. QE-8, 34 (1972).

8. Martin, J. M.; Corcoran, V. J.; Smith, W. T. IEEE J. QE-10, 191 (1974).

9. Dumitras, D. C.; Dutu, D. C.; Comaniciu, N.; Draganescu, V. Rev. Roum. Phys. 21, 225 (1976).

10. Skolnik, M. IEEE J. QE-6, 139 (1970).

2291
CSO: 8144/1033

PHYSICS

UDC 621.378.4

PARAMETRIC CONVERSION OF THE MEDIUM INFRARED REGION RADIATION IN ZINC-GERMANIUM DIPHOSPHIDE

Moscow KVANTOVAYA ELEKTRONIKA in Russian Vol 6, No 2, Feb 79 pp 357-359

[Article by N. P. Andreyeva, S. A. Andreyev, I. N. Matveyev, S. M. Pshenichnikov, N. D. Ustinov, submitted 25 Apr 78]

[Text] Computer calculations have been performed of the basic characteristics of the medium IR region parametric converter utilizing the $ZnGeP_2$ crystal pumped by the Nd^{3+}: YAG laser radiation. An experiment has been made on the CO_2 laser radiation conversion into the visible region utilizing $ZnGeP_2$ samples which feature an essential absorption. The conversion coefficient of 0.05 under laser Q-switching has been achieved, the power density being 3×10^6 w/cm^2 and the crystal length being 0.3cm. Resistance of the $ZnGeP_2$ crystal to the pulsed neodymium laser radiation and to the continuous radiation of the CO_2 laser radiation has been studied.

The prospects of using zinc-germanium diphosphide ($ZnGeP_2$) in nonlinear optics is determined by the high value of the nonlinear susceptibility tensor ($\chi_{36} = 2.7 \times 10^{-7}$ CGSE units) and the availability in it of 90° synchronism for converting the CO_2 laser radiation into the near IR region. The basic linear and nonlinear optical properties of the $ZnGeP_2$ crystal were investigated in [2-4]. The crystal has a chalcopyrite structure [1], a tetragonal symmetry (class $\bar{4}2m$), is positive and is transparent in the 0.77 - 12 micron region. It has an anomalous absorption in the region less than 1.0 micron which does not permit the achievement of its advantages, especially, at a large interaction distance. Of certain practical interest is the investigation of converters using thin (0.1 - 0.2cm) $ZnGeP_2$ crystals. In this case, first, the absorption decreases considerably due to the small distance of interaction and to the possibility of annealing crystal samples and, secondly, the visual angle, the synchronism band and the resolution are increased when the image is converted. At the same time, a reduction in the efficiency of conversion due to a reduction in the interaction distance (for example, compared to Ag3 AsS_3, $AgGaS_2$ and other

crystals) is to a certain extent compensated by the high nonlinear susceptibility of $ZnGeP_2$. In [5] are cited comparison data on theoretical quantum efficiencies of nonlinear $ZnGeP_2$, GaSe, CdSe and Ag_3AsS_3 crystals for the case of converting CO_2 laser radiation (10.6 microns) into the near IR region (0.96 microns) when pumped by radiation of a neodynium laser (1.06 microns). In this paper, for the same case, the power, angular and frequency characteristics of a converter using a $ZnGeP_2$ crystal are investigated.

To implement the experiment, the following were calculated on a computer: the geometry (the disposition of the wave vectors of interacting waves with respect to the optical axis of the crystal) of the vector of three-frequency interaction in the $ZnGeP_2$ crystal, the visual angle and the synchronism band; in this case, the dispersion characteristics, cited in [2] were used. The visual angle is determined as the angle in which the detuning multiplier $\gamma = \sin c^2 (\Delta \bar{k} l/2)$ (where $\Delta \bar{k}$ -- detuning modulus, l - length of the interaction region) pass through values zero-maximum-zero at a constant frequency of signal radiation, while the frequency band was determined as the frequency range in which the detuning multiplier passes through the same values for a constant angle of signal radiation. The calculation method coincided in its basic features with the method used for calculating converter characteristics using the $AgGaS_2$ [6] crystal. The results of the calculation are shown in Fig. 1 when θ_c-- angle between the optical axis of the crystal and the wave vector of the radiation pumping; α -- angle between the wave vectors of pumping and the signal reckoned from the pumping wave vector in the optical axis direction; β -- angle between wave vectors of pumping and output radiation at the total frequency. As may be seen, the tangent synchronism for oe-o type interaction takes place at $\theta = 82^\circ 56'$, $\alpha = o$, $\beta = o$, i.e., it coincides with the collinear and is near the 90-degree one; at a type ee-o interaction the tangent synchronism takes place at $\theta_c = 72^\circ 23'$, $\alpha = 27'$, $\beta = 2'$. The visual angle $\Delta\alpha$ within the crystal is read off as the difference between curves 1 and 3 ordinates at a fixed θ_c for region II in Fig. 1a and as the sum of curve 1 ordinates for region I in Fig. 1a.

Notice should be taken of the large values of the visual angle which may be equal to 15-20° outside of the crystal for a small length of the crystal. Also, crystal is not very critical to tune to angle θ_c and has a considerable synchronism band.

The purpose of the experimental investigations was to check the geometry of collinear interaction oe-o and to determine the real efficiency of the conversion and resistance of $ZnGeP_2$ crystal samples, with considerable absorption (about 5-10cm^{-1}), to laser radiation.

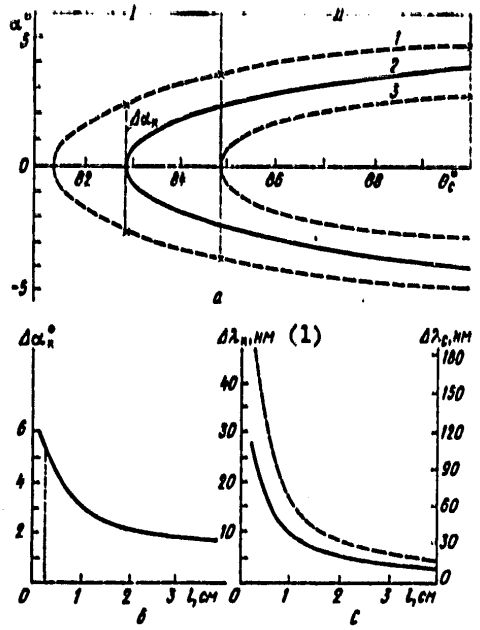

Fig. 1. Basic characteristics of a frequency converter using $ZnGeP_2$ at λ_c = 10.6 microns, λ_H = 1.064 microns, type oe-o interaction:

a -dependence of angle α on θ_c for γ = 0(1,3) and $\gamma = \gamma_{max}$ (2), l = 0.33 cm; b -- dependence of visual angle $\Delta\alpha_к$ of tangent synchronism on the length l of interaction; c -- dependence of conversion band of signal radiation $\Delta\lambda_c$(solid curve) and pumping radiations $\Delta\lambda_H$ (dashed curve) on the length of interaction l.

1. nm.

The experimental installation arrangement is shown in Fig. 2. Monocrystal 4 is 0.3cm thick and had an absorption of $8cm^{-1}$ on 1.06 micron wavelength, $10cm^{-1}$ -- on 0.96 micron and $2cm^{-1}$ on 10.6 micron wavelength. The working faces of the crystal were polished and oriented so that the normal to them was at angle θ_c = 82.5° to the optical axis while the azimuth angle in XY plane was φ = 45° (accuracy of orientation ±0.5°). Angle θ_c was set by rotating the crystal in the synchronism plane, while the mode of collinear synchronism (α = o) -- by rotating matching element 2 made of barium fluoride. A CO_2 laser with a power of about one watt was used as signal radiation oscillator 1; pumping source 9 was an yttrium-aluminum garnet oscillator, providing Q-switching at power density P_H= 3×10^6 w/cm² at pulse τ_H = 30 nanosec and a repetition frequency of 12.5 Hz; the interaction area was limited by diaphragm 3.

The selection of the converted radiation from the pumping radiation was done by interference filters with band $\Delta\lambda$ = 1.2nm and τ = 0.4 maximum transmission.

The conversion efficiency was determined by a direct method by means of measuring the power of the signal wave incident on the crystal and the power of the converted radiation at its output. The power of signal radiation and pumping radiation was measured by an IMO-2 power meter and the pulse power of converted radiation was measured by a preliminary calibrated recording arrangement consisting of an FEU-28, 7, oscillograph 8, interference filters 5 and neutral light filters 6.

The converted radiation was recorded at the converter output for values of angles θ_c, α and β close to the calculated ones (within accuracy limits of sample orientation). The converted radiation was also observed when tuning the crystal to the position of the 90-degree synchronism, but there was considerable instability in this case. The measured conversion coefficient, determined as the ratio of converted radiation power to the signal power was equal to 0.05. Taking absorption into account [7], experimental and calculated results are in fair agreement. The resistance of the $ZnGeP_2$ crystal to pulsed laser radiation at a 1.06 micron wavelength and continuous radiation at a 10.6 micron wavelength were also investigated. When irradiating the crystal by pulsed radiation with a power density of 3×10^6 w/cm^2 no damage to the sample was observed during long operation (30 min at a repetition frequency of 12.5 Hz). The sample was damaged after 5 to 10 pulses at a power density of 20×10^6 w/cm^2 and after one pulse -- at a power density of 50×10^6 w/cm^2. When the sample was irradiated by a CO_2 laser with a power density of 10 w/cm^2, it was not damaged in any way during the entire experiment (3 to 4 cycles of 30min each).

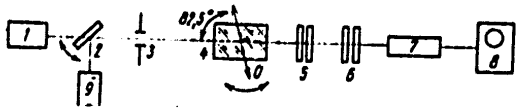

Fig. 2. Arrangement of experimental installation.

The experiment indicated that the $ZnGeP_2$ crystal is promising for use in frequency converters, however, to increase the conversion efficiency, it is necessary to reduce the absorption of thin samples in the region 0.95 - 1.1 microns to 2-4 cm^{-1}.

The samples obtained may apparently be used for fairly efficient conversion of CO_2 laser radiation in the near infrared region when using longer wavelength lasers as pumping oscillators for example, YAG lasers that generate the 1.318 micron line.

In conclusion, the authors express their gratitude to I. I. Tychin for providing monocrystalline samples.

BIBLIOGRAPHY

1. Goryunova, N. A.; Valov, Yu. A. "$A^2B^4C_2^5$ Semiconductors," Moscow, "Sov. radio," 1974.

2. Boyd, G. D. et al. Appl. Phys. Letters, 18, 301 (1971).

3. Gorban', I. S. et al. Ukr, fiz. zhurnal, 18, 9 (1975).

4. Beregulin, et al. FTP, 9, 2288 (1975).

5. Andreyev, Ye. V. et al. KVANTOVAYA ELEKTRONIKA, 4, 57, 657, (1977).

6. Il'inskiy, Yu. A.; Petnikova, V. M. "Izv. vuzov. Ser. Radiofizika," 16, 1285 (1973).

2291
CSO: 8144/1033

PHYSICS

UDC 621.378.33

HIGH-POWER CW ION LASERS WITH LONGER SERVICE LIFE

Moscow KVANTOVAYA ELEKTRONIKA in Russian Vol 6, No 2, Feb 79 pp 359-363

[Article by V. I. Donin, A. F. Shipilov, V. A. Grigor'yev, Institute of Semiconductor Physics, Siberian Department of AN USSR (Novosibirsk), submitted 11 May 1978]

[Text] Experimental results are presented on producing stable high current (~ 400A) reduced pressure discharges for CW ion gas lasers. Efforts to improve the reliability of separate elements of high-current discharge tubes received primary emphasis. A description is given of the prototype high-power ion laser MIL-1, which has been developed on the basis of the experiments performed. The service life of the laser amounts to ~ 1000 hours, the visible radiation output power level being as high as 300 watts.

At present, lasers with direct current plasma excitation in a single-component gas with ions ArII, KrII, ClII, ArIII, KrIII, etc. provide the greatest power of continuous coherent radiation in the visible and near UV regions of the spectrum. For example, [1] cites obtaining from an argon laser 0.5kw continuous blue-green radiation which is a record for the entire shortwave part of the spectrum. At the same time, the use of high-power ionic lasers is held back to a great extent by their low service life, reduced in fact to minutes at output power levels of about 100w [2]. The indicated service life of high power ionic lasers is due to the fact that for their functioning high-current stationary low pressure discharges are required, in which there is usually extensive damage to the walls of the discharge tubes electrodes, leading to the products of the damage settling on parts of the optical resonator, which disrupts its normal operation. It was noted previously in [1] that special discharge tubes and electrodes, developed in the course of high-power argon laser investigations, make it possible to achieve high levels of output power of the ion laser for about 100 hours.

This paper describes the results of the work on further increasing the reliability of parts of high-current discharge tubes of ion lasers and the design created on that basis of a continuous ion laser with a service life of about 1000 hours at an output power level of up to 300 watts.

Investigations of physical processes in high-current argon laser plasma [3 - 7] shows that in order to raise the output power of argon lasers, it is feasible to use wide tubes ($\varnothing \geqslant 10$mm) and that the development of oscillations with discharge current in such tubes has the following special features: 1) at gas pressure, optimal for output power oscillation develops only at high currents in the discharge; under discharge conditions, near optimal for oscillation, instabilities (oscillations) of discharge may arise that destroy the tube [3, 6] . From the viewpoint of increasing laser reliability, the indicated features impose the following demand on the discharge design: first, the ability to function without damage at high currents in a reduced pressure discharge and, secondly, the possibility of providing a stable existence of the discharge.

To obtain a high electron emission, we used a cold arc cathode retaining the cathode spots of the arc within it by a self-heating refractory plug. [1, 3, 9] . Such cathodes are capable of providing practically unlimited stable currents on reduced pressure discharges for long periods without cathode evaporations settling on the active part of the discharge and parts of the structure as a whole.

The cathode was made from vacuum copper with the addition of pure bismuth to the working cavity and was located perpendicularly to the longitudinal axes of the tube (Fig. 1). As shown by preliminary experiments, at such a position, the cathode transition shell, required for connecting the cathode, may serve as an additional source for originating instability in the discharge, therefore, its shape and dimensions were selected on the bases of compactness and the elimination of discharge instabilities. In particular, it should be noted that the use of smaller diameter holes for connecting the transition shell to the cathode led to the origination of instabilities in the discharge. It is appropriate to note also that the requirement of compactness, besides the purely design side, was also beneficial for metal parts of the discharge structure because of a reduction in the effects of pulverization, since at given conditions of the discharge pulverization increases with the length of the parts up to the formation of "cascade" arcs [8] .

Preliminary experiments also indicated that a gas exhaust in the anode shell unsymmetrical relative to the discharge axis may also serve as an oscillation source in the discharge, due to the side deflection of the arc column by the gas flow; to eliminate this source of instabilities a symmetrical exhaust is provided in the design of the anode shell. The anode and cathode shells are joined smoothly to the active part of the tube by small transition sections that reduce the nonuniformities of the potential distribution for the widenings of the discharge.

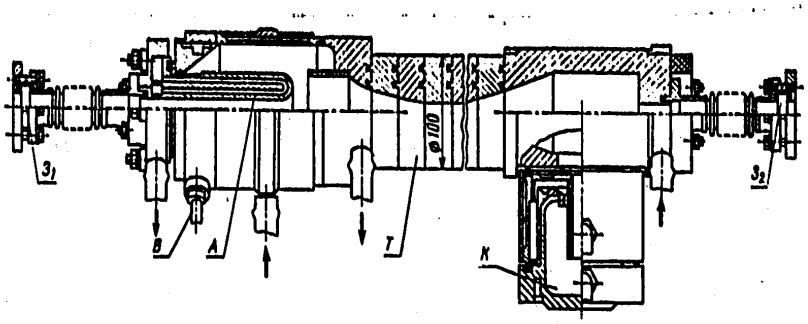

Fig. 1. High-current discharge tube:

A -- anode; K -- cathode; T -- section of pipe; B -- exhaust of vacuum-hose; 3 -- 3_2 resonator mirrors. Small cross-hatch indicates molybdenum parts, blackened areas show packing, arrows indicate water cooling.

A cylindrical anode is made of copper and is placed along the discharge axis. The anode has a central hole to pass the light radiation along the discharge axis. The anode diameters were smaller in the first versions, which increased the discharge current density at the anode and increased the possibility of forming "anode" spots of arc discharge. The formation of anode spots distrubed the normal existence of the discharge and led to the destruction of the anode up to the complete burning out of its housing where the spot was formed. The origination of anode spots in the described design was eliminated by proper selection of the dimensions and shape of the anode unit.

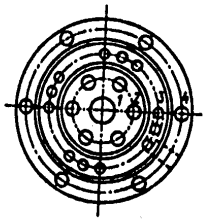

Fig. 2. Section of pipe:

1 -- Working hole; 2 -- holes for reducing the effect of electrophoresis; 3 -- cooling holes (broken line shows cooling outlet in the anode shell); 4 -- holes for tightening bolts with insulation.

Electrode units and the discharge tube were water cooled. The discharge tube was assembled with individual metal sections (Fig. 2) coated with an Al_2O_3 film in order to achieve maximum resistence to ion bombardment and to destruction by heat. Tubes of this type were used for the first time for obtaining oscillations with argon ions at lower discharge currents in [10] and, in the course of further investigations [3, 4, 6, 7], were improved for greater reliability at higher discharge currents. The active length of the tube was two meters for a discharge diameter of 16mm close to the optimal for the output characteristics of lasers with single-tune ionized atoms [11]. The length of individual sections, made of AD-1 aluminum with a subsequent coating of an oxide film anodized in oxalic acid, was 25mm, with a vacuum seal between them provided by gaskets made of thermoresistent vacuum rubber 1mm thick, with a tightening of the entire tube by means of four longitudinal brass bolts. The section around the central hole of the discharges channel had six holes each of bypass channels for eliminating the effect of electrophoresis (see Fig. 2). However, preliminary experiments indicated that tubes with increased lengths (> 1.5 meters for a 16mm diameter) and equalization of the gas pressure drop in the anode and cathode shells by means of the indicated holes, are insufficient for the normal work of the laser, because electrophoresis may create a considerable gas pressure drop directly along the active length of the discharge. As a result of such a drop in the near-cathode part of the discharge, which has lower gas pressure, instabilities that destroy the tube may develop earlier than at a given gas pressure optimal for the power of oscillation discharge currents [3, 6]. Actually, in the design of the pipe used, instabilities could have originated near the oscillation threshold. To eliminate this shortcoming, transverse slots were ground in a part of the washers in the near-cathode region of the discharge, which connect the holes of the bypass channels with the active part of the discharge.

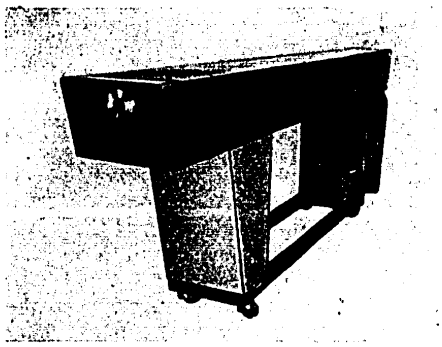

Fig. 3. High-power MIL-1 ion laser with the power supply unit.

On the basis of the described high-current discharge tube, a prototype of a high-power MIL-1 laser was developed which is shown in Fig. 3 (dimensions together with a power supply unit 40 x 110 x 310cm). The separate power supply unit for the laser was designed to locate the electric power supply switching apparatus, the firing circuit and the compact low-noise vacuum pump, connected by a flexible vacuum hose to the anode shell. A constant flow of working gas into the cathode shell is provided by a regulator from a small gas cylinder compressed to 150 atmospheres.

Laser power is provided by rectifying current from a three-phase 300-volt network in accordance with the Larionov circuit. Since the voltage of the basic rectifier (about 500 volts) is insufficient for forming the arc discharge, the initial discharge firing is done by a firing circuit using a 50 microfacad thyristor trigger charged to 3-4kv.

The power output of the laser is regulated by changing the gas pressure in the discharge by the flow regulator. In order to eliminate laser operation in modes of unstable discharge, which may originate with excessive pressure reduction, the laser has a special safety circuit which uses a selective amplifier tuned to the frequency of plasma oscillations (about 250kHz). When they appear, the circuit sends a signal to the automatic power disconnect. MIL-1 laser efficiency tests were made by filling the laser with argon and a discharge current of 400 amps.

The laser resonator was formed by two internal multilayer dielectric mirrors for the blue-greem part of the spectrum with radii of curvature $R = \infty$ and ten meters. The transmission of the output mirror was selected, in accordance with the quality of the mirrors, within limits of 4 to 8%; the other mirror was opaque. With the best mirrors, the laser provides a stable 300 watt output power on 514.5, 501.7, 496.5, 488.0, 476.5 and 457.9mm lines. The output power measurements were made to $\pm$ 10% accuracy by a system consisting of light filters and a photo-multiplier, calibrated accordingto the absolute values in the region up to a 100 watts using a standard IMO-2 power meter. Since the heating of mirrors increased with the deterioration of their quality, average quality mirrors were sprayed on the type of installation described in [12], for testing the service life of the laser. Such a choice made it possible to perform the tests under more difficult conditions of resonator operation with respect to heating. The output power in this case was 200 watts. In the mode of multiple switching the laser operated a total of 500 hours after which it was disassembled for inspection. No reduction in output or any other disturbances in laser efficiency were noted during the tests. In an inspection of the parts of the structure, no essential changes were detected that would indicate important limitations in the service life of individual parts. (On several tube sections insignificant, easily removable changes occurred, consisting of partial destruction of the oxide coating in places in contact with water and subjected to corrosion, since water used for cooling is obtained directly from ordinary water mains).

It should be noted that the presence of an autonomous sytem for pumping gas in the described type of lasers, unlike the soldered systems, practically removes limitations for their storage time and makes it possible to retune the laser quickly to operate on another optical range. Thus, we used a tube of similar design on the laboratory test stand for three years for obtaining high-power oscillation in the yellow-red and blue-green spectrum ranges on KrII and ArII transition respectively and in the UV spectrum range on KrIII and ArIII transitions. Special tests of the service life of this tube were not performed: according to approximate estimates it operated for 1000 hours and continues to operate normally at present.

We will also note that by changing the type of the optical resonator [13], it is possible to obtain high power oscillation in a one-frequency mode (version MIL-1-01). This is important for applications where, along with the high power of stationary light flows, their high monochromatism is required at the same time.

BIBLIOGRAPHY

1. Alferov, G. N.; Donin, V. I.; Yurshin, B. Ya. "Letters to ZhETF," 18, 629 (1973).

2. Kitayev, V. F.; Odintsov, A. I.; Sobolev, N. N. UFN, 99, 361 (1969).

3. Donin, V. I., Candidate dissertation IFP SO AN USSR, Novosibirsk, 1972.

4. Donin, V. I. Transaction of International Conference "Lasers and their Applications." Dresden, 1970, p 491.

5. Boersch, H.; Boscher, J.; Holder, D.; Schafer, G. Phys. Letts A, 31, 188 (1970).

6. Donin, V. I. ZhETF, 62, 1648 (1972).

7. Donin, V. I. Int. Tagung "Laser and ihre Anwendungen," Dresden, 1973. Kurzffasungen zu den Vortragen, K18.

8. Donin, V. I. "Optika i spektroskopiya," 29, 243 (1970).

9. Donin, V. I. Author's certificate No 289458, BI, No 1 (1971); PTE, No 3, 161 (1971).

10. Donin, V. I.; Klement'yev, V. M.; Chebotayev, V. P. ZhPS, 5, 388 (1966).

11. Alferov, G. N.; Donin, V. I.; Yurshin, B. Ya., ZhPS, 25, 40 (1976).

12. Glebov, Yu. A. "Opt. mekh prom," No 2, 46 (1972).

13. Alferov, G. N.; Grigor'yev, V. A.; Donin, V. I. KVANTOVAYA ELEKTRONIKA, 5, 29 (1978).

2291
CSO: 8144/1033

PHYSICS

UDC 621.373.826

HIGH-PRESSURE PERIODIC CO_2 LASER WITH THE NON-SELF-MAINTAINED DISCHARGE AND UV IONIZATION

Moscow KVANTOVAYA ELEKTRONIKA in Russian Vol 6, No 2, Feb 79 pp 370-372

[Article by Ye. A. Muratov, V. D. Pis'mennyy, A. T. Rakhimov, submitted 9 Jun 78]

[Text] Stimulated emission has been achieved from a high-pressure (250 torr) CO_2 laser under conditions of the periodic non-self-maintained discharge controlled by spark sources of the UV radiation. It is shown that the use of UV radiation sources emitting under pulse-periodic conditions makes it possible to implement quasi-CW laser operation.

Papers dedicated to the creation of CO_2 lasers at atmospheric pressure, operating in the mode of the non-self-maintained discharge using external ionization of the gas volume by UV radiation, describe the obtaining of oscillating pulses from a few to several tens of microseconds [2, 3]. The length of oscillation in such systems is due primarily to the time of exposure of the gas medium to external ionizing radiation. However, an increase in the duration of the action of pulsed UV radiation sources leads to a reduction in the light flux in the region of hard UV radiation which, strictly speaking, produces the photoionization of the gas medium. Therefore, to provide the necessary intensity of UV radiation, it is necessary to increase the energy used by the ionization source considerably which, in its turn, leads to a considerable reduction in the power efficiency of the laser.

On the other hand, an increase in the time of the action of the external ionizer on the gas medium and, as a result, an increase in the unit energy input into the non-self-maintained discharge, may be provided by using controlled UV radiation sources, operating in the mode of comparatively short pulses. Such an operating mode makes it possible, having preserved the light efficiency of the UV radiation sources, to excite the gas medium

by a non-self-maintained discharge for a fairly long time [4]. Moreover, by using the excitation arrangement by a periodic non-self-maintained discharge with a period of succession of illuminating pulses, not exceeding the characteristic relaxation time of excited N_2 and CO_2 molecules, it is possible to expect to obtain a quasi-continuous mode of laser operation for a long time.

This paper describes the obtaining of CO_2 laser oscillation at high pressure (250mm of mercury column) with a periodic non-self-maintained discharge (f = 10kHz). The periodic connection of spark sources of UV radiation made it possible to implement a quasi-continuous mode of laser operation with a characteristic length of radiation up to several hundreds of microseconds.

In our experiments, the active volume of the discharge chamber was limited by two electrodes with Chang's profile [5], with a 4.2cm gap (electrodes 40cm long, 4 cm wide). Voltage was fed to the electrodes by a storage capacitor (C = 20 microfarads). The non-self-maintained discharge was initiated by connecting two spark sources of UV radiation, made on the principle of a multigap spark discharger, located 10cm from the optical axis of the system. The source feed circuit assembled with TGI1-2500/50 thyratrons, made it possible to form a train of illumination pulses with a frequency of up to 10kHz.

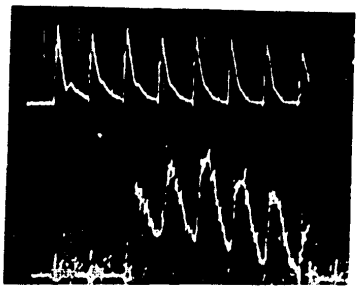

Fig. 1. Oscillograms of current pulses (20A/division) of a non-self-maintained discharge (upper beam)and radiation pulses (scan -- 100 microsec/division).

A CO_2: N_2: He = 2:68:30 gas mixture was used as the active medium to which a small amount of easily-ionized organic admixture -- dimethyl aniline -- was added. This admixture has a comparatively low ionization potential. The total pressure in the discharge chamber in the experiment was 250mm of the mercury column. The resonator of the optical system was formed by two mirrors: copper with a radius of curvature R = 5 and a flat -- made of germaniam with a 90% reflection coefficient. The current of the non-self-maintained discharge, as well as the time of oscillation, was recorded by a Ge-Au receiver.

Estimates show that under the conditions of the experiment, the time of the existence of the inverse population of CO_2 molecules was determined by the transfer time of oscillating energy from the N_2 to the CO_2 molecules and was about 3.5×10^{-4} sec. It is clear, therefore, that for a frequency of excitation pulse sequence $\gtrsim$ 3kHz, a quasi-continuous oscillation mode may be provided.

The figure shows characteristic synchronized oscillograms of the non-self-maintained discharge current and laser radiation for periodic spark sources of UV radiation with a 10kHz frequency. The 8kv voltage applied to the discharge interval was considerably lower than the breakdown voltage for the working gas mixture and the pressure in the chamber. The length of the individual current pulse of the non-self-maintained discharge was about 20 microsec.

As may be seen from the cited oscillograms, the excitation arrangement used makes it possible to achieve a unit energy contribution comparable to that characteristic for a continuous CO_2 laser, excited by an electronic beam [6]. Moreover, it may be seen that periodic excitation of the gas medium by current pulses of the non-self-maintained discharge (f = 10kHz) provides a quasi-continuous mode of laser operation during several hundreds of microsec. The considerable amplitude modulation of the radiation pulse is apparently related to the fact that, under the conditions of the experiment, pumping the gas medium at each individual pulse exceeded the corresponding threshold value slightly. The same circumstance can also explain the lack of oscillation at the moment of the appearance of the first current pulses.

It should be noted that at sufficiently high values of E/p, the development of ionization instability in non-self-maintained discharge leads to a considerable limitation of energy contribution to the discharge. On the cited oscillograms, the start of instability development corresponds to the moment oscillation ceases and the interruption of the current pulse sequence of the non-self-maintained discharge. In this case, the uniform periodic discharge turns into an arc and capacity C is discharged fully. At lower values of electrical field intensity, it is possible to maintain the mode of stable firing of the periodic discharge for a longer time. However, a reduction in the amplitude of the following current pulses in each individual series apparently related to the partial burn-out of the organic admixture leads to a noticeable reduction of the oscillation level with time.

The experimental results obtained indicated that by using periodic sources of UV radiation for irradiating the CO_2 - N_2 - He gas mixture, it is possible to maintain an optically active medium in higher pressure gas during several hundred microseconds. Investigations related to the further increase in the light and power efficiencies of such systems may be very promising for the creation of continuous high-pressure CO_2 lasers in which ionization of the gas medium is provided by UV radiation.

BIBLIOGRAPHY

1. Levin, I. S.; Javan, A. Appl. Phys. Letts, 22, 55 (1973).

2. Velikhov, Ye. P.; Muratov, Ye. A.; Pis'mennyy, V. D.; Prokhorov, A. M.; Radhimov, A. T. "Letters to ZhETF," 20, 108 (1974).

3. Clark, W. M.; Lind, R. C. Appl. Phys. Letts, 25, 284 (1974).

4. Muratov, Ye. A.; Pis'mennyy, V. D.; Rakhimov, A. T. "Fizika plazmy," 3, 405 (1977).

5. Chang, T. Y. Rev. Sci. Inst., 44, 405 (1973).

6. Velikhov, Ye. P.; Pis'mennyy, V. D.; Rakhimov, A. T. UFN, 122, 419 (1977).

2291
CSO: 8144/1033

PHYSICS

UDC 621.378.33

SELF-LOCKING OF AXIAL MODES UNDER OSCILLATION OF STIMULATED RAMAN RADIATION

Moscow KVANTOVAYA ELEKTRONIKA in Russian Vol 6, No 2, Feb 79 pp 375-377

[Article by N. V. Kravtsov, N. I. Naumkin, Scientific Research Institute of Nuclear Physics, MGU imeni M. V. Lomonosov, submitted 2 Feb 78, after revision -- 12 Jun 78]

[Text] Experimental observation is reported of self-locking of axial modes in a compressed Raman laser. Spectrum self-locking has been observed under the excitation of the stimulated emission in a high-Q long resonator.

It is known that the pumping of forced combinational radiation is usually accompanied by a change in the time characteristics of the forced radiation compared to the contour of the pumping field [1, 2]. However, the compression occuring in this case of combinational radiation pulses compared to pumping pulses is usually relatively small. The reason for such a compression are the threshold character of the origination of forced radiation in the medium with losses and the nonstationary nature of the process. In [3], supershort (3×10^{-10} sec long) pulses of Stokes radiation were obtained for inverse VKR [Stimulated Raman scattering] of a ruby laser radiation.

Of undoubted interest is the investigation of the possibility of obtaining pulses as short as possible of forced combinational radiation by using multimode pumping as shown in [4]. Below are given experimental proofs of the possibility of self-locking of the combinational radiation spectrum when the latter is pumped in a high-Q optical resonator.

2. The experimental installation consists of a ruby laser with an optical delay line (OLZ) within the resonator. The OLZ was placed in a chamber filled with compressed hydrogen at a pressure of about 50 atmospheres [5]. Mirrors of the laser resonator and the OLZ had a high coefficient of reflection ($r \sim 97\%$) on the pumping wavelength ($\lambda = 0.694$ microns), as well as on the wavelength of the first Stokes component ($\lambda = 0.975$ microns). The effective length of the laser was 7.8 meters. The ruby laser operated in the free oscillation mode and its radiation was an irregular sequence of spikes several microseconds long each. There was no noticeable synchronization of the modes within the radiation spike. The percentage of modulation at the frequency of intermode beats did not exceed 10%.

The use in experiments of a laser with a large effective length of the resonator provided multimode pumping in which there was, however, no noticeable mode synchronization, and also a possibility of a high amplification coefficient at the combinational radiation frequency even at small pumping intensities which eased the investigations of the time structure of radiation.

3. The investigation of such a laser made it possible to establish that combinational radiation, excited by multimode pumping, is a periodic sequence of short pulses with a frequency determined by the time the light passes around the resonator (c/2L). A typical oscillogram of laser radiation on a combination frequency is shown in Fig. 1. It may be seen that the radiation has a form characteristic of UKI [supershort pulses] , obtained when synchronizing longitudinal modes. The length of these pulses did not exceed 1 nanosec. We will note that the degree of synchronization of pumping radiation did not change noticeably upon origination of the VKR.

A necessary condition for the origination of a periodic sequence of short pulses at the frequency of combinational radiation is the availability at that frequency of a high-Q resonator, without which an origination of a combinational radiation in the form of an UKI train is impossible. In this case, the pulse of combinational radiation has a length comparable to the length of the pumping pulse, while its percentage of modulation at the frequency of intermode beats is found to be small.

4. The origination of synchronization of axial modes at the Stokes radiation frequency at multimode pumping is apparently the result of the operation of a mechanism considered in [4] and related to the discriminatory separation of the maximal fluctuating pulse at the resonator period due to the nonlinear law of conversion of the pumping radiation into combinational radiation. This process may also be facilitated by the "fast" component of polarizability of the medium, discovered in [6] which may be considered the compelling force also leading to the origination of self-locking.

5. Thus, the obtained results attest to the possibility of the origination in the "long" VKR active medium, placed in the optic resonator, self-locking of axial modes at the Stokes radiation frequency for intra-resonator excitation of the latter by the pumping multimode radiation.

The obtained results, taking into account [6] , where the possibility is shown of oscillation under certain conditions of several Stokes and anti-Stokes radiation components with similar intensities, increase the probability of experimental detection of extensively short light pulses (less than 10^{-14} sec long), that originate when there is a mutual synchronization of several Stokes and anti-Stokes components of combinational laser radiation [7] .

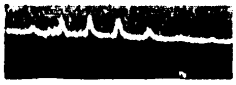

Fig. 1

BIBLIOGRAPHY

1. Grasyuk, A. Z.; KVANTOVAYA ELEKTRONIKA, 1, 485 (1974).

2. Zubov, V. A.; Krayskiy, A. V.; Prokhorov, K. A.; Sushchinskiy, M. M.; Shuvalov, I. K. ZhETF, 55, 443 (1968).

3. Culver, W. H.; Vanderlice, J. T.; Townsend, V. W. Appl. Phys. Letts., 12, 189 (1968).

4. Kuznetsova, T. I. "Letters to ZhETF," 10, 153 (1969).

5. Kravtsov, N. V.; Naumkin, N. I. FTT, 17, 3383 (1975).

6. Kravtsov, N. V.; Naumkin, N. I. "Letters to ZhETF," 21, 551 (1975).

7. Lugovoy, V. N.; Strel'tsov, V. N. KVANTOVAYA ELEKTRONIAK, 3, 1793 (1976).

2291
CSO: 8144/1033

PHYSICS

UDC 621.378.9:535.375

DIVERGENCE FROM A RAMAN LASER WITH A SLOWLY RELAXING ACTIVE MEDIUM

Moscow KVANTOVAYA ELEKTRONIKA in Russian Vol 6, No 2, Feb 79 pp 372-375

[Article by S. B. Kormer, V. D. Nikolayev, V. D. Urlin, submitted 9 Jun 78]

[Text] The formation of the angular characteristics of a liquid-nitrogen Raman laser output radiation is considered theoretically. Accumulation of vibrationally excited molecules with greater polarizability in the process of the stimulated Raman scattering is shown to be the principle mechanism of generation of optical inhomogeneities in this laser active medium. The calculated integral angular distribution of the output energy is in agreement with the experiment.

Introduction

In recent times, the great interest in combinational lasers [1-5] is explained to a great degree by the prospects of their practical applications to spectroscopy, plasma diagnostics, stimulating chemical reactions, etc. Besides retuning frequencies, these lasers make it possible to increase the brightness of a light beam. Considerable success in this direction was achieved by using liquefied gases, in particular, liquid nitrogen as the active medium [1, 4, 5] . Along with transparency in a wide range of frequencies, liquid nitrogen has high optical stability, a low Kerr [5] constant and, as was found recently, an extremely long time of oscillating relaxation τ_V [6-8] . The latter quality places it in a special position among traditional active media, since during the time of the pulse action, the energy spent on the oscillating molecules, does not have time to convert into heat and essentially destroy the optical homogeneity. As shown by an analysis performed in this paper, the basic mechanism of forming optical inhomogeneities in such a medium is due to the high polarizability of molecules in the oscillation-exicted state and the increase in their quantity in the process of the stimulated Raman scattering.

1. Opitcal Inhomogeneities of the Active Medium

It is known [9-12] that molecules in the oscillation-excited state are highly polarizable, as a result of which when their concentration increases, the refractive index of the medium increases. According to data in [10], the relative change in nitrogen polarizability is $\Delta\alpha/\alpha \approx 1.5 \times 10^{-2}$. The value of the refractive index change is related to $\Delta\alpha/\alpha$ by the following relationships:

$$\Delta n_\alpha = \frac{\Delta\alpha}{\alpha}\frac{\Delta N_1}{N_0}(n_0 - 1), \qquad (1)$$

where ΔN_1 -- population change in the first oscillating level due to stimulated Raman scattering [VKR]; N_0 -- density of the number of molecules; n_0 -- refractive index of the undisturbed medium. For $\Delta N_1 \ll N_0$, the equation describing the population of the oscillating level dynamics has the form [13]

$$\frac{\partial(\Delta N_1)}{\partial t} + \frac{\Delta N_1}{\tau_V} = \frac{g I_H I_s}{\hbar\omega_s}, \qquad (2)$$

where g -- amplification parameter of VKR; I_H, I_S -- intensities of pumping and the Stokes wave; ω_S - frequency of the dispersed radiation.

In the case of rectangular pumping pulse t_H long we find from (2)

$$\Delta N_1(t_H) = \frac{g I_H I_s \tau_V}{\hbar\omega_s}\left(1 - e^{-t_H/\tau_V}\right). \qquad (3)$$

During this time, the following amount of heat is emitted from the working substance

$$Q = \frac{\hbar\omega_K}{\tau_V}\int_0^{t_H}\Delta N_1(t)\,dt = \frac{\omega_K}{\omega_s} g I_H I_s t_H\left[1 - \frac{\tau_V}{t_H}\left(1 - e^{-t_H/\tau_V}\right)\right], \qquad (4)$$

which, under conditions of equalized pressure in the liquid, leads to a reduction in the refractive index by value [14].

$$\Delta n_T = -\frac{(n_0 - 1)\Gamma}{\rho_0 v_{ss}^2} Q, \qquad (5)$$

where ρ_0, Γ, $v_{зв}$ -- respectively density, Gryunayzen's coefficient and the speed of sound (in liquid nitrogen $\Gamma \approx 3.4$, $v_{зв} = 10^5$cm/sec, $\rho_0 = 0.8$ grams/cm^2). The energy of the oscillating quantum $\hbar\omega_н = 4.5 \times 15^{20}$ joules.

In the following, in estimating, it is convenient to deal with values averaged along the length of the working cuvette and measured in experiments. For this we will take into account that in a combinational laser with a long active medium 1

$$\frac{1}{l}\int_0^l g I_н \left(I_s^+ + I_s^-\right) dz = -\frac{\omega_s}{\omega_н}\frac{1}{l}\int_0^l \frac{dI_н}{dz}\,dz = \frac{\eta I_н(0,\,t)}{l},$$

where η -- efficiency of conversion of pumping into the Stokes component of the VKR. Then, designating by $\omega_s = \eta I_н(0) t_н / l$ the energy dispersed in 1cm^3 of medium, for $\lambda_н = 1.06$ microns and $\tau_V \gg t_н$ we will obtain

$$\Delta n_\alpha(t_н) \approx (n_0 - 1)\frac{\Delta\alpha\omega_s}{\alpha N_0 \hbar\omega_s} \approx 1{,}25\cdot 10^{-6}\omega_s = \frac{1{,}25\cdot 10^{-6}\int_0^{t_н} P_s(t)\,dt}{Sl}; \quad (6)$$

$$\Delta n_T(t_н) \approx -\frac{(n_0 - 1)\,\Gamma\omega_н\omega_s t_н}{2\rho_0 v_{зв}^2 \omega_s \tau_V} = 1{,}39\cdot 10^{-4}\omega_s \frac{t_н}{\tau_V}; \quad (7)$$

$$\Delta n_\Sigma = \Delta n_\alpha + \Delta n_T = \Delta n_\alpha (1 - t_н/t_н), \quad (8)$$

where

$$t_н = \frac{2\Delta\alpha\rho_0 v_{зв}^2 \tau_V}{\alpha\Gamma N_0 \hbar\omega_н} = 9\cdot 10^{-3}\tau_V;$$

P_s -- the power of Stokes beam with cross section S. It may be seen from (8) that the heat emitted during the VKR procees has a considerable effect on the optical homogeneity of the active medium and the divergence of the output radiation only for pumping pulse lengths $t_н \geq t_н$ (see also 12). According to 8 , the oscillating relaxation time in pure liquid nitrogen is about 56 seconds. In this case, a small amount of the dissolved admixtures of organic molecules may reduce τ_V considerably. Thus, in 7 is shown

that an admixture of methane of about 10^{-4}% leads to a reduction in τ_V to 10^{-2} seconds.*

Papers [4,5] investigated a combinational laser with pumping by the radiation of a neodymium laser in the mode of free oscillation and producing a series of spikes with a total duration of 200-600 microsec. Under such conditions, the thermal mechanism has no essential effect on Δn only in pure nitrogen with $\tau_V > 0.1$ sec or in the presence of methane admixtures to an amount less than 10^{-5}%. In [4,5], no information is given on the purity of the working medium, however, they pointed out that special measures were taken to clean it thoroughly. In these experiments, apparently $l_n < l_k$, therefore, in the following we will neglect the emission of heat in its medium in estimating the divergence of the output radiation of the combinational laser.

2. Divergence of Output Radiation

The mechanism of forming the angular radiation pattern of the output radiation in quantum oscillators with an optically inhomogeneous medium was investigated in [15-17]. It was shown that the cone aperture angle, within the limits of which the basic portion of the energy is propagated, is related to the change in refractive index Δn in the active region by relationship [17].

$$\theta \approx 2\sqrt{2\Delta n n_0 l/l_p},$$

where l -- length of active medium; l_p -- length of resonator; $n_o = 1.2$.

The specifics of the combinational laser is that the optical inhomogeneities in its medium increase with time. From the viewpoint of the speed of the electrodynamic processes in the resonator, these changes Δn (t) are slow and the width of the angular radiation pattern of the light beam follows their value parametrically. We will assume that the instananeous angular distribution of the radiation power is Gaussian:

$$F_P(\theta, t) = \frac{2P_s(t)}{\pi\theta_0^2(t)} e^{-2\theta^2/\theta_0^2(t)} \qquad (9)$$

with a characteristic angular width

$$\theta_0(t) = \left[\frac{8n_0 l}{l_p}\Delta n_\alpha(t) + \theta_n^2\right]^{1/2} = \left[B\int_0^t P_s(t)\,dt + \theta_n^2\right]^{1/2},$$

*Measured constant of attenuation by methane of the oscillating excitation of nitrogen is atout 8 x 10^{-17} cm^3/sec.

where $\theta_{н}$ -- initial divergence of radiation, due to static inhomogeneities of the refractive index and the aberration of the resonator; $B = 1.2 \times 10^{-5}$ $(\text{Slp})^{-1}$. Integrating (9) with respect to time gives an expression for a normalized integral radiation pattern

$$F_E(0) = \frac{1}{2\ln(\theta_к/\theta_н)}\left[\text{Ei}\left(-\frac{2\theta^2}{\theta_н^2}\right) - \text{Ei}\left(-\frac{2\theta^2}{\theta_к^2}\right)\right]. \qquad (10)$$

Here Ei (-x) -- integral exponent;

$$\theta_к = \sqrt{\frac{8n_0 l}{l_p}\Delta n_\alpha(l_н) + \theta_н^2}$$

is the instantaneous divergence of radiation at the end of the pulse.

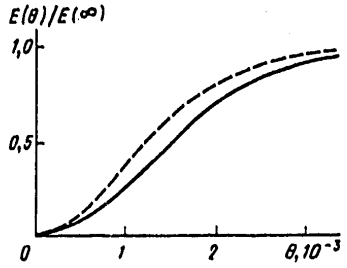

Fig. 1

The angular energy distribution corresponding to pattern (10) has the form

$$E(0) = -\frac{2\theta^2}{\theta_к^2 - \theta_н^2}\left[\text{Ei}\left(-\frac{2\theta^2}{\theta_к^2}\right) - \text{Ei}\left(-\frac{2\theta^2}{\theta_н^2}\right) + \frac{\theta_к^2}{2\theta^2}e^{-2\theta^2/\theta_к^2} - \frac{\theta_н^2}{2\theta^2}e^{-2\theta^2/\theta_н^2}\right].$$

We will note that the integral angular radiation characteristics of a combinational laser do not depend on the time behavior of its power and are fully determined by the density of the output energy. The combinational oscillator, described in [4, 5] had an active length of the medium l = 50cm

and radiated, in a beam with a cross section $1cm^2$ on the first (λ_1 = 1.41 microns) and second (λ_{21} = 2.1 microns) Stokes frequencies, 36 and 6 joules respectively. Taking into account the two Stokes components, the change in the refractive index in the medium is

$$\Delta n_a = \frac{1{,}25 \cdot 10^{-6}}{Sl}\left(E_1 + \frac{2\lambda_{21}}{\lambda_1} E_{21}\right) \approx 1{,}35 \cdot 10^{-6}.$$

It follows from experiments [4, 5] that $\theta_H/\theta_H \geq 3$. Assuming $\theta_H/\theta_H = 3$ and determining from Fig. 27 in [5] $1/1_p \approx 0.7$, we obtain the angular energy distribution shown in Fig. 1 (broken line). For comparison, there is also shown by a solid line experimental relationship E (θ) which agrees well with the calculated one. Thus, the angular characteristics of output radiation of a combination laser using liquid nitrogen are explained satisfactorily by an increase in the refractive index due to the change in the polarizability of molecules in the VKR process.

BIBLIOGRAPHY

1. Grasyuk, A. Z. KVANTOVAYA ELEKTRONIKA,1, 485 (1974).

2. Shaw, E. D.; Patel, S. K. N. Appl. Phys. Letts, 18, 215 (1971).

3. Patel, S. K. N. Appl. Phys. Letts, 19, 383 (1971).

4. Bocharov, V. V.; Grasyuk, A. Z.: Zubarev, I. G.; Kotov, A. V.; Smirnov, V. G. KVANTOVAYA ELEKTRONIKA, 1, 2185 (1974).

5. Grasyuk, A. Z.; Yefimkov, V. F.; Zubarev, I. G.; Kotov, A. V.; Smirnov, V. G. "Trudy FIAN," 91, 116 (1977).

6. Calaway, W. F.; Ewing, G. E. Chem. Phys. Letts, 30, 485 (1975).

7. Calaway, W. F.; Ewing, G. E. J. Chem. Phys., 63, 2842 (1975).

8. Brueck, S. R.; Osgood, R. M. J. Chem. Phys., 39, 568 (1976).

9. Butylkin, V. S.; Kaplan, A. Ye.; Khronopulo, Yu. G. "Izv. vuzov, Ser. Radiofizika," 12, 1792 (1969).

10. Vil'gel'mi, B.; Goyman, E. ZhPS, 19, 550 (1973).

11. Kravtsov, N. V.; Naumkin, N. I.; Protasov, V. P. KVANTOVAYA ELEKTRONIKA, 2, 1585 (1975).

12. Baklushkina, M. I.; Zel'dovich, B. Ya.; Mel'nikov, N. A.; Pimipetskiy, N. F.; Payzer, Yu. P.; Sudarkin, A. N.; Shkunov, V. V. ZhETF, 73, 831 (1977).

13. Akhmanov, S. A.; Drabovich, K. N.; Sukhorukov, A. P.; Chirkin, A. S. ZhETF, 59, 485 (1970).

14. Payzer, Yu. P. ZhETF, 52, 470 (1967).

15. Anan'yev, Yu. A. UFN, 103, 705 (1971).

16. Suchkov, A. F. "Trudy FIAN," 43, 161 (1968).

17. Kirillov, G. A.; Kormer, S. B.; Kochemasov, G. G.; Kulikov, S. M.; Murugov, V. M.; Nikolayev, V. D.; Sukharev, S. A.; Urlin, V. D. KVANTOVAYA ELEKTRONIKA, 2, 666 (1975).

2291
CSO: 8144/1033

PHYSICS

UDC 535.375

SMALL-SIGNAL WAVEFRONT REVERSAL UNDER NONTHRESHOLD REFLECTION FROM A BRILLOUIN MIRROR

Moscow KVANTOVAYA ELEKTRONIKA in Russian Vol 6, No 2, Feb 79 pp 394-397

[Article by N. G. Basov, I. G. Zubarev, A. V. Kotov, S. I. Mikhaylov, M. G. Smirnov, Physics Institute imeni P. N. Lebedev AN USSR (Moscow), submitted 2 Aug 78]

[Text] A method is suggested and implemented for small-signal wavefront reversal (OVF) under stimulated Brillouin scattering (VRMB) in a lightguide. This method may find use in nanosecond pulse wavefront reversal.

It is well known that the effect of wavefront reversal (OVF) at VRMB of spatially-inhomogeneous pumping makes it possible to compensate effectively for phase signal distortions in two-passage optical amplifiers [1, 2]. The given method, however, has a considerable shortcoming since, in view of the threshold nature of the reflection of the initiating radiation from the cuvette with the active substance, it does not permit obtaining OVF signals with an intensity lower than the threshold intensity. At small excesses above the threshold, the reflection coefficient may change strongly from one laser burst to another due to insignificant intensity variations, as well as to possible changes in the width of the pumping line [3]. All this makes the practical realization of the given effect difficult in arrangements where it is impossible or undesirable to have a signal with an intensity exceeding the threshold by many times [2, 5, 6]. This difficulty may be avoided, if a more intensive wave is sent into the cuvette with the active substance along with a weak signal wave. Then the amplification increment of the reflected signal will be determined by the intensity of the pumping waves and in the implementation of the OVF effect, there will be observed a nonthreshold reflection of the weak wave.

2. The theoretical consideration of scattering of the weak wave in the presence of a strong one will be done on the basis of a theory developed in [4] . We remind the reader that if the pumping field is represented in the form

$$E_{\text{н}} = \sum_{1}^{N} A_n e^{ik_n^{\text{н}} r},$$

and the Stokes signal field is

$$E_0 = \sum_{1}^{N} a_m e^{ik_m^{\text{с}} r}, \qquad \text{with} \qquad k_m^{\text{с}} = -k_m^{\text{н}},$$

then the system of equations describing changes in the Stokes wave amplitude along the direction of its propagation may be presented in the form

$$\frac{da_n}{dz} = \frac{g}{2} \sum_{m=1}^{N} |A_m|^2 a_n + \frac{g}{2} A_n^* \sum_{m \neq n} A_m a_m + S_n(z). \qquad (1)$$

When OVF conditions are fulfilled (see, for example [4]), the effect of number S_n (z) is negligibly small:

$$\frac{da_n}{dz} = \frac{g}{2} \sum_{m=1}^{N} |A_m|^2 a_n + \frac{g}{2} A_n^* \sum_{m \neq n} A_m a_m. \qquad (2)$$

System (2) may be solved on the assumption that

$$|A_k|^2 \ll \sum_{m \neq k} |A_m|^2, \quad k = 1, \ldots, N,$$

and the solution has the form

$$a_n(z) = a_n(0) e^{\frac{g}{2} Iz} + \frac{\sum_{m=1}^{N} A_m a_m(0)}{I} A_n^* e^{\frac{g}{2} Iz} \left(e^{\frac{g}{2} Iz} - 1 \right), \qquad (3)$$

where

$$I = \sum_{m=1}^{N} |A_m|^2, \; n = 1, \ldots, N.$$

In developing the reflected Stokes signal for the passage from spontaneous noises intensity $\Gamma = gIz \gg 1$, we, therefore, obtain from (3)

$$a_n(z) = \text{const} \cdot A_n^* e^{gIz}. \tag{4}$$

Let the pumping field consist of two components:

$$E_H = E_H^{(1)} + E_H^{(2)}, \tag{5}$$

where

$$E_H^{(1)} = \sum_{n=1}^{k} A_n e^{i k_n^H r}$$

is a strong wave and

$$E_H^{(2)} = \sum_{n=k+1}^{N} A_n e^{i k_n^H r}$$

is a weak wave, while

$$|A_{m=1, \ldots, k}| \gg |A_{m=k+1, \ldots, N}|$$

and

$$\sum_{n=1}^{k} |A_m|^2 \gg \sum_{n=k+1}^{N} |A_m|^2.$$

It follows from (4) and (5) that

$$E_c = E_c^{(1)} + E_c^{(2)} = \text{const} \cdot E_H^{(1)*} e^{ikz} + \text{const} \cdot E_H^{(2)*} e^{ikz}.$$

Thus, it has been shown that the OVF will be observed also for a weak pumping component and the presence of a strong wave permits obtaining the reflection of a weak wave as effectively as a strong wave.

3. An experimental investigation of such a mode of scattering was performed on an installation shown in Fig. 1. The radiation of a neodymium laser 1 (length of pulse $\tau \sim 25$ns, width of line $\Delta\nu_H \lesssim 5 \times 10^{-2}$cm^{-1}, divergence $\theta = 3 \times 10^{-4}$ radians, diaphragm 2 $\varnothing$ 3mm) by means of a wedge-shaped plate 3, which formed two beams, was introduced into optical amplifier 5 with an amplification coefficient for the weak signal of about 50. One of the beams imitated the weak pumping component and was attenuated by filter system 4, while the other beam was amplified without preliminary attenuation. At the amplifier exit, both beams were converged by means of glass wedges 6 to one place of phase plate 7 (the phase plate increased the "gray" divergence of the single-mode of the He-Ne laser single-mode beam with $\lambda = 0.63$ microns and 3mm diameter up to a value of $\theta \sim 2 \times 10^{-2}$ radians). The image of the illuminated part of the phase plate was transmitted by lens 8 with f=25cm to Brillouin cuvette at the entering end of light conduit 9 filled with carbon disulfide. The length of the active part of the lightguide was 70cm at a diameter of 2.5mm. Measuring complex 10 served for the determination of the energy characteristics of incident and reflected waves in both beams; moreover, photographs were taken of the intensity distribution of the radiation reflected from theBrillouin cuvette in the plane conjugated with the plane of exit diaphragm 2. Diaphragms were installed ahead of calorimeters, measuring the energy of reflected signals, the dimensions of which corresponded to the dimensions of pumping beams which made it possible to measure the reflection coefficients in the directions of weak and strong pumping waves. Experiments were made first on the OBF of each beam separately. Photographs of the corresponding distributions and the measurement data on the divergence of incident and reflected waves indicated that the value of the reversal parameter (see [2]) is near unity.

4. Fig. 2 shows the curves of the relationship between the reflection coefficient in the direction of weak wave and the intensity of the weak wave in the absence and presence of a strong wave. It may well be seen that in the absence of a strong component, the reflection has a threshold character usual for the VRMB. In the presence of a strong component, the reflection coefficient does not depend on the intensity of the weak wave and is almost equal to the reflection coefficient of the strong wave and there is no threshold. We will note that in the process of the experiments the intensity of the strong pumping component was maintained practically

constant, while the reflection coefficient of the strong wave was equal to 17.5%. Fig. 3 shows the relationship between the reflection coefficients of the weak and strong waves. In this case, the intensity of the weak wave was 1/5 of the threshold wave. It may be seen that the reflection coefficients of both beams were equal in the entire range of intensity change of the strong wave.

The given arrangement also makes it possible to obtain effective reflection and reversal of the wavefront of weak pulses the length of which is smaller than the length of the strong component of pulsing. We shortened the weak pulse to $\tau \sim 10$ns by means of a mylar film (we remind the reader that the length of the laser pulse is 25ns). The intensity of the weak component will be in the order of several percent of the strong component. The reflection coefficient of the weak component was 7% and of the strong -- 10%. This difference is explained by the fact that in the given method of shortening the pulse, its maximum falls at the rear front of the long pulse. The value of the reversal parameter of the short pulse was within limits of 0.7 - 0.9.

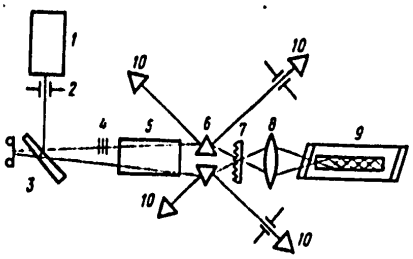

Fig. 1. Arrangement of experimental installation for investigating non-threshold signal reflection.

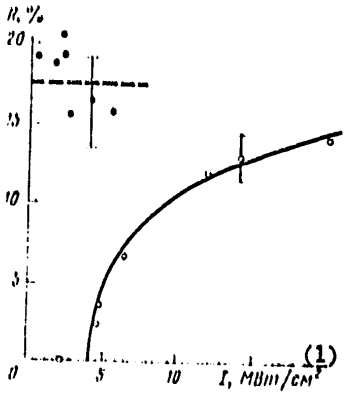

Fig. 2. Relationship between reflection coefficient of weak wave and its intensity in the absence (solid lines) and presence (broken lines) of a 30 Mw/cm^2 constant intensity strong wave.

1. Mw/cm^2

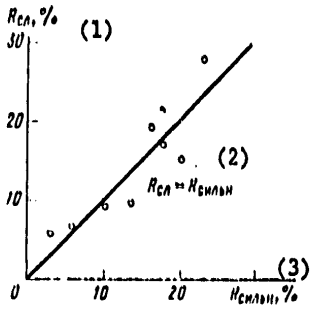

Fig. 3. Relationship between reflection coefficient of weak wave $(I_{сл} \ll I_0)$ and reflection coefficient of strong wave.

1. $R_{сл}$, %
2. $R_{сл}=R_{сильн}$
3. $R_{сильн}$, %

5. This experiment may be interpreted in terms of a four-wave shift. However, the given arrangement has a considerable advantage compared to the OVF arrangement for a degenerated four-wave shift, since here the counter waves need not be plane without fail, because the reverse (strong) Stokes wave is obtained due to the OVF and, therefore, is always comprehensively conjugated with the incident one.

BIBLIOGRAPHY

1. Nosach, O. Ya.; Popo ichev, V. I.; Ragul'skiy, V. V.; Fayzullov, F. S. "Letters to ZhETF, 16, 617 (1972).

2. Basov, N. G.; Yefimkov, V. F.; Zubarev, I. G.; Kotov, A. V.; Mironov, A. B.; Mikhaylov, S. I.; Smirnov, M. G. KVANTOVAYA ELEKTRONIKA, 5, No 4 (1978).

3. Zubarev, I. G.; Mikhaylov, S. I. KVANTOVAYA ELEKTRONIKA, 1 1239 (1974).

4. Sidorovich, V. G. ZhTF, 46, 2168 (1976).

5. Bespalov, V. I.; Betin, A. A.; Pasmanik, G. A. "Letters to ZhTF," 3, 215 (1977).

6. Borisov, V. N.; Kruzhilin, Yu. I.; Shklyarik, S. V. "Letters to ZhTF," 4, 160 (1978).

2291
CSO: 8144/1033

PHYSICS

UDC 621.378.33

AN ELECTRON-BEAM-EXCITED XeBr LASER

Moscow KVANTOVAYA ELECTRONIKA in Russian Vol 6, No 2, Feb 79 pp 400-402

[Article by I. N. Konovalov, V. F. Tarasenko, Institute of High-Current Electronics, Siberian Department of AN USSR (Tomsk), submitted 14 Aug 78]

[Text] The results are reported of an experimental investigation of the laser action in the Ar-Xe-$C_2F_4Br_2$ mixture at λ = 281.8nm. The radiation power of 3Mw and the specific radiation energy of $>$ 1 joule/liter have been achieved.

Eximer lasers using halides of noble gases are being intensively investigated at present. Oscillation has already been achieved on molecules of XeF*, KrF*, ArF*, XeCl*, KrCl*, ArCl*, XeBr*, XeI* [1-8] . Although laser radiation using halides of noble gas was first achieved on XeBr* molecules [1] , DrF and XeF lasers became the most widely used. This was due to the small radiation energies obtained in an XeBr laser when excited by electron beams [1, 3] . It was shown in [7, 8] that the efficiency of the XeBr laser increases when pumped by a fast discharge.

This paper cites the results of the experimental investigation of an XeBr laser excited by an electron beam.

An accelerator with 100-150kev electrons, 250 a/cm^2 current density in the beam and a 50ns current pulse length, was used for pumping the laser. The beam was introduced through a 20 x 1cm window into a laser tube 35cm long and 2cm in diameter, made of a steel foil 25 microns thick. The energy put into the gas was calculated by taking into account the electron scatter in the gas and the energy spectrum of the electrons outside of the foil. The distribution of the absorbed electron energy across the thickness of the gas layer was taken from [9] and the electron spectrum was determined experimentally by the foil method. The optical resonator was formed by a flat mirror with an aluminum coating and a plane-parallel quartz plate. Radiation characteristics were recorded by an IMO-2 calorimeter, FEK-22 photodiode, I2-7 oscillograph and ISP-30 spectroheliograph.

The operating efficiency of an eximer laser depends to a considerably extent on the proper choice of the halogen carrier. Thus, when exciting an XeBr laser with a rapid charge, the best results were obtained by using $C_2F_4Br_2$ and HBr [7, 8]. We investigated the effect on the efficiency of the XeBr laser of the following halogen carriers: Br_2, $C_2F_4Br_2$, $C_2H_4Br_2$, $CHBr_3$. When exciting electrons of mixtures of Ar, Xe and halogen carriers, the best results were achieved by using $C_2F_4Br_2$ and $CHBr_3$, however, $CHBr_3$ has a low pressure of saturated vapors. Mixtures with Br_2 and $C_2H_4Br_2$ gave for the same pumping smaller radiation energy by an order of magnitude. The low laser efficiency when using Br_2 was due to the strong absorption of laser radiation in Br_2. This is confirmed by the optimal concentration of Br in the mixture smaller by an order of magnitude compared to other bromine carriers.

Fig. 1 shows the relationships between the radiation energy, energy put into the gas by the electron beam and the delay time of the radiation time with respect to the start of the current pulse of the beam, and the pressure of the mixture. With an increase in pressure, maximum radiation energies are attained in mixtures with a greater content of Ar and a smaller concentration of $C_2F_4Br_2$. Delay time $_3$ decreases thereby.

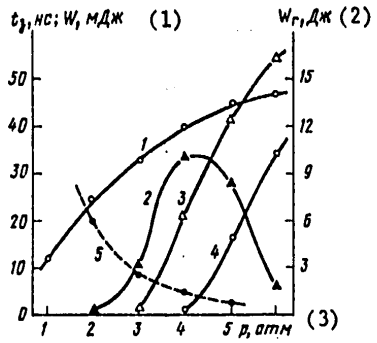

Fig. 1. Relationship between energy put into the gas from the electron beam $W_г$ (1), radiation energy W(2-4) and delay time of the radiation pulse with respect to the beam current t_3 (5), and the mixture pressure for the following ratios of components in the mixture: Xe: $C_2F_4Br_2$ = 40; Ar:Xe = 37.5 (2); 75 (3) and 150 (4).

1. t_3, ns; W , m joules
2. $W_г$, joules
3. atmospheres

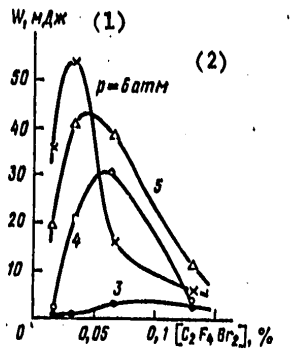

Fig. 2. Relationship between radiation energy and $C_2F_4Br_2$ content in mixture Ar:Xe = 75 at various pressures.

1. m joules 2. atmospheres

Fig. 2 shows the relationship between the energy of radiation and the percentage of $C_2F_4Br_2$ content at various pressures in the mixture. For a mixture pressure of six atmospheres, the optimal pressure of $C_2F_4Br_2$ at 20°C was 1.8×10^{-3} atmospheres. Fig. 3 shows oscillograms of the beam current, laser radiation and the laser radiation spectrum. A short radiation pulse at the half-height and a high peak power are characteristic of the XeBr laser. The radiation spectrum is a symmetrical line 0.4mm wide with a center on wavelength λ = 2818nm.

The investigations show that in energy characteristic the XeBr laser with an electron beam excitation is not inferior to an XeF laser. A 3Mw radiation power and a unit radiation energy $>$ 1 joule/liter were obtained using an Ar:Xr: $C_2F_4Br_2$ = 2000:40:1 mixture. The efficiency of oscillation with respect to the energy put into the gas from the beam was about 0.4%.

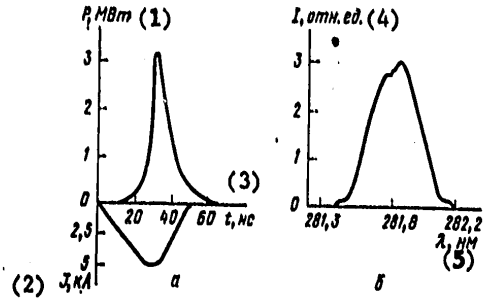

Fig. 3. Oscillograms of beam current pulses and laser radiation (a) and spectrum of laser radiation (b) in mixture Ar:Xe:$C_2F_4Br_2$ = 2000:40:1 at a pressure of 5 atm.

1. Mw
2. J, kA
3. ns
4. relative units
5. nm

The authors thank Yu. I. Bychkov for his support and A. G. Yastremskiy for calculating the energy put into the gas by the electron beam.

BIBLIOGRAPHY

1. Searles, S. K.; Hart, G. A. Appl. Phys. Letts, 27, 243 (1975).

2. Hoffman, J. M.; Hays, A. K.; Tisone, G. C. Appl. Phys. Letts, 28, 538 (1976).

3. Searles, S. K.; Appl. Phys. Letts, 28, 602 (1976).

4. Waynant, R. W. Appl. Phys. Letts, 30, 234 (1977).

5. Basov, N. G.; Brunin, A. N.; Danilyvich, V. A.; Kerimov, O. M.; Milanich, A. I.; Khodkevich, D. D. "Letters to ZhTF," 3, 1297 (1977).

6. Kudryavtsev, Yu. A. "Radioelectronics Abroad," No 4, 106 (1978).

7. Lisitsyn, V. N.; Razhev, A. M.; Chermenko, A. A. KVANTOVAYA ELEKTRONIKA, 5, 424 (1978).

8. Sze, R. C.; Scott, P. B. Appl. Phys. Letts, 32, 479 (1978).

9. Yevdokimov, O. B.; Ponomarev, V. B. "Izv. vuzov. Ser. Fizika," No 3, 159 (1978).

2291
CSO: 8144/1033

PHYSICS

UDC 621.378.33

AN ELECTRIC DISCHARGE LASER UTILIZING $SF_6 + H_2$ MIXTURE PUMPED BY AN INDUCTIVE STORAGE

Moscow KVANTOVAYA ELEKTRONIKA in Russian Vol 6, No 2, Feb 79 pp 408-411

[Article by A. F. Zapol'skiy, K. B. Yushko, submitted 9 Jun 78, after revision -- 5 Sep 78]

[Text] Results are presented of experimental studies of an electric-discharge chemical laser utilizing an $SF_6 + H_2$ mixture with an inductive storage in the pumping scheme. An inductive storage circuit is described which makes it possible to obtain a uniform longitudinal electric discharge without preionization in a laser cell with a volume of 3.7 liters under mixture pressure of up to 46mm Hg. The laser energy amounted to 6.9 joules, the signal being 40Mw, when the energy stored in the capacitor bank was equal to 3kjoules. The maximum energy output of 6.2 joules/liter has been achieved from the volume of 0.29 liters under the $SF_6 + H_2$ (3: 1) mixture pressure of 68mm Hg.

To obtain short oscillating pulses in an HF laser by initiating a chemical reaction by means of an electronic beam or a high-current discharge, usually a low-inductive capacitor bank is used which is charged to high voltages. An Arkad'yev-Marx oscillator and a double forming line [1 - 4] are widely used elements in arrangements for feeding lasers. It is also well known that by using an inductive storage arrangement, it is possible to obtain high-power electric signals 0.1 to 1.0 microseconds long [5, 6] on the load.

This paper gives the results of the experimental investigation of an HF laser operation with about an 0.1 microsecond oscillating pulse. It is pumped by inductive storage, loaded on the resistance of the plasma discharge in the working medium of the laser. An arrangement of longitudinal discharges was investigated. An $SF_6 - H_2$ mixture usually used in electric-charge HF lasers [3, 4, 7-9] was employed as the working substance.

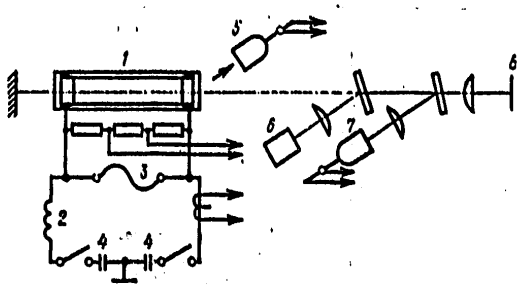

Fig. 1. Arrangement of experimental installation: 1 -- cuvette with SF_6 - H_2 mixture; 2 -- storage inductance; 3 -- circuit breaker; 4 -- IK-50-3 capacitors; 5 -- FEK-14 photoelement; 6 -- IKT-1 calorimeter; 7 -- detector; 8 -- shield of illuminated photographic printing paper.

Ivestigations were performed on the installation shown in Fig. 1. Two IK-50-3 capacitors (4), connected in series, were charged to +25kv and -25kv. Their capacitances of 1.5 microfarads were discharged through two controlled spark gaps and a working storage inductance through the resistance of circuit breaker 3.

The circuit breaker consisted of copper wire 0.06mm in diameter and 35 cm long placed in a polyethylene tube filled with a silicon carbide powder with about 10 micron grains. The powder served as an arc-quenching material and, at the same time, reduced the effect of the shock wave originating when the electric rupture of the wires occurred.

Laser curvette 1 with the SF_6 - H_2 mixture was connected in parallel with the circuit breaker or the inductance. The cuvette, 38mm in diameter and a distance of 35cm between ring electrodes made of stainless steel (volume 0.29 liters), was made of caprolan. The cuvette windows of IR quartz were aligned with each other with one window serving as the output window of the resonator. A gold-coated dead mirror could be placed instead of one of the cuvette's windows. When studying the oscillation spectrum, a window made of a BaF_2 crystal served as the output mirror of the resonator.

Maximum voltage across the cuvette electrodes was obtained at a working inductance of 2.1 microhenries (the total inductance of the loop was 2.5 microhenries).

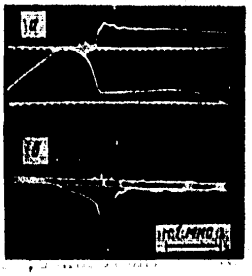

Fig. 2. Typical signal oscillograms:

a) upper beam -- light signal from discharge plasma into the laser cuvette; lower beam -- current pulse (marks every 200ns); b) upper beam -- oscillating signal; lower beam -- voltage pulses across electrodes of laser cuvette; U_C = 50kv, U_{max} = 290kv; I_{max} = 36ka, E_r = 0.85 joules; p = 46mm Hg; mixture SF_6: H_2 = 4:1

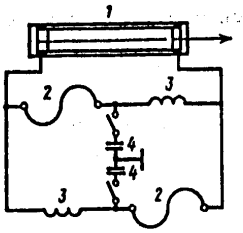

Fig. 3. Arrangement of inductive storage

1 -- laser cuvette; 2 -- circuit breakers; 3 -- storage inductances; 4 -- IK-50-3 capacitors.

Fig. 2 shows typical signal oscillograms. Since there was no preliminary ionization of the mixture, the maximum working pressure was limited by the value of the voltage applied to the cuvette electrodes.

To obtain a discharge at higher pressures of the working mixture, the inductive storage was connected into a circuit shown in Fig. 3. A parallel connection of additional inductances and a circuit breaker made it possible not only to almost double the voltage applied to the cuvette electrodes, but also increased the switched power due to a reduction in the length of the current and voltage signals.

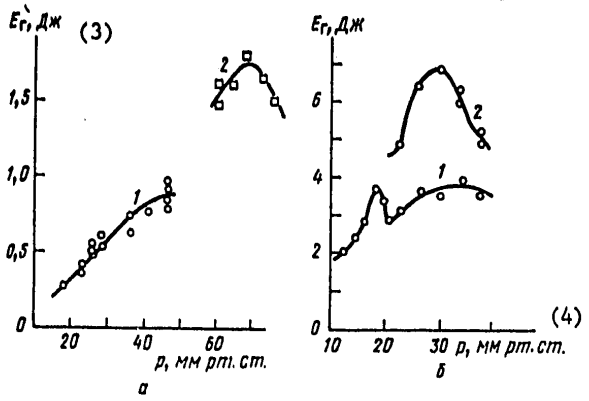

Fig. 4. Relationships between oscillation energy $E_г$ and pressure of working mixture p in the cuvette:

a) 0.29 liter cuvette; U_C = 50kv; connection in accordance with arrangement in Fig. 1, mixture SF_6 - H_2 = 4:1 (1) and according to arrangement Fig. 3, mixture SF_6: H_2 = 3:1 (2); b -- 3.7 liter cuvette; connected in accordance with arrangement in Fig. 3; mixture SF_6: H_2 = 3:1, U_C = 50kv (1) and 63kv (2)

3. joules 4. mmHz

The relationship between the oscillation energy and pressure of mixture SF_6: H_2 = 4:1 when the storage is operated in accordance with the arrangement in Fig. 1 is shown in Fig. 4a (curve 1). Maximum oscillating energy attained 1 joule for a signal length at the half-height in 100ns. The distribution of oscillation energy on the output mirror was fairly uniform. Transition lines $P_2(8)$ and $P_2(9)$ of the excited HF molecule were the most intensive in the radiation spectrum.

With the storage working in accordance with the arrangement in Fig. 3 with the previous capacitor bank, the maximum oscillation energy was attained

at 3.0 microhenry inductances and 45cm long circuit breakers. The maximum oscillation power obtained from a 0.29 liter cuvette was increased to 1.8 joules (see Fig. 4a, curve 2).

The formed voltage pulse with an amplitude $>$ 500kv made it possible to obtain a uniform electric discharge in a 3.7 liter cuvette with an internal diameter of 9.6cm and 51cm length of the active part. (A similar method for creating a volume charge, but with a different electrode configuration and a feed from an Arkad'yev-Marx oscillator, was proposed in [4]). The relationship between energy oscillation and pressure in the SF_6 - H_2 mixture for this case is shown in Fig. 4b. The maximums in the cited relationships were observed as the most uniform energy distribution at the output mirror of the resonator (Fig. 5). A reduction in the oscillation energy at pressures higher than 30mm Hg was due to a reduction in the efficiency of the energy transfer from the storage to the electric discharge.

The maximum oscillation energy was 6.9 joules at a 40Mw signal and a technical energy efficiency of 0.23%. Fig. 6 shows oscillograms of oscillation signals when the laser operates with an arrangement of an inductive storage shown in Fig. 3.

Fig. 5. Distribution of laser radiation over the cross section in the near zone (picture of a burn on the illuminated photographic printing paper);

E_r = 6.3 joules; p = 34mm Hg, mixture SF_6: H_2 = 3:1, V_K = 3.7 liters.

Thus, the results of this paper show that the use of an inductance storage in the feed circuit of the electric discharge HF laser makes it possible to form a uniform longitudinal electric discharge in cuvettes with considerable volumes at pressures of working mixture SF_6 - H_2 of tens of mm Hg and obtain high power oscillation pulses about 1 microsecond long.

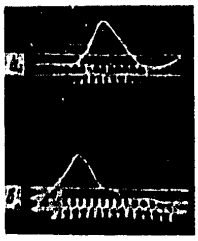

Fig. 6. Oscillograms of oscillation signals taken off a 0.29 liter cuvette (a, P_{max} = 17mw, 20ns marks) and 3.7 liter cuvettes (b, P_{max} = 31Mw, 40ns marks).

BIBLIOGRAPHY

1. Gerber, R. A.; Patterson, E. L.; Blair, L. S.; Grenier, N. R. Appl. Phys. Letters, 25, 281 (1974).

2. Osgood, R. M.; Mooney, Jr., D. L. Appl. Phys. Letts, 26, 201 (1975).

3. Schilling, P.; Decker, G. Infrared Phys. 16, 103 (1976).

4. Pavlovskiy, A. I.; Bosamykin, V. S.; Karelin, V. I.; Nikol'skiy, V. S. KVANTOVAYA ELEKTRONIKA, 3, 601 (1976).

5. Kind, D.; Salge, I.; Schiweck, L; Nevi, G. Electrotechn. Z-A, 92, 46 (1971).

6. Koval'chuk, B. M.; Kotov, Yu. A.; Mesyats, G. A. ZhTF, 34, 215 (1974).

7. Batovskiy, O. M.; Vasil'yev, G. K.; Markov, Ye. F.; Tal'roze, V. L. "Letters to ZhETF," 9, 341 (1969).

8. Dolgov-Savel'yev, G. G.; Podminogin, A. A. KVANTOVAYA ELEKTRONIKA, edited by Basov, N. G. No 4 (10), 69 (1972).

9. Arnold, C. P.; Wenzel, R. C. IEEE J. QE-9, 491 (1973).

2291
CSO: 8144/1033

PHYSICS

UDC 621.378.33

RADIATION PULSE LENGTHENING IN A SECTIONALIZED CO_2 LASER WITH SUCCESSIVE EXCITATION OF WORKING MEDIUM

Moscow KVANTOVAYA ELEKTRONIKA in Russian Vol 6, No 2, Feb 79 pp 417-421

[Article by V. P. Kudryashov, V. V. Osipov, V. V. Savin, Institute of Atmosphere Optics, Siberian Department of AN USSR (Novosibirsk), submitted 1 Sep 77]

[Text] The theoretical and experimental analysis is given of sectionalized CO_2 lasers with successive excitation of separate sections. Optimization of separate section parameters has been performed (gas composition and pressure, energy contribution) which made it possible to obtain long (up to 100 μs) high-power radiation pulses under electric discharge excitation. It is shown that under the successive excitation of two sections, the laser radiation pulse duration is 2.5 times longer than that of radiation pulses obtained under both independent and simultaneous excitation of separate sections.

When using pulsed CO_2-lasers with high peak radiation power for technological purposes, a dense plasma forms on the machined surface, which shields the target from the laser radiation [1]. The radiation pulse of typical lasers contain a comparatively short initial peak (50-100ns) accompanied by a long drop (1-2 microseconds), during which the radiation power is an order of magnitude smaller than the peak. For technological lasers, it is more feasible to have radiation pulses of smaller power but longer ones (about 100ms) with a high unit energy of radiation.

At present, several types of CO_2 lasers are known in which long (about 10 microsec) radiation pulses are obtained: 1) CO_2 lasers with low pressure (about 100mm Hg) when the small collision frequency provides a long time of existence of inverse population [2]. 2) CO_2 lasers at atmospheric pressure with a high concentration of nitrogen in the $CO_2 + N_2 + He$ mixture (a higher effective lifetime of the upper laser level is provided by the

transfer of energy from the vibration-excited nitrogen molecules [3]); 3) CO_2 laser, excited by a nonindependent charge controlled by an electron beam. The time of inversion existence may be close to the duration of the electron beam[4].

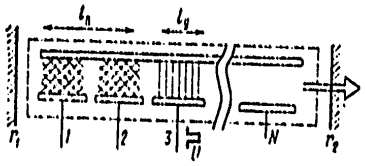

Fig. 1. Arrangement of multisectional laser.

The use of the first two types of CO_2 lasers does not provide for two of the above conditions due to the low density of active molecules and, therefore, the low unit radiation energy. By the excitation of the working medium by electron ionization, it is possible to obtain long smooth radiation pulses with high unit power take-off, however, higher power characteristics are achieved nevertheless by shorter durations of pumping since, in this case, the pumping power increases and, therefore, also the gain of the active medium and the energy introduced into the working medium [5-7].

Higher parameters may be obtained by using sectionalized excitation of the active medium in electrodischarge and electroionization lasers. In this case, individual sections of the working medium are excited in sequence, varying the delay time and the energy contribution when exciting the individual sections, which makes it possible to obtain almost any given radiation pulse shape. The total radiation pulse length in such a system may be increased to $l_{\Sigma} = N\tau_c$, where τ_c -- length of pulse generated by the individual section and N = number of sections.

Fig. 1 shows schematically a laser consisting of N sections with total length L, placed in a common resonator with coefficients r_1 and r_2 of the mirrors. Let in any moment of time one section be excited, for example 3, while the preceding ones (1, 2) were used up and represent an absorbing medium. The absorption is related to the higher gas temperature, determined by the value of the energy contribution. To determine the maximum radiation pulse length at a given length of the active medium and a certain method for its excitation, we will write the condition for quasistationary oscillation:

$$gl_y = g_n l_n + g_0 L, \qquad (1)$$

where g -- given in the amplification region; $g_0 = -\ln(r_1 r_2)/(2L)$ -- loss coefficient in resonator mirror; l_y and l_n -- lengths of amplifying and absorbing regions respectively. Designating by l_i the length of the i-th section, we obtain the relationship which determines its minimum length:

$$l_i = \left(g_0 L + g_n \sum_{k=1}^{n-1} l_k\right) \Big/ g. \qquad (2)$$

As an example, we will consider a multisectional laser with an nonindependent excited discharge controlled by a 10ms electron beam. In this case, a gain of about 3 x 10^{-2}cm [8] can be maintained in the active medium. Let the lengths of the individual sections be equal, then at the moment of radiation oscillation of the last section, when the absorbing section has a maximum length, relationship (1) acquires the form:

$$gl_y = g_n(L - l_y) + g_0 L,$$

from where it follows that

$$l_y/L = (g_n + g_0)/(g + g_n). \qquad (3),$$

We will use the following parameter values for estimating purposes: L = 300cm, r, r_2 = 0.5, temperature of absorbing medium T = 470K which corresponds to an energy contribution of 0.2 joules/cm^3 to mixture CO_2: N_2 = 1.2 at atmospheric pressure. By determining the equilibruim population in the lower laser level, we obtain for the absorption coefficient at given levels g_n = 2.5 x 10^{-3} cm^{-1} and for resonator losses g_0 = 1.2 x 10^{-3} cm^{-1}. By substituting these values into (3), we obtain Ly/L=1/9, i.e., N = 9. This means that the length of the radiation pulse for the sequential excitation of sections may exceed by nine times the radiation pulse length, generated by an individual section, i.e., may be 90 microseconds under conditions of our example. If resonator losses are reduced by increasing the reflection coefficient of mirrors, it is possible to increase the number of sections: in our example at r_1 r_2 = 0.8, N = 11.

Naturally, the cited estimates give the lower limit for N and t_z. If expression (2) is used for determining the lengths of the following sections, then for l_1 = 30cm, we obtain $r_1 r_2$ = 0.5, N = 14 and for $r_1 r_2$ = 0.8, N = 20 (Fig. 2), which corresponds to pulse lengths of 140 and 200 microsec respectively.

The obtained results show that lengths of radiation pulses in the order of 100 microsec may also be obtained with considerably shorter pumping of individual sections, which is characteristic for an independent discharge and this is not related to a considerable increase in the total length L (Fig. 2).

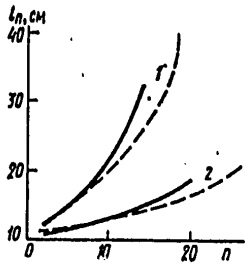

Fig. 2. Relationships between the length of individual section and its ordinal number for $r_1 r_2$ = 0.5 (1) and 0.8 (2) at L = 300 (solid lines) and 400cm (broken lines).

Numerical modeling of nonstationary kinetic processes in a CO_2 laser [9] makes it possible to calculate the shape of the radiation pulse of a multisectional laser with an electrodischarge excitation. The calculation was made for three sections 40, 30 and 30cm long for an energy contribution of 0.21 joules/cm^3 and a mixture of CO_2; N_2: He = 1: 2: 3 at atmospheric pressure. The results of calculations shown in Fig. 3 indicate that in oscillating radiations by all sections except the first, there may be no high-power peaks and the amplitudes of the output radiation is found to be fairly smooth. By a gradual increase of pumping power of individual sections, it is possible to obtain radiation with increasing power (Fig. 3b), i.e., in principle it is possible to form radiation pulses of any given shape.

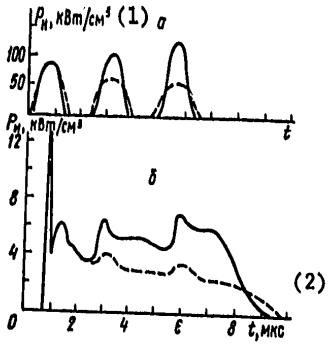

Fig. 3. Relationships between pumping power (a), radiation (b) and time, calculated for mixture C_2: N_2: He = 1: 2: 3 for p = latm and average unit energy contributions 0.2 (broken lines and 0.3 joules/cm^3 (solid lines).

1. kw/cm^3
2. microseconds

For experimental implementation of multisectional excitation, it is necessary to determine the optimal values of the composition and pressure of the gas pressure, as well as the energy contribution that produces the longest individual radiation pulse with high unit energy. These experiments were performed on an electrodischarge laser with a 3 x 4 x 74cm volume of the active medium [10].

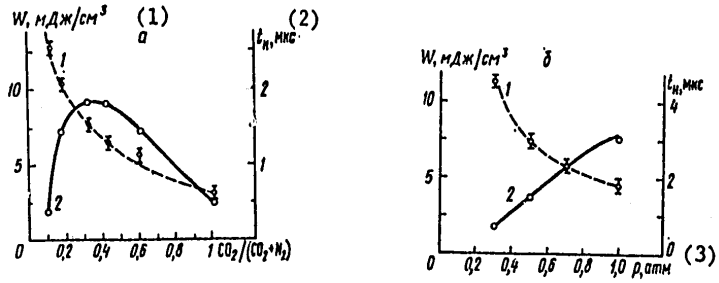

Fig. 4. Relationships between the length (1) and energy (2) of radiation, and composition (a) and pressure (b) when one section is operating.

1. m joules/cm^3
2. microseconds
3. atmospheres

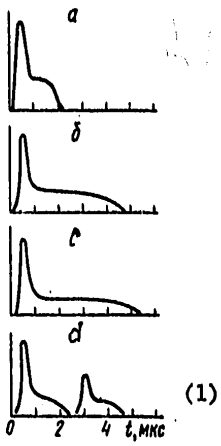

Fig. 5. Oscillograms of radiation pulses obtained at energy contributions of 0.25 joules/cm^3 to the first sections and 0.12 joules/cm^3 to the second sections; delays between connections of sections and the radiation energies are respectively 0 microsec and 11.4 m joules/cm^3 (a); 1.5 and 11.0 (b); 2.0 and 9.7 (c); 2.5 and 2.9 (d).

1. microseconds

For the experimental implementation of multisectional excitation, it is necessary to determine the optimal values of the composition and the pressure of the gas mixture, as well as the energy contribution that produces the longest individual radiation pulse with high unit energy. These experiments were performed on an electrodischarge laser with a 3 x 4 x 74cm volume of active medium [10].

Fig. 4a shows the relationships between the length and energy of the radiation pulse depending upon the composition of the CO_2 - N_2 - He mixture at atmospheric pressure and an 0.2 joules/cm^3 energy contribution typical for a CO_2 laser with an electrodischarge system of radiation. An increase in the pulse length with an increase in the nitrogen concentration in the mixture is due to the greater time of inversion existence caused by the long time needed for transfering the energy from N_2 to CO_2.

At the same time, the gain drops due to a reduction in the concentration of CO_2 molecules [9], nearing the loss coefficient in the resonator, as a result of which the radiation energy is reduced. For the utilized resonator (gold mirror and germanium plate) the optimal mixture composition CO_2: N_2: He = 1: 4: 5.

The effect of pressure on the characteristics of the radiation pulse is shown in Fig. 4b. The cited data was obtained for mixture CO_2: N_2: He = 1: 4: 5 for a fixed unit energy contribution W/p = 0.2 joules/(cm^3 atm).

Sectionalized excitation experiments were performed on an electrodischarge laser consisting of two sections with volumes of active medium 3 x 4 x 34 and 3 x 4 x 40cm. The sections were excited by two Marx oscillators with "shock" 0.016 and 0.02 microfarad capacitors for a charging voltage of each stage of about 50kv. The delay between the section starts was produced by means of G5-15 and GI-10 oscillators and an electronic delay circuit with an operating accuracy no worse than 100ns.

Fig. 5 shows oscillograms of radiation pulses obtained for various delays. It may be seen that with a longer delay, the length of the radiation pulse increases from two to five microseconds for an insignificant reduction in radiation energy (oscillograms a-c). A further increase in the delay leads to independent operation of the sections, as a consequence of which the radiation energy reduces sharply. This is explained by the fact that the energy contribution to the second section is chosen in such a way that the gain during its operation is only slightly higher than the loss coefficient in the resonator. It is precisely under such conditions that it is possible to obtain a smooth radiation pulse in the operation of a multisectional laser (Fig. 5a). However, these conditions are not beneficial for the independent oscillation of the radiation of the second section, therefore, the total radiation energy for the independent operation of sections decreases noticeably. It is clear that an increase of energy contribution to the second section will lead to a jump in radiation power at the moment it is connected in (Fig. 3b). Thus, by regulating the energy contribution and the delay length in connecting individual sections, we have the possibility of obtaining any required signal shape (rectangular, incremental, etc.). We will note that by sectionalizing the electrode system, it is possible not only in the longitudinal direction (along the resonator axis), but also transversly, which opens up possibilities for increasing further the length of the laser radiation pulses.

In conclusion, the authors express their gratitude to Yu. Bychkov for useful discussions of the described results.

BIBLIOGRAPHY

1. Andreyev, S. I.; Verzhikovskiy, I. V.; Dymshits, Yu. I. ZhTF, 40, 1436 (1970).

2. Girard, A. Optics Comms, 11, 346 (1974).

3. Girard, A.; Beaulieu, A. J. IEEE J. QE10, 521 (1974).

4. Velikhov, Ye. P.; Zemtsov, Yu. K.; Kovalev, A. S.; Persiyantsev, I. G.; Pis'mennyy, V. D.; Rakhimov, A. G. "Letters to ZhETF," 19, 364 (1976).

5. Basov, N. G.; Belanov, E. M.; Danilyvich, V. A. et al. "Letters to ZhETF," 14, 421 (1971).

6. Bychkov, Yu. I.; Osipov, V. V.; Savin, V. V. ZhTF, 46, 1444 (1976).

7. Savic, P.; Keker, M. M. Canad. J. Phys., 55, 325 (1977).

8. Leland, V. T. KVANTOVAYA ELEKTRONIKA, 3, 855 (1976).

9. Bychkov, Yu. I.; Kudryashov, V. P.; Osipov, V. V.; Savin V. V. KVANTOVAYA ELEKTRONIKA, 3, 1558 (1976).

10. Bychkov, Yu. I.; Kudryashov, V. P.; Osipov, V. V. KVANTOVAYA ELEKTRONIKA, 1, 1256 (1974).

2291
CSO: 8144/1033

END